

The Role of Signaling Pathways during the development of Hepatocellular Carcinoma

by

Susie Lee

DISSERTATION

Submitted in partial satisfaction of the requirements for the degree of

DOCTOR OF PHILOSOPHY

in

Pharmaceutical Sciences and Pharmacogenomics

in the

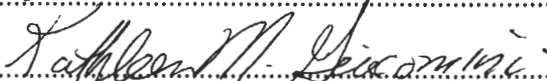
GRADUATE DIVISION

of the

UNIVERSITY OF CALIFORNIA, SAN FRANCISCO

Approved:







.....

Committee in Charge

UMI Number: 3390107

All rights reserved

INFORMATION TO ALL USERS

The quality of this reproduction is dependent upon the quality of the copy submitted.

In the unlikely event that the author did not send a complete manuscript and there are missing pages, these will be noted. Also, if material had to be removed, a note will indicate the deletion.



UMI 3390107

Copyright 2010 by ProQuest LLC.

All rights reserved. This edition of the work is protected against unauthorized copying under Title 17, United States Code.



ProQuest LLC
789 East Eisenhower Parkway
P.O. Box 1346
Ann Arbor, MI 48106-1346

Acknowledgements

None of this work would have been possible without the support of many people. First of all, I am grateful to my advisor, Dr. Xin Chen, for giving me the opportunity to learn and explore a new area of research. Her support was instrumental in the completion of this dissertation. I want to thank my thesis committee members, Dr. Kathleen Giacomini and Dr. Andrei Goga for their thoughtful advice on my dissertation. I would also like to thank Sandra Huling of the UCSF Liver Center and collaborator, Dr. Diego Calvisi of the Ernst Moritz Arndt University of Greifswald for their contributions to my research.

I thank all former and current lab members of the Chen Lab: Mohini, Ji, Jude, Coral, Cindy, and Micheal for their help, collaborations, and making the lab a more pleasant place to be in.

I express my deepest gratitude to my parents for the sacrifices they have made so that I could achieve my dream. To my brothers, Won Fung and Jeffrey, my god-parents, Henry and Pandita, my friends, especially Judy, and my Dear Jon, thank you all for being there for me through my tough and good times during graduate school.

Co-Author Acknowledgements

Chapter 2 was previously published in *Hepatology*, 2008, 47(4):1200-10 and is reproduced in adherence with *Hepatology* copyright policy.

Work in this chapter was done in collaboration with co-first author, Coral Ho, who performed microarray and CGH analysis of human HCC, as well as immunohistochemical staining of mouse tissue samples. Co-first author Susie Lee generated the murine model, followed by RT-PCR and Western Blot analysis of these samples, and wrote part of the manuscript for this study.

Chapter 4 was previously published in *Cancer Research*, 2009, 69(1):253-61 and is reproduced in adherence with *Cancer Research* copyright policy.

This work is done in collaboration with co-first author, Mohini Patil, who performed RT-PCR and Western blot analysis of CCND1/c-Met samples and immunohistochemical analysis of samples from c-Met transgenic, β -cat/c-Met injected FVB, and CCND1/c-Met mice as well as wrote the manuscript. Co-first author Susie Lee generated the CCND1/c-Met FVB mice and β -cat/c-Met injected CCND1 null mice for this study, used western blot to analyze samples from β -cat/c-Met injected CCND1 $-/-$ mice, and edited the manuscript.

Chapter 5 was previously published in *Molecular Cancer Research*, 2009 7:1937-1945 and is reproduced in adherence with *Molecular Cancer Research* copyright policy.

Work in this chapter is done in collaboration with co-first author, Chuan-Rui Xu, who performed all *in vitro* analysis. Co-first author, Coral Ho performed microarray

analysis of human HCC, and immunohistochemical analysis of mouse liver samples. Co-first author Susie Lee generated the murine model, followed by RT-PCR and Western blot analysis of these samples, and wrote part of the manuscript.

The Role of Signaling Pathways during the development of Hepatocellular Carcinoma

Susie Lee

Abstract:

The roles of genetic alterations in human hepatocellular carcinoma (HCC) are poorly understood. This dissertation's goals are to examine whether these de-regulated genes are sufficient to promote liver tumorigenesis and characterize the resulting effects on cellular processes and signaling pathways.

We first describe the role of receptor tyrosine kinase (RTK) feedback inhibitor Sprouty2 (Spry2) during hepatocarcinogenesis. We expressed dominant negative form of Spry2 (Spry2Y55F) and/or activated β -catenin into mouse hepatocytes and found that both factors are sufficient to induce liver tumorigenesis *in vivo*. Proliferation and angiogenesis as well as MAPK signaling are up-regulated in Spry2Y55F/ β -catenin induced HCC. However, the loss of Spry2 function alone is not capable of promoting MAPK activity. A correlation between the over-expression of RTK c-Met and down-regulation of Spry2 has been identified in human HCC. To investigate the synergistic effects of c-Met and Spry2 during hepatocarcinogenesis, we injected c-Met and/or Spry2Y55F into Ink4A/ARF null mice. Co-expression of both factors resulted in the development of HCC. The tumors displayed increases in MAPK and AKT activity. These findings demonstrate the role of Spry2 as a tumor suppressor in hepatocarcinogenesis.

We next analyzed the role of cell cycle regulator cyclin D1 (CCND1) in hepatocarcinogenesis. Co-expression of CCND1 and c-Met resulted in the development of HCC *in vivo*. Although, this cyclin is a downstream target of β -catenin, the absence of CCND1 did not deter β -catenin/c-Met induced liver tumorigenesis in mice. These results indicate that CCND1 is sufficient, but not required for β -catenin/c-Met induced hepatocarcinogenesis.

Finally, we describe the role of polycomb repressor Bmi1 in liver carcinogenesis. We expressed Bmi1 and/or activated Ras (RasV12) and found that both factors cooperate to promote hepatocarcinogenesis *in vivo*. Although Bmi1 is a known inhibitor of Ink4A/ARF, we found no evidence that Bmi1 does so during tumorigenesis. Our study indicates that Bmi1 cooperates with RasV12 to induce liver carcinogenesis in an Ink4A/ARF independent manner.

Taken altogether, our studies have validated clinical findings and demonstrated that combinations of MAPK signaling factors and genes, including CCND1 and Bmi1, are sufficient to promote hepatocarcinogenesis.

Table of Contents

Title Page	i
Acknowledgements	iii
Abstract	vi
List of Tables	xii
List of Figures	xiii
Chapter 1	
Introduction to Hepatocellular Carcinoma and Signaling Pathways	1
Introduction: Hepatocellular Carcinoma	1
Ras/MAPK Signaling Pathway	2
Akt Pathway	5
Wnt Pathway	8
Cyclin D1	10
Ink4A and Arf Pathways	13
Summary of Chapters	15
Chapter 2	16

Chapter 3	17
Chapter 4	18
Chapter 5	18
References	20

Chapter 2

Integration of genomic analysis and <i>in vivo</i> transfection to identify	27
--	-----------

Sprouty 2 as a candidate tumor suppressor in liver cancer

Introduction	27
Materials and Methods	29
Results	33
Discussion	51
References	56

Chapter 3

Suppression of Spry2 promotes unrestrained activation of c-Met	59
---	-----------

signaling during hepatocarcinogenesis

Introduction	59
Materials and Methods	62
Results	64
Discussion	74
References	78
Chapter 4	
Role of Cyclin D1 as a Mediator of c-Met and β-catenin Induced	80
Hepatocarcinogenesis	
Introduction	80
Materials and Methods	82
Results	86
Discussion	103
References	108

Chapter 5

Bmi1 functions as an Oncogene Independent of Ink4A/Arf	112
Repression in Hepatic Carcinogenesis	
Introduction	112
Materials and Methods	113
Results	118
Discussion	136
References	140
Chapter 6	
Summary and Conclusions	144
References	151

List of Tables

Chapter 2

Table 2.1: Primers used for real-time PCR analysis	33
Table 2.2: Candidate Oncogenes and Tumor Suppressor Genes Identified by correlating Expression arrays and aCGH data	36-37
Table 2.3: Tumor Development in Mouse co-injected with Ras/ Δ -N90- β -catenin or Spry2Y55F/ Δ N90- β -catenin	41

Chapter 5

Table 5.1: Primers used for real-time PCR analysis	115
Table 5.2: Summary of HCC cell lines used in the study	118
Table 5.3: Cell cycle distribution of SK-Hep1 cells infected with pLKO.1 or Bmi1/pLKO.1	123
Table 5.4: Statistics of positive stained cells for transfected hepatocytes	134

List of Figures

Chapter 1

- Figure 1.1: Simplified diagram of Ras signaling depicting MAPK and other Ras effector pathways 4
- Figure 1.2: Simplified diagram of Akt pathway depicting regulation of Akt and its downstream targets 6
- Figure 1.3: Wnt Pathway 9
- Figure 1.4: Diagram of CCND1 regulation of the cell cycle 11
- Figure 1.5: Ink4A and ARF 14

Chapter 2

- Figure 2.1: Correlation between DNA copy number variations and global gene expression patterns 34
- Figure 2.2: Overexpression of EGFP-Spry2 inhibits HCC cell growth *in vitro* 38
- Figure 2.3: Hydrodynamic injection and sleeping beauty mediated somatic integration to stably express target gene in mouse hepatocytes 39
- Figure 2.4: Co-expression of RasV12/ Δ N90- β -catenin or Spry2Y55F/ Δ N90- β -catenin induces liver cancer formation in mice 42
- Figure 2.5: Overexpression of AFP in mouse tumor samples induced by Spry2Y55F/ Δ N90- β -catenin and RasV12/ Δ N90- β -catenin 43

Figure 2.6: Co-expression of Spry2Y55F and Δ N90- β -catenin in mouse liver tumor cells	45
Figure 2.7: Activation of ERK, but not Akt in liver tumors induced by Spry2Y55F/ Δ N90- β -catenin	47
Figure 2.8: Immunohistochemical staining of liver tumor cells and surrounding non-tumor cells	50
Figure 2.9: Real-time RT-PCR analysis of gene expression in normal liver, non-tumor liver, HCCs from Spry2Y55F/ Δ N90- β -catenin and RasV12/ Δ N90- β -catenin injected mice	51
Figure 2.10: EGFR expression in wildtype liver, non-tumor liver, and Spry2Y55F/ Δ N90- β -catenin tumor samples	54
 Chapter 3	
Figure 3.1: Over-expression of c-Met induces preneoplastic lesions	65
Figure 3.2: Over-expression of c-Met and dominant-negative form of Spry2 (Spry2Y55F) cooperates with the loss of Ink4A/Arf to induce liver carcinogenesis <i>in vivo</i>	67
Figure 3.3: Co-expression of c-Met and Spry2Y55F in mouse liver tumor	69-70
Figure 3.4: Overview of cell proliferation, apoptosis, and angiogenesis in c-Met/Spry2Y55F tumors	71-72
Figure 3.5: Activation of ERK and AKT signaling in c-Met/Spry2Y55F tumors	73

Chapter 4

Figure 4.1: Cyclin D1 is induced in hMet/ β -catenin tumors	88-89
Figure 4.2: Cyclin D1 is not a direct target of activated β -catenin in Normal hepatocytes	90-91
Figure 4.3: Cyclin D1 cooperates with hMet to induce HCC in mice	92
Figure 4.4: Gross images of liver tumors	93
Figure 4.5: Molecular features of liver tumors induced by hMet/CCND1	95-96
Figure 4.6: Accelerated tumor development induced by hMet/ Δ N90- β -catenin in cyclin D1 knockout mice	97
Figure 4.7: Molecular features of liver tumors induced by hMet/ Δ N90- β -catenin in different Cyclin D1 genetic backgrounds	99
Figure 4.8: Array CGH plots of tumors induced by hMet and β -catenin in wildtype and CCND1 null mice	100
Figure 4.9: Expression in D-type cyclins and Cdks in mouse liver tissues	102
Figure 4.10: Decreased expression of Cdk4 in liver tumors induced by c-Met and β -catenin from mice with different CCND1 genetic backgrounds	103

Chapter 5

Figure 5.1: Bmi1 expression and its correlation with Ink4A/Arf expression in human HCC samples	117
Figure 5.2: Cell growth inhibition in Hep3B cells when Bmi1 is knock knock down was validated by a second shRNA construct	119

Figure 5.3: Down-regulation of Bmi1 and its effects on its target gene expression in human HCC cells	119-20
Figure 5.4: Silencing Bmi1 expression leads to decreased cell growth in human HCC cells	121
Figure 5.5: Cell cycle regulated genes expression decreased partly in Bmi1 knockdown Hep3B cells	122
Figure 5.6: BrdU labeling assay showed decreased proliferation activity in Bmi1 knockdown Huh7 cells	122
Figure 5.7: Bmi1 knock down in SK-Hep1 cells resulted in cell cycle blockages in S and G/M phases	122
Figure 5.8: Bmi1 cooperates with activated Ras (RasV12) to promote hepatic carcinogenesis <i>in vivo</i>	126-27
Figure 5.9: Characterization of liver tumors induced by Bmi1/RasV12	129
Figure 5.10: Up-regulation of p16Ink4A and p19Arf in liver tumor samples induced by Bmi1/RasV12	130
Figure 5.11: Regulation of p16Ink4A and p19Arf expression by RasV12 and/or Bmi1 in primary hepatocytes	132-33
Figure 5.12: Ras does not induce senescence in mouse hepatocytes	133
Figure 5.13: H-Ras and RASSF1A expression in HCC samples showed no correlation between Bmi1 and H-Ras, as well as Ras inhibitor RASSF1A	135

Chapter 1

Introduction to Hepatocellular Carcinoma and Signaling Pathways

Introduction: Hepatocellular Carcinoma

Hepatocellular carcinoma (HCC) is one of the most common cancers world-wide [1]. Surgery is the only curable option available, although only a minority of diagnosed patients will qualify for this treatment. This leaves the rest to other types of standard therapy, like chemo and radiotherapy. Unfortunately, these therapeutic options often have little clinical success. Consequently, this primary form of liver cancer is highly lethal, with many of the cases not surviving past one year [2, 3].

HCC has a broad epidemiology, ranging from chronic exposure to alcohol or aflatoxins, to fatty liver disease and metabolic disorders, as well as hepatitis viral infections [4]. In fact, hepatitis comprises of approximately 80% of the cases [5]. Although many studies have demonstrated the capability of the hepatitis viruses to indirectly and directly induce liver tumor formation, the role of these infections during hepatocarcinogenesis is still poorly understood [6]. Additionally, cirrhosis or scarring of the liver tissue is often an underlying condition in many of these liver cancer patients. Due to the variety of these pre-existing liver diseases, HCC has been considered to be a complex malignancy and difficult to treat.

The complexity of this disease also comes from the accumulation of various genetic and epigenetic changes, which occur during the progression to liver cancer.

Molecular analyses of these alterations in HCC have identified a multitude of deregulated signaling pathways that affect cellular processes, like cell cycle and apoptosis. There is mounting evidence that these pathways, such as Ras/MAPK, p53, and Wnt/ β -catenin signaling, play important roles during hepatocarcinogenesis [7]. Furthermore, the approval of sorafenib, an inhibitor of Raf kinase, Vascular endothelial growth factor receptor (VEGFR), and other kinases, for treatment of HCC shows considerable promise for molecular targeted therapy [8]. Therefore, a better understanding of the implicated pathways during liver carcinogenesis may give way to novel therapeutics. The mechanisms of the Ras/MAPK, Akt, Wnt/ β -catenin, Cyclin D1, and Ink4A/ARF signaling systems and their roles during the progression of cancer will be comprehensively described in the following sections.

Ras/Mitogen Activated Protein Kinase (MAPK) Pathway

In the presence of extracellular signals, such as growth factors, GTPase Ras interacts with various effectors, such as Ras-like guanine exchange factor (Ral-GEF) and phosphatidylinositol 3-kinase (PI3K). The binding of Ras to these factors subsequently leads to the activation of a range of signaling cascades, including the Ral and Akt pathways, thus coupling the cellular responses to external stimuli [9, 10].

Of particular interest is the Ras/MAPK pathway, whose roles in development and cancer have been well documented. Ras/MAPK signaling is initiated when growth factors bind to receptor tyrosine kinases (RTK) and results in the phosphorylation and activation of these receptors (Figure 1.1). Adaptor proteins, growth factor binding protein 2 (Grb2) and Grb2-associated binder 1 (Gab1), as well as signal relay protein Sh2-domain

containing tyrosine phosphatase 2 (Shp2) are then localized to the plasma membrane. This is followed by the recruitment of guanine exchange factor son-of-sevenless (SOS). SOS then stimulates Ras by inducing the guanine nucleotide exchange from GDP to GTP. Activated Ras binds to and induces the phosphorylation of Raf, which initiates a signaling cascade through the phosphorylation of mitogen-activated and extracellular signal-regulated kinase (MEK) and then extracellular signal-regulated kinase (ERK). This signaling activity eventually leads to the transcription of factors responsible for cell proliferation. A number of negative regulators are also involved in the control of Ras/MAPK activity. Sprouty (Spry) family members have been identified as feedback inhibitors of the pathway. In particular, mechanistic studies have demonstrated that Sprouty2 (Spry2) may interact with Grb2 or Raf to inhibit Ras/MAPK signaling [11, 12]. Dual-specificity phosphatases (DUSP) have also been found to antagonize this pathway by dephosphorylating ERK [13]. The number of identified regulators indicates that the maintenance of Ras/MAPK activity is clearly essential to cell survival.

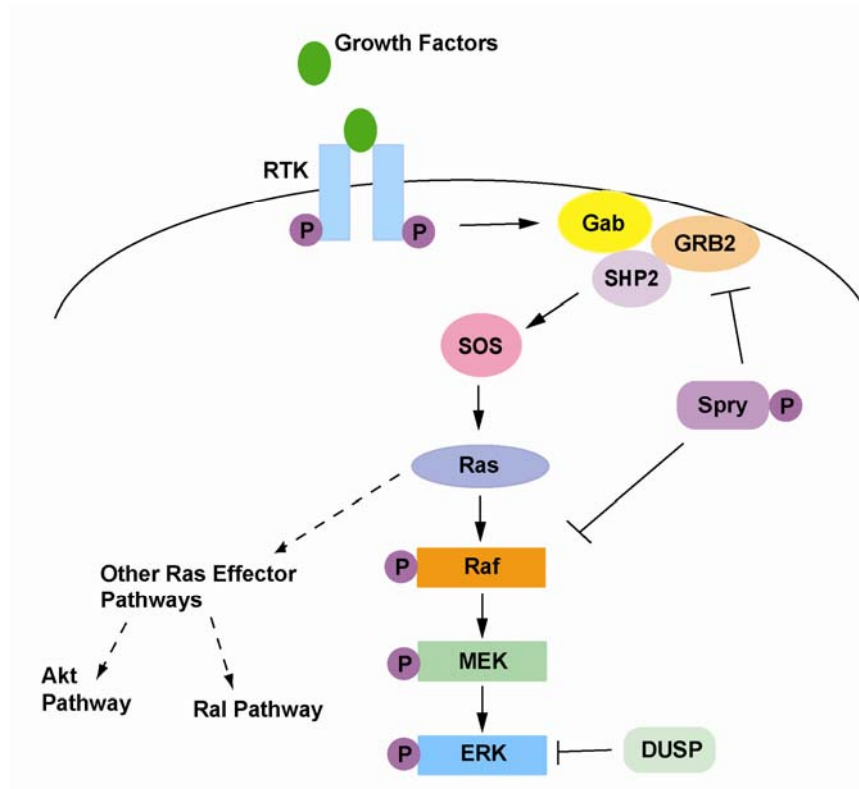


Figure 1.1 Simplified diagram of Ras signaling depicting MAPK and other Ras Effector pathways

Deregulation of Ras/MAPK signaling has been implicated in multiple forms of cancer. Activating *Ras* mutations are among the more common genetic alterations of this pathway, with an occurrence of 30% in malignancies, including pancreatic, lung, and colorectal cancers (COSMIC/Sanger Institute website). Furthermore, mouse models carrying constitutively active mutations of this GTPase have demonstrated Ras to be a potent inducer of cancers, such as pancreatic and lung carcinoma [14, 15]. However, the rate of incidence appears to depend on tumor type. *Ras* mutations, for instance, have been found in 90% of pancreatic cancer cases, whereas, its incidence rate in lung cancer is only 20% [16, 17]. In addition to Ras mutations, MAPK signaling can also be stimulated

by alterations of other factors in the pathway, such as RTKs. The epidermal growth factor receptor (EGFR) is mutated in 40% of all lung cancer patients and confirmed to have an oncogenic role in lung adenoma murine models [18]. Interestingly, lung cancer cases, carrying *Ras* mutations, lacked *EGFR* perturbations. This finding suggests that these two mutations are mutually exclusive, since they are both regulators of the same pathway. This may also be the case for HCC, where MAPK signaling is up-regulated in the presence of wildtype Ras in almost all liver cancer cases [19]. Studies have implicated the over-expression of RTK, c-Met as well as the down-regulation of tumor suppressor, Spry2 in human liver carcinogenesis [20, 21]. Altogether, these findings indicate that over-activation of the MAPK pathway occurs via the de-regulation of factors other than Ras in hepatocarcinogenesis. Chapters 2 and 3 will describe the roles of Spry2 and c-Met during the development of HCC in greater detail.

Akt Pathway

Akt signaling is essential to the regulation of cell survival and cycle as well as translation. Initiation of this pathway begins with the activation of PI3K by RTK signaling as well as Ras (Figure 1.2). PI3K then phosphorylates phosphatidylinositol-4,5-bisphosphate (PIP₂), to produce phosphatidylinositol-3,4,5-trisphosphate (PIP₃) at the plasma membrane. This is followed by the recruitment and phosphorylation of the Akt kinase at 2 residues, serine at amino acid position 473 (Ser473) and threonine at position 308 (Thr308) (Figure 1.2). Thr308 is phosphorylated by phosphoinositide-dependent protein kinase-1 (PDK-1), another indirect target of PI3K. However, phosphorylation of this residue can be inhibited by the dephosphorylation of PIP₃ by phosphatase and tensin

homolog (PTEN). The mechanism by which Ser473 is phosphorylated is still debatable. Studies have suggested that this serine residue is either phosphorylated by a component of the mammalian target of rapamycin (mTor) complex, rictor or autophosphorylated [22, 23]. Furthermore, although both residues need to be phosphorylated in order to activate Akt, phosphorylation of Ser473 alone has been shown to be sufficient to induce Akt signaling [24]. As previously mentioned, Akt activity controls various pathways, such as promoting cell survival through the phosphorylation and subsequent sequestration of pro-apoptotic protein, Bcl2-associated agonist of cell death (BAD) [25]. Akt signaling is also known for its activation of the mTor pathway, which leads to an increase in translation via the up-regulation of targets like ribosomal protein S6 (RpS6) [26].

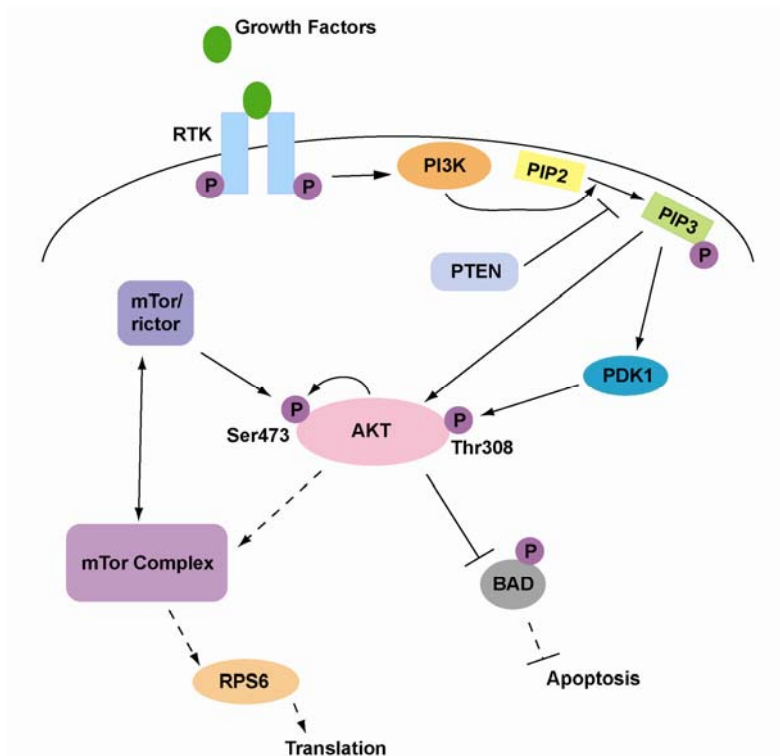


Figure 1.2 Simplified diagram of Akt pathway depicting regulation of Akt and its downstream targets.

Given its role in cell survival, it's not surprising that up-regulation of Akt signaling is prevalent in many cancers. Over-activation of Akt can be attributed to genetic/epigenetic aberrations of certain factors in this pathway, notably PI3K and PTEN. In fact, activating mutations of PI3K or deficiencies in PTEN expression, due to deletions or inactivating mutations, has been implicated in breast, prostate, endometrial, and ovarian carcinomas [27-31]. Inactivation of PTEN has also been detected in approximately 10% of HCC cases [32]. Furthermore, a murine study demonstrated that the specific loss of PTEN expression in hepatocytes induced the development of HCC in 60% of the mice [33]. The presence of PI3K mutations in liver cancer, however, is unclear, since studies have found the frequency of these genetic alterations to vary from no mutations to 35% among human HCC samples [34, 35]. Additionally, since RTK signaling is capable of stimulating Akt, it is probable that RTK hyper-activity is another mechanism by which the Akt pathway is de-regulated during tumorigenesis. Over-activation of EGFR has been found to result in the up-regulation of Akt signaling in cancers, like lung and liver carcinomas [36, 37]. Aberrant Akt signaling may be required for liver tumor development as indicated by studies involving rapamycin. This mTor inhibitor has been shown to reduce tumor proliferation and angiogenesis, as well as, increase apoptosis in HCC xenograft mice [38]. In addition, the combination of sorafenib and rapamycin enhanced the suppression of tumor proliferation and angiogenesis, suggesting that Akt activity in combination with Ras/MAPK signaling may have a synergistic effect on liver tumorigenesis [39, 40].

Wnt Pathway

Wnt signaling can be divided into 2 pathways: canonical, which signals through transcriptional co-factor β -catenin, and non-canonical, which transfers the Wnt signal to c-Jun N-terminal kinase (c-JNK) or Ca^{2+} pathways [41, 42]. This section will focus on the canonical system.

In the absence of Wnt signaling, β -catenin is phosphorylated by a protein complex, consisting of adenomatous polyposis coli (APC), axin, and glycogen synthase kinase (GSK3 β) (Figure 1.3). Phosphorylation of β -catenin leads to its ubiquitination and subsequent degradation. As a result, transcription remains inhibited by the repressor, groucho. Wnt signaling is activated when Wnt ligands bind to receptor Frizzled (Fz) and co-receptor low density lipoprotein receptor-related protein (LRP). This interaction leads to the phosphorylation of phosphoprotein Dishevelled (Dvl), which then inhibits GSK3 β and causes the disassociation of the APC protein complex. β -catenin, therefore, accumulates in the cytosol and eventually translocates to the nucleus, where it displaces groucho to interact with transcription factors T-cell factor/lymphoid enhancing factor (TCF/LEF) and initiate transcription of downstream genes. Some of these downstream targets include cyclin D1 (CCND1) and cMyc, which are important to the regulation of cell cycle and survival.

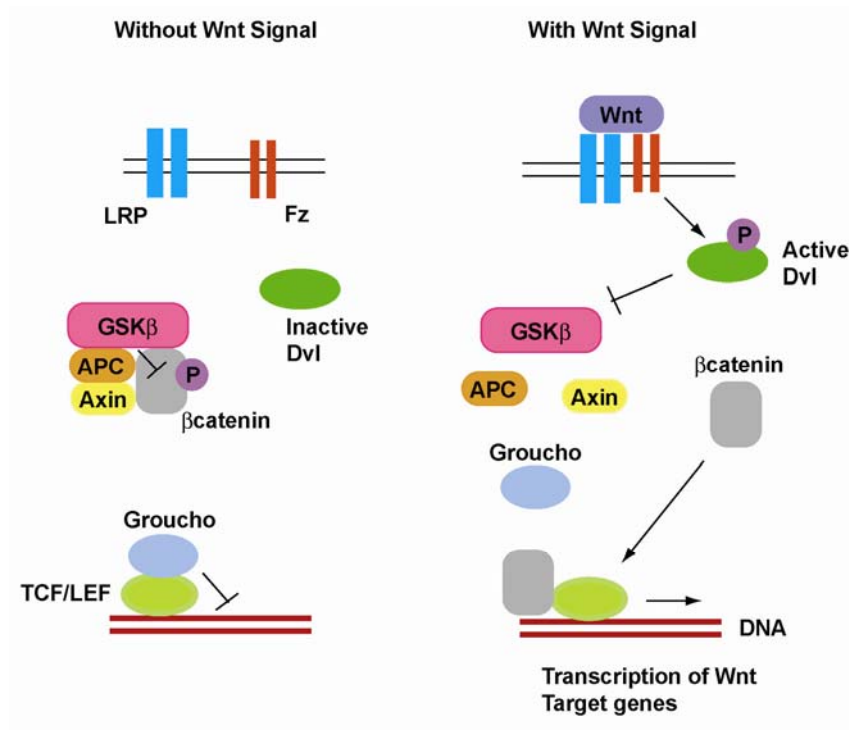


Figure 1.3 Wnt Pathway

Wnt signaling is essential to embryonic development, but its over-activation has also been implicated in carcinogenesis. Inactivating mutations of APC and activating β -catenin mutations are among the more frequent causes of Wnt over-stimulation in cancers. In particular, alterations of APC are present in 90% of colorectal cancer cases [43]. APC mutations are rare in HCC; however, hypermethylation of the APC promoter has been implicated in 53% of the cases [44-47]. β -catenin mutations have also been detected in 30% of HCC [48].

Murine studies have been performed to assess the role of constitutively active Wnt signaling during hepatocarcinogenesis. Interestingly, the over-expression of a dominant stable form of β -catenin in mice led to hepatomegaly or the enlargement of the liver, but did not promote the development of HCC [49]. It was later discovered that the

co-expression of both mutant forms of β -catenin and Ras induced hepatocarcinogenesis in all mice [50]. This cooperation between β -catenin and the Ras signaling pathway during hepatocarcinogenesis is further validated by another mouse model, where the combination of constitutively active β -catenin and c-Met also resulted in liver tumorigenesis [51]. Yet, another study demonstrated that the liver specific loss of Apc in a mouse model not only resulted in activation of the Wnt pathway, but also the development of HCC [52]. All of these findings suggest that the role of Wnt signaling in liver carcinogenesis may be complex.

Cyclin D1

As mentioned before, CCND1, a downstream target of β -catenin, is an important regulator of the cell cycle. In resting cells, retinoblastoma protein (pRb) is bound to the E2F transcription factor and prevents the transcription of genes that would have allowed the cell to transition from G1 to S phase. However, upon the presence of mitogenic signals, CCND1 begins to accumulate and eventually interacts with cyclin dependent kinase 4/6 (Cdk4/6) to form a complex (Figure 1.4) [53, 54]. This CCND1/Cdk4/6 complex, in turn, phosphorylates pRb, causing it to dissociate from E2F. Additionally, this complex also sequesters Cdk inhibitors p21Cip (p21) or p27Kip (p27), which frees Cdk2 to associate with cyclin E (CCNE). The CCNE/Cdk2 complex also phosphorylates pRb to further facilitate its separation from E2F. E2F then initiates the transcription of genes that support S phase entry. In addition, CCND1 has been found to have Cdk independent functions, where this cyclin is capable of associating with transcription factors and modulating transcriptional activity [55]. For instance, when CCND1 interacts

with transcriptional co-regulator p300, this results in the repression of the basic helix-loop-helix protein BETA2/NeuroD [56]. CCND1 activity is known to be repressed by a number of factors, including GSK3 β and p16^{Ink4A}. GSK3 β , in particular, has been found to target CCND1 for nuclear export and proteolysis by phosphorylating the threonine residue at amino acid position 286 [57]. The mechanisms by which p16^{Ink4A} inhibits CCND1 will be described in the next section.

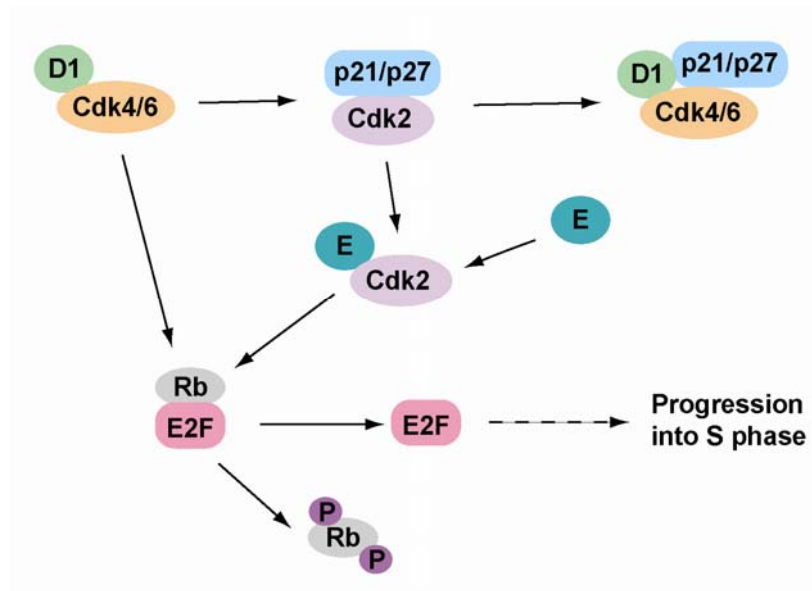


Figure 1.4 Diagram of CCND1 regulation of the cell cycle. D1 refers to CCND1 and E refers to CCNE.

Over-expression of CCND1 has been reported in a number of cancers, including colon and breast carcinomas [58, 59]. In particular, over-expression of this cyclin has been detected at variable frequencies (from 11 to 58%) in human HCC [60-62]. Amplification of this gene at chromosome 11q13 has been described as one of the mechanisms leading to CCND1 over-expression in a number of cancers, including breast

carcinoma and HCC, where it is detected in 11 to 13% of the cases [63, 64]. Furthermore, since CCND1 is activated in response to Wnt/ β -catenin signaling, it is possible that over-activation of β -catenin also leads to elevated levels of this cyclin protein. Although human HCC samples have been examined for an association between β -catenin and CCND1 expressions, the findings, so far, have been inconclusive, as some studies found there to be a positive correlation, while others did not [65-67].

Evidence of CCND1's role as an oncogene has been demonstrated in various studies. In particular, the over-expression of this cyclin in specific tissues, including the mammary gland and liver, has led to the development of mammary and hepatocellular carcinoma in these transgenic mice [68, 69]. However, both mouse models require periods of 15 months for mammary carcinoma or 17 months for HCC to develop. Clearly, the long latencies of these mice suggest that CCND1 needs additional oncogenic factors in order to fully promote carcinogenesis. Such factors may include the de-regulation of upstream signaling pathways that utilize CCND1's activity or other cooperating oncogenes. This was the case in a finding where the combination of CCND1 and Myc was found to induce lymphomas more rapidly than the expression of either transgene *in vivo* [70]. Mouse models have also been generated to assess the requirement of CCND1 in mammary carcinogenesis driven by various oncogenes. The results demonstrated that the loss of CCND1 confers resistance to mammary tumorigenesis induced by RTK, ErbB2 or Ras [71]. However, the same study also found that the absence of this cyclin did not deter mammary tumorigenesis induced by β -catenin or Myc. Yet, CCND1 deficiency reportedly reduced the formation of intestinal adenomas in mice carrying APC

mutations [72]. These studies indicate that the role of CCND1 in tumorigenesis appears to be dependent on the type of tissue and oncogene.

Ink4A and ARF Pathways

The locus at chromosome 9p2, also known as the cyclin dependent kinase inhibitor 2A (CDKN2A) gene, encodes two distinct inhibitors, Ink4A and ARF [73]. Each repressor has a unique promoter and 1st exon, which then splices into a common 2nd and 3rd exon (Figure 1.4). As a result, this generates a different reading frame for each of these inhibitors.

Ink4A and ARF each regulate their respective pathways. Ink4A, also known as p16^{INK4A}, is a member of a group of cell cycle inhibitors that regulate the retinoblastoma (RB) pathway. Cell cycle entry is initiated by the phosphorylation and subsequent inhibition of cell cycle inhibitor pRb by the cyclin dependent kinase 4/6 (CDK 4/6) and CCND1 complex. p16^{INK4A} prevents the association of this complex, which in turn stops cell cycle progression (Figure 1.5). ARF, also known as p19^{ARF} in mice and p14^{ARF} in humans, regulates the p53 pathway by binding to ubiquitin ligase mouse double minute 2 homolog (MDM2). This prevents the ubiquitination of transcription factor p53 and therefore stabilizes it. At this point, p53 either induces cell cycle arrest or apoptosis. Studies have suggested that the expression of p16^{INK4A} and ARF can be regulated together or separately. The expression of p16^{INK4A} for instance, increases in response to DNA damage, while transcription factor cMyc induces ARF expression [74, 75]. The Ras/MAPK and transforming growth factor beta (TGF- β) signaling pathways, however, were found to be capable of up-regulating both inhibitors [76-78]. In addition, the

expression of p16^{INK4A} and ARF has been demonstrated to be repressed by T box proteins (Tbx) and polycomb group protein Bmi1 [79, 80]. Chapter 5 will describe Bmi1 in more detail.

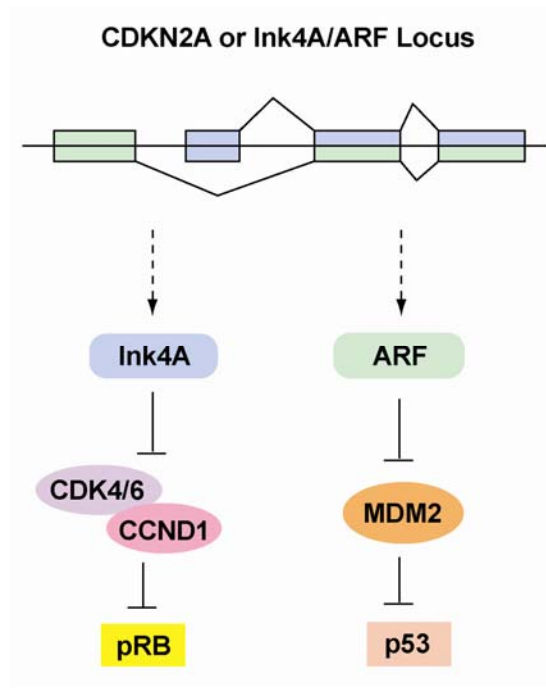


Figure 1.5 Ink4A and ARF: Diagram of the CDKN2A locus showing the open reading frames for Ink4A (in blue) and ARF (in green). Followed by a diagram of the Ink4A/ARF pathways

The Ink4A/ARF locus is partially or wholly inactivated by genetic or epigenetic alterations in a variety of cancers, including glioblastomas and colorectal cancer [81, 82]. In HCC, p16^{INK4A} is frequently inactivated in 45 to 60% of the patients [83, 84]. However, p14^{ARF} inactivation, by methylation and to a lesser degree deletions, has been detected in only 15% of HCC cases. Interestingly, the concomitant loss of p16^{INK4A} and p14^{ARF} is rare in liver cancer, where the frequency is only 7%.

To understand the roles of p16^{INK4A} and ARF during tumorigenesis, mouse models carrying specific deletions of p16^{INK4A}, p19^{ARF}, or both have been generated [85, 86]. These mice have no observable defects, although, they are all prone to developing lymphomas and sarcomas. p16^{INK4A} null mice, in particular, have been found to also spontaneously develop melanomas [87]. The tumor phenotype of the double knock-out mice is more severe. The tumor latency of these animals, for instance, is much shorter (38 weeks) compared to p16^{INK4A} -/- (76 weeks) and p19^{ARF} -/- (62 weeks) mice [88, 89]. But, primary liver tumors have not been observed in any of these murine models. One finding, however, demonstrated that the transient transfection of p19^{ARF} null mouse liver with an oncogenic form of *Ras* induces HCC in all animals, thus indicating that a second oncogenic hit is needed to drive the progression into liver carcinogenesis [90].

Summary of Chapters

HCC is a heterogeneous disease, as indicated by the number of de-regulated genes and signaling pathways that have been identified in clinical studies. But, it remains unclear whether these genetic aberrations play a role in hepatocarcinogenesis. Transgenic and knock out murine models have been generated to assess the mechanisms by which these potential oncogenes and tumor suppressors promote liver carcinogenesis. Overall, their findings suggest that a single genetic alteration is not sufficient to promote HCC formation. When co-expressed with another oncogene, however, this genetic alteration can induce liver tumorigenesis. While these studies have indicated that the combined de-regulation of 2 or more genes may stimulate the development of HCC, the difficulty of testing these different combinations lies in the mouse models. Unless these

transgenic and knock out mice are readily available, the process of making such models to analyze these genetic combinations can be time-consuming and expensive.

This dissertation's studies will examine whether certain combinations of potential oncogenes and tumor suppressors are sufficient to promote hepatocarcinogenesis *in vivo*. Specifically, the hydrodynamic injection and sleeping beauty transposon system will be used to stably transfect these genes into adult mouse hepatocytes. This method will allow us to quickly generate transiently transfected mice for the studies. The tumors from these mouse models will be further characterized to assess how the cellular processes are affected and identify the pathways activated by these oncogenic factors during liver tumorigenesis.

Chapter 2

Data from microarray and array-based comparative genomic hybridization (CGH) analyzes of human HCC samples were compared to determine the correlation between gene expression changes and DNA copy number variation. The comparison uncovered 76 genes which were up-regulated and amplified due to an increase in DNA copy number. Another set of 37 genes were also found to be down-regulated and deleted. One of these down-regulated genes is Spry2. Therefore, this study investigated the role of Spry2 as a potential tumor suppressor during liver carcinogenesis. We and others demonstrated that the over-expression of Spry2 repressed HCC cell proliferation. To investigate the role of Spry2 as a potential tumor suppressor *in vivo*, we co-expressed a dominant negative form of Spry2 (Spry2Y55F) with constitutively activated β -catenin into mouse hepatocytes by hydrodynamic injection and sleeping beauty transposon integration. The combination of

both Spry2Y55F and β -catenin led to a neoplastic phenotype in the mice. Furthermore, these tumors displayed elevated MAPK signaling as well as the de-regulation of genes involved in cell proliferation, apoptosis, and angiogenesis. Altogether, the data provides evidence that the inhibition of Spry2 activity cooperates with other oncogenes to promote liver carcinogenesis in murine models.

Chapter 3

Spry2 has been implicated as a tumor suppressor in the development of HCC (Chapter2). Recent clinical data suggests there to be a correlation between the loss of Spry2 activity and over-expression of c-Met in HCC cases (Calvisi et al, unpublished data). Additionally, *in vitro* analysis has demonstrated that Spry2 regulates both MAPK and AKT signaling in response to activation of c-Met. Therefore, the studies in this chapter examined the synergistic relationship between Spry2 and c-Met during hepatocarcinogenesis, using the aforementioned methods to express Spry2Y55F and/or c-Met in Ink4A/ARF null mice. Interestingly, while mice injected with only Spry2Y55F did not develop any tumors, c-Met expressing mice developed preneoplastic lesions. In contrast, the co-expression of Spry2Y55F and c-Met induced HCC in these injected animals. Increases in proliferation and angiogenesis were detected in these tumor nodules. Furthermore, the Spry2Y55F/c-Met induced tumors showed up-regulation of both MAPK and AKT signaling pathways. These findings suggest that the coordinated deregulation of Spry2 and c-Met may be a pivotal mechanism triggering unrestrained activation of Ras/MAPK signaling in human hepatocarcinogenesis.

Chapter 4

β -catenin and c-Met have been demonstrated to cooperatively induce the development of HCC *in vivo*. Cell cycle regulator, CCND1 is a downstream target of β -catenin. In order to determine the role of CCND1 in β -catenin and c-Met induced hepatocarcinogenesis, the interactions between these three components during liver tumorigenesis were examined in mouse models. The co-expression of CCND1 and c-Met stimulated the development of liver tumors. However, these tumors had a longer latency period as well as a lower frequency, and appeared to be more benign compared to those induced by β -catenin/c-Met. In addition, when β -catenin and c-Met were co-injected into CCND1 null mice, the absence of this cyclin did not deter tumorigenesis in these animals. In fact, a moderate accelerated tumor growth and increased tumor malignancy was observed in these mice. Further analysis detected an up-regulation of cyclin D2 (CCND2) expression in CCND1 null tumor samples, indicating that CCND2 may replace CCND1 in hepatic tumorigenesis. Together, these results suggest that CCND1 functions as a mediator of β -catenin during HCC pathogenesis, although other factors may be required to fully propagate β -catenin signaling. Moreover, our data suggest that CCND1 expression is not essential for liver tumor development induced by c-met and β -catenin.

Chapter 5

Bmi1 is a polycomb group proto-oncogene that has been implicated in multiple tumor types. Analysis of previous microarray data in our lab found this transcriptional regulator to be over-expressed in human HCC. Based on this finding, the role of Bmi1 in liver carcinogenesis was evaluated in this chapter. Our *in vitro* studies found that the loss

of Bmi1 expression reduced proliferation and perturbed cell cycle regulation in HCC cell lines. To investigate the role of Bmi1 during the development of liver cancer *in vivo*, Bmi1 and/or an activated form of Ras (RasV12) was stably expressed into mouse hepatocytes. While Bmi1 or RasV12 alone is not sufficient to promote hepatocarcinogenesis, the co-expression of both factors induced liver tumorigenesis in the mice. Tumors induced by Bmi1/RasV12 resembled human HCC by deregulation of genes involved in cell proliferation, apoptosis, and angiogenesis. Intriguingly, although Bmi1 is thought to be an important repressor of the Ink4A/Arf locus, it does not appear to affect Ink4A/Arf expression in hepatocytes based on our *in vitro* and *in vivo* findings. In summary, these studies demonstrate that Bmi1 can cooperate with other oncogenic signals to promote hepatic carcinogenesis *in vivo*. Yet Bmi1 functions independent of Ink4A/Arf repression in liver cancer development.

References:

1. Parkin, D.M., F. Bray, J. Ferlay, and P. Pisani, *Global cancer statistics, 2002*. CA Cancer J Clin, 2005. **55**(2): 74-108.
2. Perry, J.F., H. Poustchi, J. George, G.C. Farrell, G.W. McCaughan, and S.I. Strasser, *Current approaches to the diagnosis and management of hepatocellular carcinoma*. Clin Exp Med, 2005. **5**(1): 1-13.
3. Llovet, J.M. and J. Bruix, *Molecular targeted therapies in hepatocellular carcinoma*. Hepatology, 2008. **48**(4): 1312-27.
4. Bosch, F.X., J. Ribes, M. Diaz, and R. Cleries, *Primary liver cancer: worldwide incidence and trends*. Gastroenterology, 2004. **127**(5 Suppl 1): S5-S16.
5. Caldwell, S. and S.H. Park, *The epidemiology of hepatocellular cancer: from the perspectives of public health problem to tumor biology*. J Gastroenterol, 2009. **44 Suppl 19**: 96-101.
6. Di Bisceglie, A.M., *Hepatitis B and hepatocellular carcinoma*. Hepatology, 2009. **49**(5 Suppl):S56-60.
7. Aravalli, R.N., C.J. Steer, and E.N. Cressman, *Molecular mechanisms of hepatocellular carcinoma*. Hepatology, 2008. **48**(6): 2047-63.
8. Llovet, J.M., S. Ricci, V. Mazzaferro, P. Hilgard, E. Gane, J.F. Blanc, A.C. de Oliveira, A. Santoro, J.L. Raoul, A. Forner, M. Schwartz, C. Porta, S. Zeuzem, L. Bolondi, T.F. Greten, P.R. Galle, J.F. Seitz, I. Borbath, D. Haussinger, T. Giannaris, M. Shan, M. Moscovici, D. Voliotis, and J. Bruix, *Sorafenib in advanced hepatocellular carcinoma*. N Engl J Med, 2008. **359**(4): 378-90.
9. Schubert, S., K. Shannon, and G. Bollag, *Hyperactive Ras in developmental disorders and cancer*. Nat Rev Cancer, 2007. **7**(4):295-308.
10. Karnoub, A.E. and R.A. Weinberg, *Ras oncogenes: split personalities*. Nat Rev Mol Cell Biol, 2008. **9**(7): 517-31.
11. Martinez, N., C.A. Garcia-Dominguez, B. Domingo, J.L. Oliva, N. Zarich, A. Sanchez, S. Gutierrez-Eisman, J. Llopis, and J.M. Rojas, *Sprouty2 binds Grb2 at two different proline-rich regions, and the mechanism of ERK inhibition is independent of this interaction*. Cell Signal, 2007. **19**(11): 2277-85.
12. Brady, S.C., M.L. Coleman, J. Munro, S.M. Feller, N.A. Morrice, and M.F. Olson, *Sprouty2 association with B-Raf is regulated by phosphorylation and kinase conformation*. Cancer Res, 2009. **69**(17): 6773-81.
13. Boutros, T., E. Chevet, and P. Metrakos, *Mitogen-activated protein (MAP) kinase/MAP kinase phosphatase regulation: roles in cell growth, death, and cancer*. Pharmacol Rev, 2008. **60**(3): 261-310.
14. Jackson, E.L., N. Willis, K. Mercer, R.T. Bronson, D. Crowley, R. Montoya, T. Jacks, and D.A. Tuveson, *Analysis of lung tumor initiation and progression using conditional expression of oncogenic K-ras*. Genes Dev, 2001. **15**(24): 3243-8.
15. Hingorani, S.R., E.F. Petricoin, A. Maitra, V. Rajapakse, C. King, M.A. Jacobetz, S. Ross, T.P. Conrads, T.D. Veenstra, B.A. Hitt, Y. Kawaguchi, D. Johann, L.A. Liotta, H.C. Crawford, M.E. Putt, T. Jacks, C.V. Wright, R.H. Hruban, A.M.

- Lowy, and D.A. Tuveson, *Preinvasive and invasive ductal pancreatic cancer and its early detection in the mouse*. *Cancer Cell*, 2003. **4**(6): 437-50.
16. Brose, M.S., P. Volpe, M. Feldman, M. Kumar, I. Rishi, R. Guerrero, E. Einhorn, M. Herlyn, J. Minna, A. Nicholson, J.A. Roth, S.M. Albelda, H. Davies, C. Cox, G. Brignell, P. Stephens, P.A. Futreal, R. Wooster, M.R. Stratton, and B.L. Weber, *BRAF and RAS mutations in human lung cancer and melanoma*. *Cancer Res*, 2002. **62**(23): 6997-7000.
 17. Cowgill, S.M. and P. Muscarella, *The genetics of pancreatic cancer*. *Am J Surg*, 2003. **186**(3): 279-86.
 18. Kosaka, T., Y. Yatabe, H. Endoh, H. Kuwano, T. Takahashi, and T. Mitsudomi, *Mutations of the epidermal growth factor receptor gene in lung cancer: biological and clinical implications*. *Cancer Res*, 2004. **64**(24):8919-23.
 19. Calvisi, D.F., S. Ladu, A. Gorden, M. Farina, E.A. Conner, J.S. Lee, V.M. Factor, and S.S. Thorgeirsson, *Ubiquitous activation of Ras and Jak/Stat pathways in human HCC*. *Gastroenterology*, 2006. **130**(4): 1117-28.
 20. Chen, X., S.T. Cheung, S. So, S.T. Fan, C. Barry, J. Higgins, K.M. Lai, J. Ji, S. Dudoit, I.O. Ng, M. Van De Rijn, D. Botstein, and P.O. Brown, *Gene expression patterns in human liver cancers*. *Mol Biol Cell*, 2002. **13**(6): 1929-39.
 21. Kaposi-Novak, P., J.S. Lee, L. Gomez-Quiroz, C. Coulouarn, V.M. Factor, and S.S. Thorgeirsson, *Met-regulated expression signature defines a subset of human hepatocellular carcinomas with poor prognosis and aggressive phenotype*. *J Clin Invest*, 2006. **116**(6): 1582-95.
 22. Toker, A. and A.C. Newton, *Akt/protein kinase B is regulated by autophosphorylation at the hypothetical PDK-2 site*. *J Biol Chem*, 2000. **275**(12): 8271-4.
 23. Sarbassov, D.D., D.A. Guertin, S.M. Ali, and D.M. Sabatini, *Phosphorylation and regulation of Akt/PKB by the rictor-mTOR complex*. *Science*, 2005. **307**(5712): 1098-101.
 24. Alessi, D.R., M. Andjelkovic, B. Caudwell, P. Cron, N. Morrice, P. Cohen, and B.A. Hemmings, *Mechanism of activation of protein kinase B by insulin and IGF-I*. *EMBO J*, 1996. **15**(23): 6541-51.
 25. Datta, S.R., A. Brunet, and M.E. Greenberg, *Cellular survival: a play in three Akts*. *Genes Dev*, 1999. **13**(22): 2905-27.
 26. Hennessy, B.T., D.L. Smith, P.T. Ram, Y. Lu, and G.B. Mills, *Exploiting the PI3K/AKT pathway for cancer drug discovery*. *Nat Rev Drug Discov*, 2005. **4**(12): 988-1004.
 27. Barbareschi, M., F. Buttitta, L. Felicioni, S. Cotrupi, F. Barassi, M. Del Grammastro, A. Ferro, P. Dalla Palma, E. Galligioni, and A. Marchetti, *Different prognostic roles of mutations in the helical and kinase domains of the PIK3CA gene in breast carcinomas*. *Clin Cancer Res*, 2007. **13**(20): 6064-9.
 28. Saal, L.H., P. Johansson, K. Holm, S.K. Gruvberger-Saal, Q.B. She, M. Maurer, S. Koujak, A.A. Ferrando, P. Malmstrom, L. Memeo, J. Isola, P.O. Bendahl, N. Rosen, H. Hibshoosh, M. Ringner, A. Borg, and R. Parsons, *Poor prognosis in carcinoma is associated with a gene expression signature of aberrant PTEN tumor suppressor pathway activity*. *Proc Natl Acad Sci U S A*, 2007. **104**(18): 7564-9.

29. Shayesteh, L., Y. Lu, W.L. Kuo, R. Baldocchi, T. Godfrey, C. Collins, D. Pinkel, B. Powell, G.B. Mills, and J.W. Gray, *PIK3CA is implicated as an oncogene in ovarian cancer*. Nat Genet, 1999. **21**(1): 99-102.
30. Suzuki, H., D. Freije, D.R. Nusskern, K. Okami, P. Cairns, D. Sidransky, W.B. Isaacs, and G.S. Bova, *Interfocal heterogeneity of PTEN/MMAC1 gene alterations in multiple metastatic prostate cancer tissues*. Cancer Res, 1998. **58**(2): 204-9.
31. Tashiro, H., M.S. Blazes, R. Wu, K.R. Cho, S. Bose, S.I. Wang, J. Li, R. Parsons, and L.H. Ellenson, *Mutations in PTEN are frequent in endometrial carcinoma but rare in other common gynecological malignancies*. Cancer Res, 1997. **57**(18): 3935-40.
32. Yao, Y.J., X.L. Ping, H. Zhang, F.F. Chen, P.K. Lee, H. Ahsan, C.J. Chen, P.H. Lee, M. Peacocke, R.M. Santella, and H.C. Tsou, *PTEN/MMAC1 mutations in hepatocellular carcinomas*. Oncogene, 1999. **18**(20): 3181-5.
33. Horie, Y., A. Suzuki, E. Kataoka, T. Sasaki, K. Hamada, J. Sasaki, K. Mizuno, G. Hasegawa, H. Kishimoto, M. Iizuka, M. Naito, K. Enomoto, S. Watanabe, T.W. Mak, and T. Nakano, *Hepatocyte-specific Pten deficiency results in steatohepatitis and hepatocellular carcinomas*. J Clin Invest, 2004. **113**(12): 1774-83.
34. Lee, J.W., Y.H. Soung, S.Y. Kim, H.W. Lee, W.S. Park, S.W. Nam, S.H. Kim, J.Y. Lee, N.J. Yoo, and S.H. Lee, *PIK3CA gene is frequently mutated in breast carcinomas and hepatocellular carcinomas*. Oncogene, 2005. **24**(8): 1477-80.
35. Tanaka, Y., F. Kanai, M. Tada, Y. Asaoka, B. Guleng, A. Jazag, M. Ohta, T. Ikenoue, K. Tateishi, S. Obi, T. Kawabe, O. Yokosuka, and M. Omata, *Absence of PIK3CA hotspot mutations in hepatocellular carcinoma in Japanese patients*. Oncogene, 2006. **25**(20): 2950-2.
36. Engelman, J.A., P.A. Janne, C. Mermel, J. Pearlberg, T. Mukohara, C. Fleet, K. Cichowski, B.E. Johnson, and L.C. Cantley, *ErbB-3 mediates phosphoinositide 3-kinase activity in gefitinib-sensitive non-small cell lung cancer cell lines*. Proc Natl Acad Sci U S A, 2005. **102**(10): 3788-93.
37. Villanueva, A., D.Y. Chiang, P. Newell, J. Peix, S. Thung, C. Alsinet, V. Tovar, S. Roayaie, B. Minguez, M. Sole, C. Battiston, S. Van Laarhoven, M.I. Fiel, A. Di Feo, Y. Hoshida, S. Yea, S. Toffanin, A. Ramos, J.A. Martignetti, V. Mazzaferro, J. Bruix, S. Waxman, M. Schwartz, M. Meyerson, S.L. Friedman, and J.M. Llovet, *Pivotal role of mTOR signaling in hepatocellular carcinoma*. Gastroenterology, 2008. **135**(6): 1972-83, 1983 e1-11.
38. Wang, Z., J. Zhou, J. Fan, S.J. Qiu, Y. Yu, X.W. Huang, and Z.Y. Tang, *Effect of rapamycin alone and in combination with sorafenib in an orthotopic model of human hepatocellular carcinoma*. Clin Cancer Res, 2008. **14**(16): p. 5124-30.
39. Huynh, H., V.C. Ngo, H.N. Koong, D. Poon, S.P. Choo, C.H. Thng, P. Chow, H.S. Ong, A. Chung, and K.C. Soo, *Sorafenib and Rapamycin Induce Growth Suppression in Mouse Models of Hepatocellular Carcinoma*. J Cell Mol Med, 2009.
40. Newell, P., S. Toffanin, A. Villanueva, D.Y. Chiang, B. Minguez, L. Cabellos, R. Savic, Y. Hoshida, K.H. Lim, P. Melgar-Lesmes, S. Yea, J. Peix, K. Deniz, M.I. Fiel, S. Thung, C. Alsinet, V. Tovar, V. Mazzaferro, J. Bruix, S. Roayaie, M.

- Schwartz, S.L. Friedman, and J.M. Llovet, *Ras pathway activation in hepatocellular carcinoma and anti-tumoral effect of combined sorafenib and rapamycin in vivo*. *J Hepatol*, 2009. **51**(4): 725-33.
41. Veeman, M.T., J.D. Axelrod, and R.T. Moon, *A second canon. Functions and mechanisms of beta-catenin-independent Wnt signaling*. *Dev Cell*, 2003. **5**(3): 367-77.
 42. Giles, R.H., J.H. van Es, and H. Clevers, *Caught up in a Wnt storm: Wnt signaling in cancer*. *Biochim Biophys Acta*, 2003. **1653**(1): 1-24.
 43. Miyoshi, Y., H. Nagase, H. Ando, A. Horii, S. Ichii, S. Nakatsuru, T. Aoki, Y. Miki, T. Mori, and Y. Nakamura, *Somatic mutations of the APC gene in colorectal tumors: mutation cluster region in the APC gene*. *Hum Mol Genet*, 1992. **1**(4): 229-33.
 44. Edamoto, Y., A. Hara, W. Biernat, L. Terracciano, G. Cathomas, H.M. Riehle, M. Matsuda, H. Fujii, J.Y. Scoazec, and H. Ohgaki, *Alterations of Rb1, p53 and Wnt pathways in hepatocellular carcinomas associated with hepatitis C, hepatitis B and alcoholic liver cirrhosis*. *Int J Cancer*, 2003. **106**(3): 334-41.
 45. Ishizaki, Y., S. Ikeda, M. Fujimori, Y. Shimizu, T. Kurihara, T. Itamoto, A. Kikuchi, M. Okajima, and T. Asahara, *Immunohistochemical analysis and mutational analyses of beta-catenin, Axin family and APC genes in hepatocellular carcinomas*. *Int J Oncol*, 2004. **24**(5): 1077-83.
 46. Yang, B., M. Guo, J.G. Herman, and D.P. Clark, *Aberrant promoter methylation profiles of tumor suppressor genes in hepatocellular carcinoma*. *Am J Pathol*, 2003. **163**(3): 1101-7.
 47. Csepregi, A., C. Rocken, J. Hoffmann, P. Gu, S. Saliger, O. Muller, R. Schneider-Stock, N. Kutzner, A. Roessner, P. Malfertheiner, and M.P. Ebert, *APC promoter methylation and protein expression in hepatocellular carcinoma*. *J Cancer Res Clin Oncol*, 2008. **134**(5): 579-89.
 48. Taniguchi, K., L.R. Roberts, I.N. Aderca, X. Dong, C. Qian, L.M. Murphy, D.M. Nagorney, L.J. Burgart, P.C. Roche, D.I. Smith, J.A. Ross, and W. Liu, *Mutational spectrum of beta-catenin, AXIN1, and AXIN2 in hepatocellular carcinomas and hepatoblastomas*. *Oncogene*, 2002. **21**(31): 4863-71.
 49. Harada, N., H. Miyoshi, N. Murai, H. Oshima, Y. Tamai, M. Oshima, and M.M. Taketo, *Lack of tumorigenesis in the mouse liver after adenovirus-mediated expression of a dominant stable mutant of beta-catenin*. *Cancer Res*, 2002. **62**(7): 1971-7.
 50. Harada, N., H. Oshima, M. Katoh, Y. Tamai, M. Oshima, and M.M. Taketo, *Hepatocarcinogenesis in mice with beta-catenin and Ha-ras gene mutations*. *Cancer Res*, 2004. **64**(1): 48-54.
 51. Tward, A.D., K.D. Jones, S. Yant, S.T. Cheung, S.T. Fan, X. Chen, M.A. Kay, R. Wang, and J.M. Bishop, *Distinct pathways of genomic progression to benign and malignant tumors of the liver*. *Proc Natl Acad Sci U S A*, 2007. **104**(37): 14771-6.
 52. Colnot, S., T. Decaens, M. Niwa-Kawakita, C. Godard, G. Hamard, A. Kahn, M. Giovannini, and C. Perret, *Liver-targeted disruption of Apc in mice activates beta-catenin signaling and leads to hepatocellular carcinomas*. *Proc Natl Acad Sci U S A*, 2004. **101**(49): 17216-21.

53. Coqueret, O., *Linking cyclins to transcriptional control*. Gene, 2002. **299**(1-2): 35-55.
54. Massague, J., *G1 cell-cycle control and cancer*. Nature, 2004. **432**(7015): 298-306.
55. Fu, M., C. Wang, Z. Li, T. Sakamaki, and R.G. Pestell, *Minireview: Cyclin D1: normal and abnormal functions*. Endocrinology, 2004. **145**(12): 5439-47.
56. Ratineau, C., M.W. Petry, H. Mutoh, and A.B. Leiter, *Cyclin D1 represses the basic helix-loop-helix transcription factor, BETA2/NeuroD*. J Biol Chem, 2002. **277**(11): 8847-53.
57. Diehl, J.A., M. Cheng, M.F. Roussel, and C.J. Sherr, *Glycogen synthase kinase-3beta regulates cyclin D1 proteolysis and subcellular localization*. Genes Dev, 1998. **12**(22): 3499-511.
58. Arber, N., H. Hibshoosh, S.F. Moss, T. Sutter, Y. Zhang, M. Begg, S. Wang, I.B. Weinstein, and P.R. Holt, *Increased expression of cyclin D1 is an early event in multistage colorectal carcinogenesis*. Gastroenterology, 1996. **110**(3): 669-74.
59. Buckley, M.F., K.J. Sweeney, J.A. Hamilton, R.L. Sini, D.L. Manning, R.I. Nicholson, A. deFazio, C.K. Watts, E.A. Musgrove, and R.L. Sutherland, *Expression and amplification of cyclin genes in human breast cancer*. Oncogene, 1993. **8**(8): 2127-33.
60. Joo, M., Y.K. Kang, M.R. Kim, H.K. Lee, and J.J. Jang, *Cyclin D1 overexpression in hepatocellular carcinoma*. Liver, 2001. **21**(2): 89-95.
61. Ito, Y., N. Matsuura, M. Sakon, E. Miyoshi, K. Noda, T. Takeda, K. Umeshita, H. Nagano, S. Nakamori, K. Dono, M. Tsujimoto, M. Nakahara, K. Nakao, N. Taniguchi, and M. Monden, *Expression and prognostic roles of the G1-S modulators in hepatocellular carcinoma: p27 independently predicts the recurrence*. Hepatology, 1999. **30**(1): 90-9.
62. Azechi, H., N. Nishida, Y. Fukuda, T. Nishimura, M. Minata, H. Katsuma, M. Kuno, T. Ito, T. Komeda, R. Kita, R. Takahashi, and K. Nakao, *Disruption of the p16/cyclin D1/retinoblastoma protein pathway in the majority of human hepatocellular carcinomas*. Oncology, 2001. **60**(4): 346-54.
63. Zhang, Y.J., W. Jiang, C.J. Chen, C.S. Lee, S.M. Kahn, R.M. Santella, and I.B. Weinstein, *Amplification and overexpression of cyclin D1 in human hepatocellular carcinoma*. Biochem Biophys Res Commun, 1993. **196**(2): 1010-6.
64. Nishida, N., Y. Fukuda, T. Komeda, R. Kita, T. Sando, M. Furukawa, M. Amenomori, I. Shibagaki, K. Nakao, M. Ikenaga, and et al., *Amplification and overexpression of the cyclin D1 gene in aggressive human hepatocellular carcinoma*. Cancer Res, 1994. **54**(12): 3107-10.
65. Inagawa, S., M. Itabashi, S. Adachi, T. Kawamoto, M. Hori, J. Shimazaki, F. Yoshimi, and K. Fukao, *Expression and prognostic roles of beta-catenin in hepatocellular carcinoma: correlation with tumor progression and postoperative survival*. Clin Cancer Res, 2002. **8**(2): 450-6.
66. Zucman-Rossi, J., S. Benhamouche, C. Godard, S. Boyault, G. Grimber, C. Balabaud, A.S. Cunha, P. Bioulac-Sage, and C. Perret, *Differential effects of inactivated Axin1 and activated beta-catenin mutations in human hepatocellular carcinomas*. Oncogene, 2007. **26**(5): 774-80.

67. Ueta, T., M. Ikeguchi, Y. Hirooka, N. Kaibara, and T. Terada, *Beta-catenin and cyclin D1 expression in human hepatocellular carcinoma*. *Oncol Rep*, 2002. **9**(6): 1197-203.
68. Wang, T.C., R.D. Cardiff, L. Zukerberg, E. Lees, A. Arnold, and E.V. Schmidt, *Mammary hyperplasia and carcinoma in MMTV-cyclin D1 transgenic mice*. *Nature*, 1994. **369**(6482): 669-71.
69. Deane, N.G., M.A. Parker, R. Aramandla, L. Diehl, W.J. Lee, M.K. Washington, L.B. Nanney, Y. Shyr, and R.D. Beauchamp, *Hepatocellular carcinoma results from chronic cyclin D1 overexpression in transgenic mice*. *Cancer Res*, 2001. **61**(14): 5389-95.
70. Bodrug, S.E., B.J. Warner, M.L. Bath, G.J. Lindeman, A.W. Harris, and J.M. Adams, *Cyclin D1 transgene impedes lymphocyte maturation and collaborates in lymphomagenesis with the myc gene*. *EMBO J*, 1994. **13**(9): 2124-30.
71. Yu, Q., Y. Geng, and P. Sicinski, *Specific protection against breast cancers by cyclin D1 ablation*. *Nature*, 2001. **411**(6841): 1017-21.
72. Hulit, J., C. Wang, Z. Li, C. Albanese, M. Rao, D. Di Vizio, S. Shah, S.W. Byers, R. Mahmood, L.H. Augenlicht, R. Russell, and R.G. Pestell, *Cyclin D1 genetic heterozygosity regulates colonic epithelial cell differentiation and tumor number in ApcMin mice*. *Mol Cell Biol*, 2004. **24**(17): 7598-611.
73. Sharpless, N.E., *INK4a/ARF: a multifunctional tumor suppressor locus*. *Mutat Res*, 2005. **576**(1-2): 22-38.
74. Pavey, S., S. Conroy, T. Russell, and B. Gabrielli, *Ultraviolet radiation induces p16CDKN2A expression in human skin*. *Cancer Res*, 1999. **59**(17): 4185-9.
75. Zindy, F., C.M. Eischen, D.H. Randle, T. Kamijo, J.L. Cleveland, C.J. Sherr, and M.F. Roussel, *Myc signaling via the ARF tumor suppressor regulates p53-dependent apoptosis and immortalization*. *Genes Dev*, 1998. **12**(15): 2424-33.
76. Zhu, J., D. Woods, M. McMahon, and J.M. Bishop, *Senescence of human fibroblasts induced by oncogenic Raf*. *Genes Dev*, 1998. **12**(19): 2997-3007.
77. Lin, A.W. and S.W. Lowe, *Oncogenic ras activates the ARF-p53 pathway to suppress epithelial cell transformation*. *Proc Natl Acad Sci U S A*, 2001. **98**(9): 5025-30.
78. Vijayachandra, K., W. Higgins, J. Lee, and A. Glick, *Induction of p16ink4a and p19ARF by TGFbeta1 contributes to growth arrest and senescence response in mouse keratinocytes*. *Mol Carcinog*, 2009. **48**(3): 181-6.
79. Jacobs, J.J., K. Kieboom, S. Marino, R.A. DePinho, and M. van Lohuizen, *The oncogene and Polycomb-group gene bmi-1 regulates cell proliferation and senescence through the ink4a locus*. *Nature*, 1999. **397**(6715): 164-8.
80. Brummelkamp, T.R., R.M. Kortlever, M. Lingbeek, F. Trettel, M.E. MacDonald, M. van Lohuizen, and R. Bernards, *TBX-3, the gene mutated in Ulnar-Mammary Syndrome, is a negative regulator of p19ARF and inhibits senescence*. *J Biol Chem*, 2002. **277**(8): 6567-72.
81. Fulci, G., M. Labuhn, D. Maier, Y. Lachat, O. Hausmann, M.E. Hegi, R.C. Janzer, A. Merlo, and E.G. Van Meir, *p53 gene mutation and ink4a-arf deletion appear to be two mutually exclusive events in human glioblastoma*. *Oncogene*, 2000. **19**(33): 3816-22.

82. Burri, N., P. Shaw, H. Bouzourene, I. Sordat, B. Sordat, M. Gillet, D. Schorderet, F.T. Bosman, and P. Chaubert, *Methylation silencing and mutations of the p14ARF and p16INK4a genes in colon cancer*. Lab Invest, 2001. **81**(2): 217-29.
83. Tannapfel, A., F. Geissler, H. Witzigmann, J. Hauss, and C. Wittekind, *Analysis of liver allograft rejection related genes using cDNA-microarrays in liver allograft specimen*. Transplant Proc, 2001. **33**(7-8): 3283-4.
84. Matsuda, Y., *Molecular mechanism underlying the functional loss of cyclindependent kinase inhibitors p16 and p27 in hepatocellular carcinoma*. World J Gastroenterol, 2008. **14**(11): 1734-40.
85. Serrano, M., H. Lee, L. Chin, C. Cordon-Cardo, D. Beach, and R.A. DePinho, *Role of the INK4a locus in tumor suppression and cell mortality*. Cell, 1996. **85**(1): 27-37.
86. Kamijo, T., F. Zindy, M.F. Roussel, D.E. Quelle, J.R. Downing, R.A. Ashmun, G. Grosveld, and C.J. Sherr, *Tumor suppression at the mouse INK4a locus mediated by the alternative reading frame product p19ARF*. Cell, 1997. **91**(5): 649-59.
87. Krimpenfort, P., K.C. Quon, W.J. Mooi, A. Loonstra, and A. Berns, *Loss of p16Ink4a confers susceptibility to metastatic melanoma in mice*. Nature, 2001. **413**(6851): 83-6.
88. Serrano, M., *The INK4a/ARF locus in murine tumorigenesis*. Carcinogenesis, 2000. **21**(5): 865-9.
89. Sherr, C.J., *Parsing Ink4a/Arf: "pure" p16-null mice*. Cell, 2001. **106**(5): p. 531-4.
90. Carlson, C.M., J.L. Frandsen, N. Kirchhof, R.S. McIvor, and D.A. Largaespada, *Somatic integration of an oncogene-harboring Sleeping Beauty transposon models liver tumor development in the mouse*. Proc Natl Acad Sci U S A, 2005. **102**(47): 17059-64.

Chapter 2

Integration of genomic analysis and *in vivo* transfection to identify

Sprouty 2 as a candidate tumor suppressor in liver cancer¹

Introduction

Hepatocellular carcinoma (HCC), is among the top five causes of cancer-related deaths in the world [1]. Epidemiological and molecular genetic studies have demonstrated that hepatitis B (HBV) or hepatitis C (HCV) are major risk factors for HCC development, especially when accompanied by liver cirrhosis. Treatment options of HCC are limited, and the five year survival rate for HCC patients remains approximately at 7% in the US (<http://www.cancer.org/>).

Development of HCC is a multi-step process. However, the molecular genetics and signaling pathways underlying hepatic carcinogenesis are still poorly understood [2]. Molecular events frequently observed in HCC include mutations in *p53* and *β-catenin*, and aberrant CpG island methylation of *APC*, *E-cadherin*, and *p16*. Among them, mutations of *β-catenin* occur in 15 to 30% of human HCCs [3, 4]. These mutations tend to be point mutations or deletions at the N-terminus that lead to the stabilization of β -catenin. This stabilized β -catenin translocates into the nucleus and binds to the TCF transcriptional factors to activate downstream genes. Another important pathway involved in HCC pathogenesis is the Ras/ERK signaling pathway. Mouse models have

¹ This chapter was published in a manuscript entitled: Integration of genomic analysis and in vivo transfection to identify Sprouty2 as a candidate tumor suppressor in liver cancer; Lee, S.A., Ho, C, Roy, R, Kosinski, C, Patil, M.A., Tward A.D., Fridlyand, J, Chen X.; *Hepatology*, 2008, 47(4):1200-10. I thank the co-author and all other authors who contributed to this work. First co-authors, Susie Lee and Coral Ho contributed equally to this work.

demonstrated that activated Ras (RasV12) alone is not sufficient to induce HCC *in vivo* [5, 6]. However, activated Ras and β -catenin together can promote hepatic carcinogenesis in mice. There is ubiquitous activation of the Ras/ERK pathway in human HCC, but Ras family members are rarely mutated [7-9]. So how does Ras/ERK signaling become activated in human HCCs? One possible mechanism is the down-regulation of Spry2 in human HCCs [10].

Spry2 belongs to the Sprouty family of proteins, which are evolutionarily conserved inhibitors of RTKs [11-13]. Upon activation of RTKs, Spry2 becomes phosphorylated at a conserved N-terminal tyrosine residue (Y55), and binds to a series of intracellular signaling molecules, including Raf, Grb2 and Cbl. This ultimately leads to the down-regulation of ERK phosphorylation and RTK signaling. Mutation of this conserved N-terminal tyrosine of Spry2 (Spry2Y55F) generates a dominant-negative Spry2 protein that enhances growth factor dependent ERK signaling [14, 15]. In addition, Spry2 may interact with other signaling molecules, including caveolin, FRS2 and PTP1B to regulate other cellular processes, including cell growth and migration. Spry2 expression appears to be down-regulated in several tumor types, including HCC, breast, and prostate cancers [16, 17]. This is thought to lead to abnormal activation of Ras/ERK signaling in tumor cells and promote tumor development. However most current studies are limited to *in vitro* or xenograft analysis of Spry functions. It is clearly imperative to investigate whether blocking Spry activity contributes to tumorigenesis, using *in vivo* mouse models.

DNA microarray technology provides a powerful tool to identify genes that are associated with tumor cells by surveying global gene expression in an unbiased way.

Using this technology, we and several groups have reported the expression profiles of liver cancer cell lines and human samples [18-21]. Such genomic studies provide us with a large number of genes that are differentially expressed by tumor and non-tumor liver cells, as well as genes that may serve as prognostic markers. To characterize the molecular genetics of HCCs, we applied array based comparative genomic hybridization (CGH) to study the DNA copy number variations among HCC samples [22]. We identified recurrent DNA copy number gains at 1q, 8q and 20q, as well as DNA copy number losses at 1p, 4q, 8p, 13q, 16q and 17p. However, genes altered within these chromosomal regions remain largely unknown.

One of the major challenges during the post genome era is how to effectively study the functions of large numbers of genes identified from genomic studies, especially *in vivo*. The traditional methods using transgenic or knockout mice are both time consuming and expensive. Recently, we and another group reported that the combination of hydrodynamic injection and sleeping beauty mediated somatic gene integration is an efficient and flexible method to target long term gene expression in mouse hepatocytes and induce liver cancer *in vivo* [23, 24]. In this manuscript, we showed that this approach can be readily integrated into oncogenomic studies to study the functional significance of candidate genes' role in liver tumorigenesis *in vivo*.

Materials and Methods

Constructs and reagents

Mouse Spry2 cDNA was kindly provided by Dr. Gail Martin of UCSF; the hyperactive sleeping beauty construct (pCMV/SB) by Dr. Mark Kay of Stanford University; and

pCaggs-RasV12 by Dr. David Largaespada of University of Minnesota. The pT3-EF1 α vector containing duplicated inverted repeats (IR) for sleeping beauty mediated integration and EF1 α promoter (pT3-EF1 α) used for injected was described by Tward *et al.* Spry2Y55F was generated by site-directed mutagenesis using QuikChange (Stratagene, La Jolla, CA). Spry2Y55F (with a C-terminal V5 tag) and Δ N90- β -catenin were cloned into pT3-EF1 α via the Gateway PCR cloning strategy (Invitrogen, Carlsbad, CA). All plasmids were purified using the Endotoxin free Maxi prep kit (Sigma, St. Louis, MO) before injecting into mice.

Statistical analysis of microarray and array CGH data

The expression data of the 4863 cDNA clones used in the previous gene expression analysis were retrieved [25]. Mapping position for these cDNA clones was assigned using the NCBI genome assembly, accessed through the UCSC genome browser database. Of the 4863 cDNA clones, 4354 cDNA clones have chromosomal mapping information and were used for further analysis. The gene expression clones were mapped to the BAC clone within 1Mb of the gene expression clone which had the highest Pearson correlation between copy number and gene expression. Correlation was computed for each clone and a correlation coefficient of 0.35 was used as the cut-off to identify clones having positive correlation between copy number and gene expression. *P* values were obtained based on permutation analysis, and were corrected for multiple testing by controlling for the false discovery rate.

Hydrodynamic injection and mouse monitoring

The procedures were described as previously [24]. In brief, plasmids were diluted in 2 mL of 0.9% NaCl, filtered, and injected into the lateral tail vein of a six to eight week old FVB/N mice in 5 to 7 seconds. All mice were housed, fed, monitored and treated in accordance with protocols approved by the committee for animal research at the University of California, San Francisco.

Histology

Animals were euthanized and their livers were removed and rinsed in PBS. Samples collected from the livers were either frozen in dry ice for RNA and protein extraction or fixed overnight in freshly prepared cold 4% paraformaldehyde. Fixed tissue samples were embedded in paraffin. Five micron sections were placed on slides and stained with hematoxylin and eosin.

Immunohistochemistry

Paraffin tissue sections were dewaxed with xylene and hydrated in graded alcohols. Antigen retrieval was performed by boiling slides for 10 minutes in sodium-citrate buffer (10mM, pH 6.0). Following antigen retrieval, the slides were treated with primary antibodies at room temperature or overnight at 4°C. The slides then were incubated with biotinylated secondary antibody, followed by ABC immunodetection (Vector Laboratories, Burlingame, CA) using DAB to reveal antibody binding. Antibodies and dilutions were as follows: anti-phospho-ERK, 1:100 (Cell Signalling Technology, Beverly, MA); anti-V5, 1:1000 (Invitrogen); anti- β -catenin, 1:200 and anti-E-cadherin,

1:1000 (BD Bioscience, San Jose, CA); anti-PODXL1 1:200 (Applied Genomics, Burlingame, CA); and anti-Ki67, 1:150 (Lab vision, Fremont, CA).

Preparation of lysates and Western blotting

Liver tissues were lysed in M-PER mammalian protein extraction buffer (Pierce, Rockford, IL) plus proteinase inhibitor cocktail (Roche, Palo Alto, CA) and Halt phosphatase inhibitor cocktail (Pierce). Protein content of the lysate was quantified using the BCA protein assay (Pierce). Western blotting was performed as described [24]. Antibodies were used as follows: anti-phospho-ERK, 1:1000, anti-ERK, 1:1000 antiphospho-AKT, 1:1000, and anti-AKT 1:1000 (Cell Signaling Technology); anti-V5 1:5000 (Invitrogen); anti- β -catenin, 1:1000 (BD Bioscience); and anti-phospho-tyrosine, 1:1000 (kindly provided from Dr. Bishop of UCSF).

Real-time RT-PCR

Total RNA was extracted from frozen liver tissues using Trizol (Invitrogen) and digested with DNase I to remove any genomic DNA contamination. Sybergreen based real-time RT-PCR was carried out as described, and rRNA was used as an internal control [25]. Transcript quantification was performed in triplicate for every sample and reported relative to rRNA. The primer pairs are listed in Table 2.1.

Gene Name	Forward Primer	Reverse Primer
AFP	TCTGCTGGCACGCAAGAAG	TCGGCAGGTTCTGGAAACTG
CyclinB1	TTGTGTGCCCAAGAAGATGCT	GTACATCTCCTCATATTTGCTTGCA
CyclinD1	CGTGGCCTCTAAGATGAAGGA	CCTCGGGCCGGATAGAGTAG
P21	CACAGCGATATCCAGACATTCAG	CGGAACAGGTCGGACATCAC
Survivin	GCCACGCATCCCAGCTT	TTTGAAAATACCACTGTCTCCTTCTC
E-Cadherin	TGTGGGTCAGGAAATCACATCTT	CCAAATCCGATACGTGATCTTCT
CyclinE1	TGCCAAGATTGACAAGACTGTGA	TCCACGCATGCTGAATTATCA

Primers for real-time PCR of angiogenesis genes are the same as described.

Table 2.1 Primers used for real-time PCR analysis

Results

Contribution of genomic DNA copy number variation to global gene expression changes in human HCC samples

To determine whether genomic DNA copy number variations contribute to global gene expression pattern changes, we examined the correlation between gene expression values and the corresponding DNA copy number changes from 44 human HCC samples with both expression array and array CGH data. Of the 4354 cDNA clones analyzed, 747 cDNA clones (or 17.2% of total cDNA clones analyzed), representing approximately 542 unique genes, show statistical significant correlation between expression values and DNA copy number variations (correlation >0.35 and adjusted P value is 0.016 with FDR less than 7.9%. Data not shown). To illustrate whether DNA copy numbers influence gene expression, we compared the pairwise correlation of gene expression data with CGH values of BAC clones close to the locus where each gene is located at (diagonal), or CGH values of BAC clones located at other region of the genome. We found pairs of regions

along the diagonal have higher positive correlation (medium correlation approximately 0.135) than the off-diagonal pairs (medium correlation, approximately 0.005) (Fig. 2.1A). A heatmap of the pairwise correlation between gene expression and copy number also demonstrates the positive correlation along the diagonal (Fig. 2.1B).

Overall, our data confirm that genomic DNA copy number variations contribute to the regulation of regional gene expression profiles in human HCC samples.

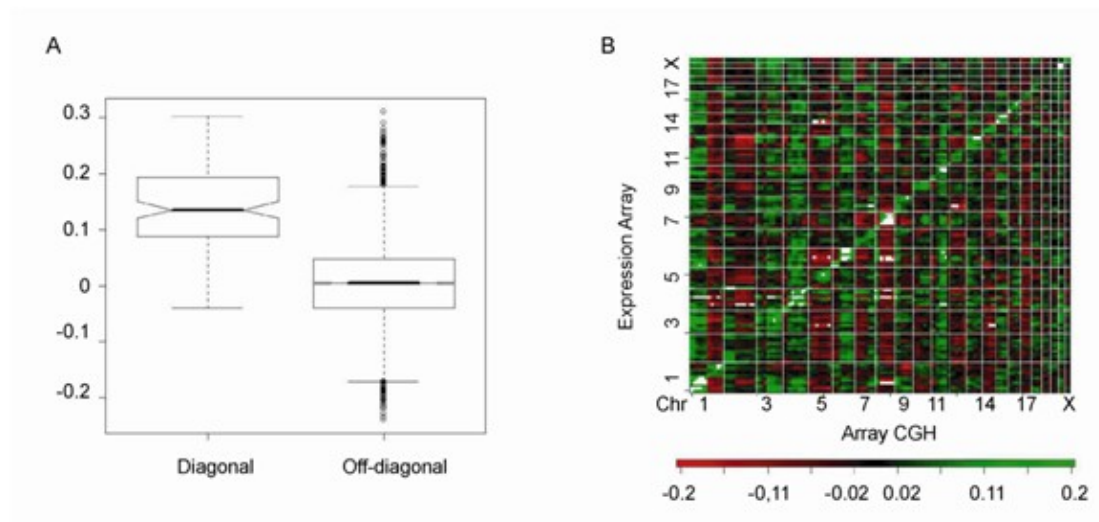


Figure 2.1 Correlation between DNA copy number variations and global gene expression patterns. Each chromosomal arm was divided into equal number of parts or bins of size 20Mb and then average pairwise Pearson correlation between gene expression and copy number was calculated for all pairs of binned regions. (A) Box plots of correlation between pairs along the diagonal (cDNA clones with surrounding BAC clones) and pairs off diagonal (cDNA clones with unrelated BAC clones). (B) Heatmap of the average correlation between gene expression and copy number.

Identification of candidate oncogenes or tumor suppressor genes for human HCCs

To pinpoint candidate oncogenes or tumor suppressor genes, we applied 2 criteria to the list of 747 cDNA clones. First, we searched for genes that showed consistent gain or loss in at least 8 (or approximately 20%) tumor samples. Second, we matched the gene list with the 1,946 cDNA clones that were identified to be differentially expressed among non-tumor liver and HCC samples in our previous study [25]. Thus, we narrowed our list to 134 cDNA clones, representing 113 unique genes (Table 2.2). Among these genes, 76 genes are up-regulated in HCC samples and are frequently amplified at the genomic DNA level, whereas the remaining 37 genes are down-regulated in HCC samples and are frequently deleted at the genomic DNA level. These 2 sets of genes represent potential candidate oncogenes or tumor suppressor genes, respectively, for HCC pathogenesis. One of the genes identified from our screening is Jab1/CSN5, a gene that we previously demonstrated to be highly expressed in HCCs and this is frequently amplified. This confirms the reliability of our genome-wide correlation analysis.

Genes that are up-regulated and are frequently amplified in human HCCs

Gene Symbol	Chr	Percentage Gained/Lost*	Fold of Up/Down-Regulation †	Gene Symbol	Chr	Percentage Gained/Lost*	Fold of Up/Down-Regulation †
SF3B4	1q	68.2	2.28	NEU1	6p	25.0	2.22
APH1A	1q	68.2	1.68	EHMT2	6p	25.0	2.32
KIAA0460	1q	65.9	2.01	RDBP	6p	25.0	1.98
PRUNE	1q	65.9	2.63	PFDN6	6p	20.5	1.66
SNX27	1q	65.9	2.07	CUTA	6p	20.5	1.62
ILF2	1q	65.9	1.94	XPO5	6p	18.2	1.80
NICE-3	1q	65.9	1.99	SLC29A1	6p	18.2	2.06
UBAP2L	1q	65.9	2.23	NUP205	7q	22.7	1.48
UBE2Q1	1q	65.9	1.96	TRIM24	7q	22.7	2.01
PYGO2	1q	65.9	2.44	MULK	7q	22.7	1.59
FLAD1	1q	65.9	2.56	KCNH2	7q	22.7	1.64
FDPS	1q	63.6	2.70	ATP6V1H	8q	29.5	1.53
DAP3	1q	63.6	2.03	ARMC1	8q	34.1	1.76
MEF2D	1q	63.6	1.64	CSN5/JAB1	8q	34.1	1.56
PRCC	1q	63.6	2.08	ARFGEF1	8q	34.1	1.52
NCSTN	1q	63.6	1.97	NCOA2	8q	36.4	1.87
B4GALT3	1q	63.6	1.70	RDH10	8q	36.4	1.64
TMCO1	1q	61.4	1.86	PLEKHF2	8q	45.5	1.76
BAT2D1	1q	61.4	1.72	PGCP	8q	45.5	1.63
SMG7	1q	56.8	1.78	MTDH	8q	45.5	1.64
UCHL5	1q	54.5	1.51	LAPTM4B	8q	50.0	2.58
JARID1B	1q	52.3	1.65	RPL30	8q	45.5	1.56
SNRPE	1q	50.0	2.09	YWHAZ	8q	50.0	1.85
NUCKS1	1q	47.7	1.58	ZNF706	8q	50.0	1.63
CD46	1q	47.7	1.74	EST	8q	47.7	2.06
LPGAT1	1q	50.0	1.88	FAM83H	8q	45.5	2.25
INTS7	1q	50.0	1.75	SIAHBP1	8q	45.5	1.64
PPP2R5A	1q	50.0	1.70	GPAA1	8q	45.5	1.77
CNIH4	1q	47.7	2.07	CYC1	8q	45.5	1.71
NUP133	1q	45.5	2.06	MAF1	8q	45.5	1.98
GNPAT	1q	45.5	1.91	LOC441383	8q	45.5	1.73
TOMM20	1q	45.5	1.62	CBX1	17q	18.2	1.66
ARID4B	1q	45.5	1.53	WDR68	17q	20.5	1.71
GGPS1	1q	45.5	2.09	NDRG3	20q	22.7	2.06
GMNN	6p	18.2	3.64	PPGB	20q	31.8	1.91
HIST1H2BK	6p	20.5	1.89	NCOA3	20q	29.5	1.65
CSNK2B	6p	25.0	1.49	ARFGEF2	20q	29.5	1.74
MSH5	6p	20.5	2.10	PRPF6	20q	25.0	1.71

Genes that are down-regulated and are frequently deleted in human HCCs

EPHA2	1p	18.2	3.57	C6orf75	6q	27.3	1.68
UGT2B7	4q	34.1	3.01	ECHDC1	6q	22.7	1.53
UGT2B4	4q	34.1	2.17	ENPP1	6q	22.7	1.50
SAS10	4q	34.1	1.62	SLC7A2	8p	38.6	3.21
CXCL1	4q	38.6	3.98	DOCK5	8p	36.4	1.54
CXCL2	4q	38.6	3.31	FGFR1	8p	27.3	1.88

ANTXR2	4q	47.7	2.18	PTS	11q	22.7	2.00
FAM13A1	4q	43.2	2.25	SPRY2	13q	40.9	2.31
BDH2	4q	45.5	3.24	PROZ	13q	29.5	3.00
CFI	4q	45.5	1.95	FLJ12874	14q	25.0	1.67
LARP2	4q	43.2	1.88	SGPP1	14q	27.3	1.63
TDO2	4q	38.6	2.99	C14orf4	14q	29.5	1.50
CTSO	4q	38.6	1.59	GSTZ1	14q	29.5	4.74
CBR4	4q	43.2	1.75	ACSM3	16p	20.5	3.01
KLKB1	4q	45.5	2.88	LOC57149	16p	20.5	1.72
FAM46A	6q	22.7	1.82	CDH1	16q	50.0	1.61
PNRC1	6q	25.0	2.04	EIF4A1	17p	59.1	1.56
BACH2	6q	25.0	1.67	SHMT1	17p	34.1	2.36
LOC619208	6q	22.7	1.95				

* Percentage of HCC samples with gain or loss at the specific gene loci.

† Average fold of up-regulation or down-regulation of the gene comparing HCC versus nontumor liver samples.

Table 2.2 Candidate Oncogenes and Tumor Suppressor Genes Identified by Correlating Expression Arrays with aCGH Data

Long term *in vivo* delivery of target genes in mouse hepatocytes and induction of HCC by hydrodynamic transfection

One of the genes identified from our genomic analysis to be down-regulated and frequently deleted is Spry2, a well-characterized RTK/Ras pathway inhibitor. Our *in vitro* studies showed that overexpression of Spry2 inhibits HCC cell growth (Fig. 2.2). The results are consistent with other *in vitro* studies that demonstrate Spry2 inhibits tumor cell proliferation. To determine whether Spry2 is a bona fide tumor suppressor for hepatic carcinogenesis, we investigated whether the loss of Spry2 activity contributes to liver cancer development using *in vivo* mouse models.

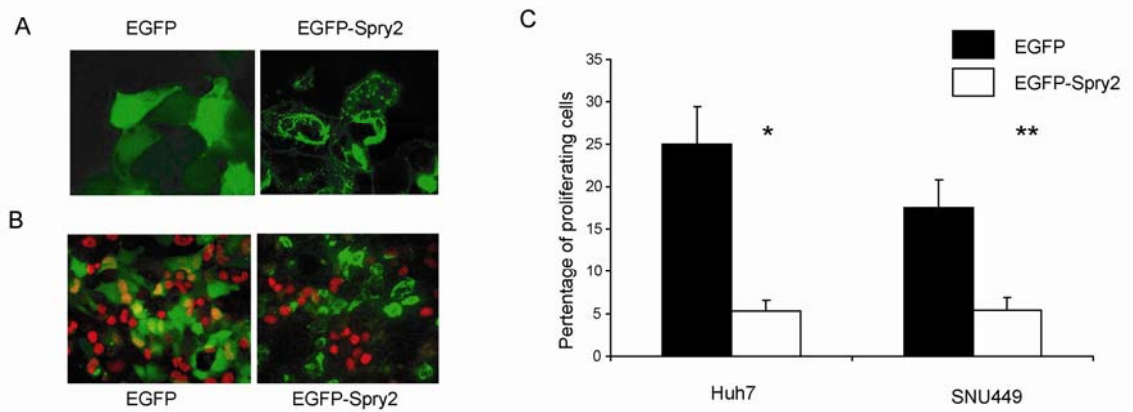


Figure 2.2 Overexpression of EGFP-Spry2 inhibits HCC cell growth *in vitro*. (A) Confocal microscopy analysis of cellular localization of EGFP and EGFPSpry2; (B) Representative images of reduced BrdU positive (red) in EGFP-Spry2 transfected (green) Huh7 cells (C) Quantitative measurement of reduced BrdU labeling in EGFP-Spry2 transfected Huh7 and SNU449 HCC cells. * p=0.01 and **p=0.002.

Because it has been shown that activated Ras and β -catenin cooperate to induce HCC development, we hypothesized that loss of Spry2 function together with activated β -catenin will also lead to hepatocarcinogenesis in mice. Spry2 knockout mice have been generated [26]. However, these Spry2 null mice have a shortened life span and most die within 1 to 2 months after birth, therefore are not suitable for this study. To address our hypothesis, we took an alternative approach in which we used hydrodynamic transfection with a transposable vector to stably express exogenous genes in mouse liver [27]. Most recently, we and another group showed that this method can be used to develop mouse models for liver cancer. We therefore generated a well-characterized dominant negative form of Spry2, Spry2Y55F (with a C-terminal V5 tag) to block endogenous Spry2 function, as well as a stabilized and activated β -catenin (Δ N90- β -catenin) for

hydrodynamic transfection (Fig. 2.3A). After injecting into mice, long term expression of each of the transfected genes can be detected in 5 to 10% of the hepatocytes by immunohistochemistry (Fig. 2.3B & C). The transfection efficiency is similar to what has been described and our previous experience.

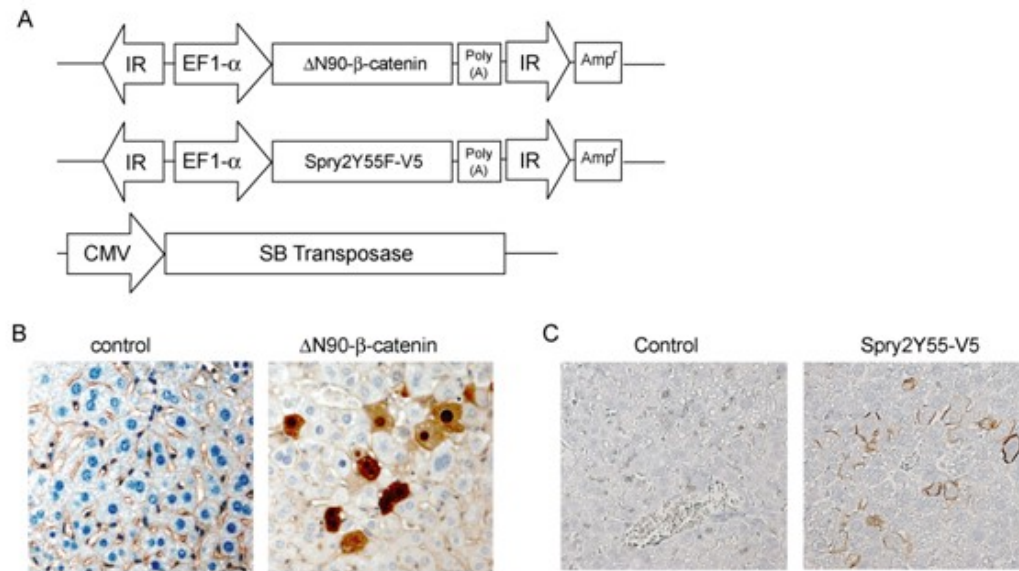


Figure 2.3 Hydrodynamic injection and sleeping beauty mediated somatic integration to stably express target gene in mouse hepatocytes. (A) Map of the constructs used in the study. IR: Inverted Repeats; EF1- α : EF1- α promoter; SB: sleeping beauty. (B) Immunohistochemical staining of β -catenin of control liver and Δ N90- β -catenin injected liver harvested 2 weeks post injection; (C) Immunohistochemical staining of control and Spry2Y55F-V5 injected liver harvested 22 weeks post injection using anti-V5 antibody.

To further prove the reliability of our approach, we determined whether RasV12 and Δ N90- β -catenin can cooperate to induce liver cancer in mice using hydrodynamic

transfection. Consistent with previous reports, we found that although none of the RasV12 or Δ N90- β -catenin injected mice developed liver tumors, coexpression of RasV12 and Δ N90- β -catenin induced liver cancer formation in 67% of the mice (8/12) at 18 weeks post injection (Fig. 2.4 and Table 2.3). In all cases, there were too many tumor nodules in the mouse liver to be counted.

Spry2Y55F cooperates with Δ N90- β -catenin signaling to induce liver cancer development in mice

To test our hypothesis that loss of Spry2 function cooperates with activated β -catenin to promote HCC development *in vivo*, we expressed Spry2Y55F, or Δ N90- β -catenin alone or Spry2Y55F plus Δ N90- β -catenin into mouse hepatocytes. All animals were sacrificed between 18 to 29 weeks post injection and liver tissues were examined grossly and histologically for tumors. Analysis of these samples revealed that half of the mice (7/14) co-expressing Spry2Y55F and Δ N90- β -catenin developed liver tumors (Fig. 2.4 and Table 2.3), whereas no tumors were observed in mice injected with Spry2Y55F or Δ N90- β -catenin alone (Fig. 2.4B). Interestingly, we noticed differences between tumors induced by RasV12/ Δ N90- β -catenin and Spry2Y55F/ Δ N90- β -catenin. In particular, mice co-expressing Spry2Y55F/ Δ N90- β -catenin have lower tumor incidence (1-4 nodules per mouse) in comparison with the numerous tumors found in RasV12/ Δ N90- β -catenin mice. Furthermore, while RasV12/ Δ N90- β -catenin can induce tumorigenesis as early as 13 weeks post injection, Spry2Y55F/ Δ N90- β -catenin requires longer latency (~24 weeks) for tumor development.

Injection	Code	Sex	Age (Weeks Old)	Weeks Post injection	Tumor*	Number of Tumors	Tumor Size (mm)†
Y55FSpry2 + Δ N90- β -catenin	YB-F1.1	F	26	18	N		
	YB-F1.2	F	26	18	N		
	YB-F1.3	F	32	24	Y	1	5
	YB-F1.4	F	32	24	N		
	YB-M1.1	M	29	22	N		
	YB-M1.2	M	34	27	Y	2	4, 18
	YB-M1.3	M	36	29	N		
	YB-M1.4	M	36	29	Y	4	3, 2, 15, 16
	YB-M1.5	M	36	29	Y	1	1
	YB-F2.1	F	37	29	N		
	YB-F2.2	F	37	29	N		
	YB-F2.3	F	37	29	Y	1	1
	YB-F2.4	F	37	29	Y	1	14
	YB-F2.5	F	37	29	Y	1	10
	RasV12 + Δ N90- β -catenin	RB-F1.1	F	21	13	N	
RB-F1.2		F	21	13	Y	TMTC	ND
RB-F1.3		F	21	13	Y	TMTC	ND
RB-F1.4		F	21	13	Y	TMTC	ND
RB-M1.1		M	21	14	Y	TMTC	ND
RB-M1.2		M	26	18	N		
RB-M1.3		M	26	18	N		
RB-M1.4		M	26	18	N		
RB-F2.1		F	26	18	Y	TMTC	ND
RB-F2.2		F	23	16	Y	TMTC	ND
RB-F2.3		F	23	16	Y	TMTC	ND
RB-F2.4		F	26	18	Y	TMTC	ND

Abbreviations: F, female; M, male; TMTC, too many to count.

* Tumor: Y, liver tumor in liver; N, no tumor nodules observed in liver.

† ND: Not determined. Because there are too many tumor nodules in the mouse liver, it is difficult to distinguish the boundary of each individual tumor nodule. Therefore the tumor size was not determined.

Table 2.3 Tumor Development in Mouse co-injected with RasV12/ Δ N90- β -catenin or Spry2Y55F/ Δ N90- β -catenin

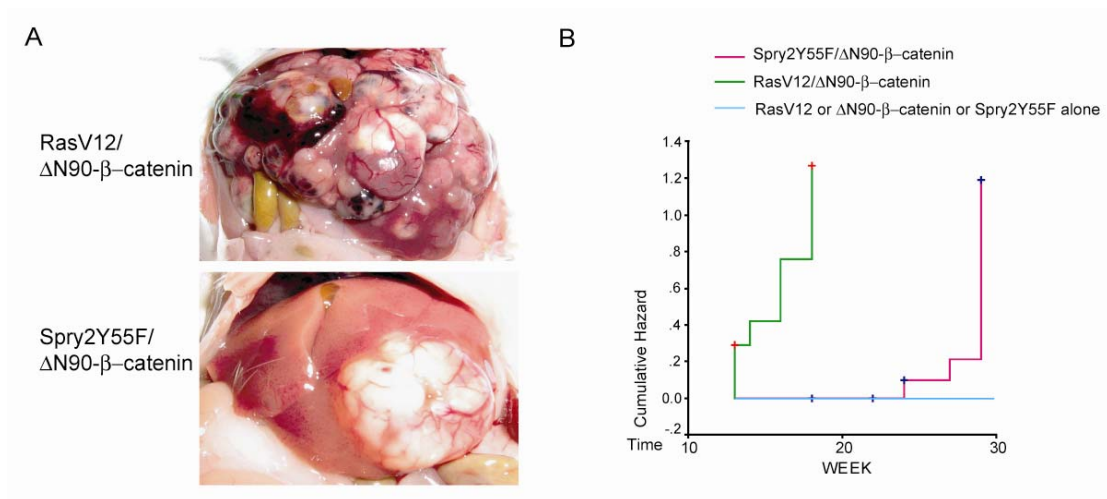


Figure 2.4 Co-expression of RasV12/ΔN90-β-catenin or Spry2Y55F/ΔN90-β-catenin induces liver cancer formation in mice. (A) Representative gross image of liver tumors from RasV12/ΔN90-β-catenin or Spry2Y55F/ΔN90-β-catenin co-injected mice. Note that there are numerous tumor nodules in RasV12/ΔN90-β-catenin mice and one tumor nodule in Spry2Y55F/ΔN90-β-catenin mice. (B) Tumor development incident curves in mice.

Histological examination of liver tumor samples from Spry2Y55F/ΔN90-β-catenin mice revealed that tumor cells morphologically appear to be of hepatocellular origin and the neoplastic cells display cytological atypia and frequent trabecular disorganization, which are consistent with HCC (Fig. 2.6A). Real-time RT-PCR analysis revealed the high expression of liver tumor marker α -fetoprotein (Fig. 2.5), further supporting that Spry2Y55F and ΔN90-β-catenin cooperate to induce HCC *in vivo*.

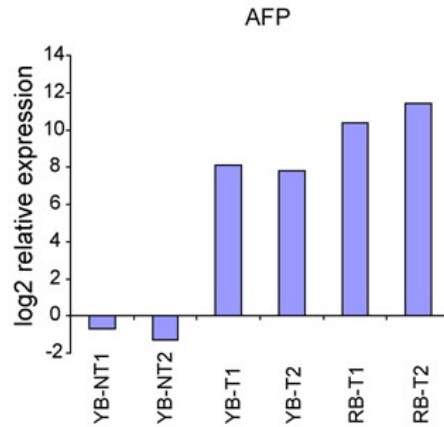


Figure 2.5 Overexpression of AFP in mouse tumor samples induced by Spry2Y55F/ Δ N90- β -catenin and RasV12/ Δ N90- β -catenin. Real-time RT-PCR analysis was performed in normal liver (n=2), non-tumor liver tissues (n=2), HCCs from Spry2Y55F/ Δ N90- β -catenin injected mice (n=2), as well as HCCs from RasV12/ Δ N90- β -catenin injected mice (n=2). Expression of each gene was calculated relative to rRNA and the expression values of two normal liver tissues were averaged, set to 1 and used to normalize all the rest of the samples. YB-NT: non-tumor liver tissues from Spry2Y55F/ Δ N90- β -catenin injected mice; YB-T: tumor liver tissues from Spry2Y55F/ Δ N90- β -catenin injected mice; and RB-T: tumor liver tissues from RasV12/ Δ N90- β -catenin injected mice

Co-expression of Spry2Y55F and Δ N90- β -catenin in mouse HCC samples

We next examined whether all tumor nodules co-express Spry2Y55F and Δ N90- β -catenin. Immunohistochemistry with anti- β -catenin and anti-V5 antibodies demonstrated that all tumor cells exhibit nuclear/cytoplasmic staining of β -catenin as well as membrane expression of Spry2Y55F (Fig. 2.6B and C). These results are

consistent with the Western blot analysis in which Spry2Y55-V5 and Δ N90- β -catenin are detected only in the HCC samples (Fig. 2.6D). Furthermore, the western blot depicts tumor tissues displaying a predominant lower band of β -catenin, which indicates that the activation of β -catenin in tumor cells is not due to random mutations of the endogenous β -catenin (which are typically point mutations) during tumorigenesis. Scattered Spry2Y55F or Δ N90- β -catenin-expressing cells are observed in the adjacent non-tumor liver by immunostaining (Fig. 2.6B and C), but their expression levels maybe too low to be detected by Western blotting. Together our analysis supports that all tumor cells coexpress Spry2Y55F and Δ N90- β -catenin and the expression of both Spry2Y55F and Δ N90- β -catenin promotes liver cancer formation *in vivo*.

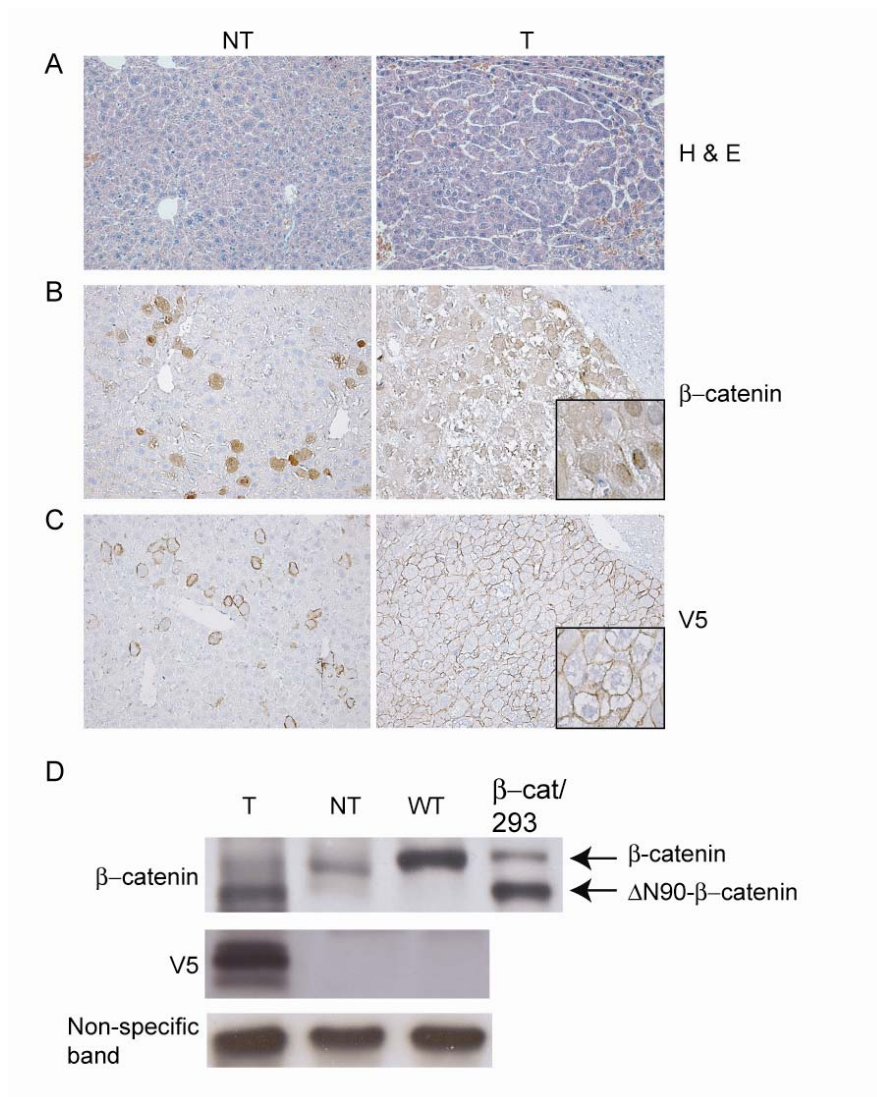


Figure 2.6 Co-expression of Spry2Y55F and Δ N90- β -catenin in mouse liver tumor cells. (A) H&E staining of liver samples from non-tumor liver tissues (NT) or HCC liver tissues (T); (B and C) immunohistochemical staining of β -catenin and V5, respectively (Original magnifications, x200). Insets are higher magnification (x400) images showing specific staining of β -catenin and Spry2Y55F in tumor cells; (D) Western blotting analysis of lysate from tumor (T), non-tumor (NT) or wildtype (WT) liver tissues using anti- β -catenin and V5 antibodies. For Δ N90- β -catenin detection, 239 cells transfected with pCMV/ Δ N90- β -catenin was used as positive control.

Activation of ERK pathway in mouse liver tumors

We next investigated the molecular mechanisms of Spry2Y55F in promoting HCC development by assaying the activity of key signaling components that may be downstream of Spry, including ERK and protein kinase Akt. Using immunohistochemical staining, we found that although non-tumor liver cells have no detectable levels of phospho-ERK, liver tumor cells display high levels of phospho-ERK (Fig. 2.7A). This observation is verified by western blotting (Fig. 2.7B). Total ERK expression remains unchanged in all samples. We observed no evidence of phospho-Akt expression in either non-tumor liver tissues or liver tumor tissues (Fig. 2.7C). These results indicate that Spry2Y55F up-regulates ERK signaling, but has no effect on the Akt pathway.

To validate that phospho-ERK signaling observed in tumor samples is due to ectopic Spry2Y55F expression, but not due to the activation of the upstream RTKs, we measured the expression levels of total phosphorylated tyrosine by Western blotting. We found the tumor showed no increase in the expression of total phosphorylated tyrosine (Fig. 2.7D), suggesting that there is no overall increased activation of RTKs in tumor cells.

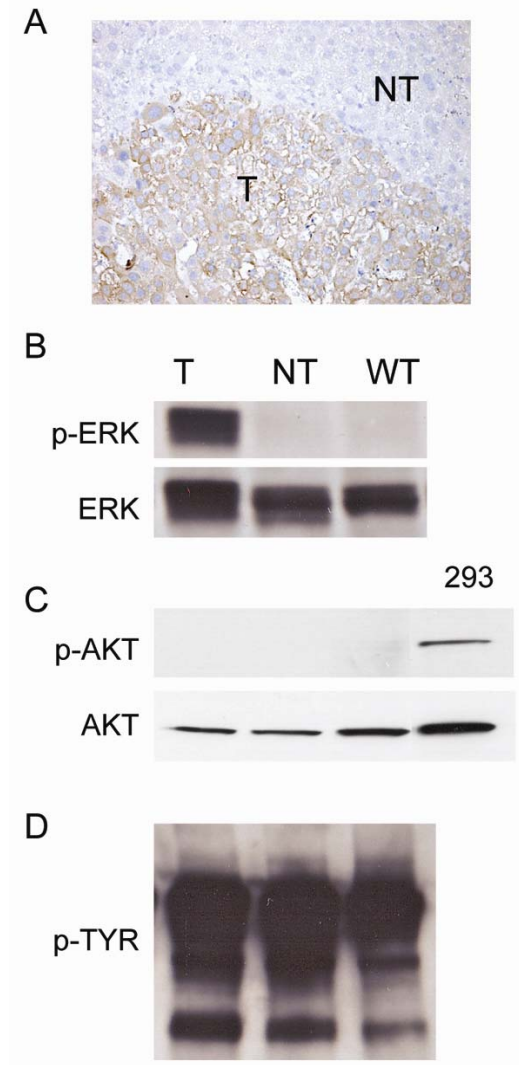


Figure 2.7 Activation of ERK, but not Akt in liver tumors induced by Spry2Y55F/ Δ N90- β -catenin. (A) Immunohistochemical staining of liver tumor cells (T) and surrounding non-tumor cells (NT) using anti-phospho-ERK antibody (Original magnifications, x200); (B-D) Western blot analysis of liver tissues from wildtype mice (WT); non-tumor liver (NT) and tumor (T) tissues for phospho-ERK, ERK, phospho-Akt, Akt and phospho-tyrosine. For the analysis of Akt status, 293 cells were used as positive control.

Molecular features of HCCs induced by Spry2Y55F and Δ N90- β -catenin

To determine whether liver tumors induced by Spry2Y55F/ Δ N90- β -catenin resemble a subset of human HCCs, we characterized the molecular features of these mouse liver tumor samples. Ki67 staining revealed that tumor cells are highly proliferative (Fig. 2.8A). Furthermore, these tumor cells show high expression of genes involved in cell cycle and cell proliferation, including cyclins B1, D1 and E1 (Fig. 2.9A-C). Expression of a Cdk inhibitor, p21Cip1, is also increased in the HCC samples (Fig. 2.9D). p21Cip may be induced as a feedback inhibitor in response to the abnormal cell proliferation and has been reported to be frequently up-regulated in human HCCs [28]. In addition, tumor cells express high levels of the anti-apoptotic protein, Survivin (Fig. 2.9E). Survivin has also been reported to be highly expressed in human HCC samples [29].

We next examined the expression of the cell-cell adhesion molecule, E-cadherin. In the normal liver, hepatocytes show weak staining of E-cadherin around the periportal area. However, liver tumor samples induced by Spry2Y55F/ Δ N90- β -catenin were found to have E-cadherin expression in virtually all neoplastic hepatocytes (Fig. 2.8B). The increased expression of E-cadherin in the tumor cell is also supported by RT-PCR analysis (Fig. 2.9F). The up-regulation of E-cadherin has been reported in multiple mouse liver cancer models, including HCCs induced by c-Myc/E2F1 or c-Myc/transforming growth factor- α [30].

One hallmark of HCC is the change in endothelial cells. In humans, while sinusoidal endothelial cells surrounding the normal hepatocytes do not express endothelial markers CD34 or podocalyxin kcl (PODXL1), the endothelial cells of HCC

stain positively for these markers [31]. This change in expression of these markers represents fundamental differences between endothelial cell structures in the normal liver and cancerous liver tissues. Using an antibody against PODXL1, we demonstrated that although the normal liver sinusoid endothelial cells does not express PODXL1, the endothelial cells in tumor tissues induced by Spry2Y55F/ Δ N90- β -catenin express this marker at high levels (Fig. 2.8C).

The change in expression of endothelial cell markers in the mouse HCC samples implies that angiogenesis occurs during tumor development. We next investigated whether there are changes of expression of genes involved in angiogenesis. Although we did not detect any changes in the expression levels for angiogenic factors vascular endothelial growth factor (VEGF), VEGF120, and Ang1, as well as their receptors FLT1 and FLK1 in tumor versus non-tumor liver tissue (data not shown), we observed an increase in the expression of Ang2 in Spry2Y55F/ Δ N90- β -catenin induced HCCs (Fig. 2.9G). The data suggest that the up-regulation of Ang2 may be a key factor in promoting angiogenesis in our mouse model. Interestingly, Ang2 overexpression has been observed in human HCCs and is associated with tumor invasion and increased tumor microvessel densities [32].

Although there are striking differences in tumor latency and incidence between the Spry2Y55F/ Δ N90- β -catenin and RasV12/ Δ N90- β -catenin injected mice, molecular features of both tumors are very similar, which include elevated expression of cyclins, Survivin, E-cadherin, p21Cip1, and Ang2 in all HCC samples examined. These observations support that the 2 sets of oncogenes share similar cellular responses and elicit similar molecular changes during hepatic carcinogenesis.

Altogether our studies support that HCCs induced by Spry2Y55F/ Δ N90- β -catenin mimic a subset of human HCCs, characterized by the deregulation of genes associated with cell proliferation, apoptosis and angiogenesis.

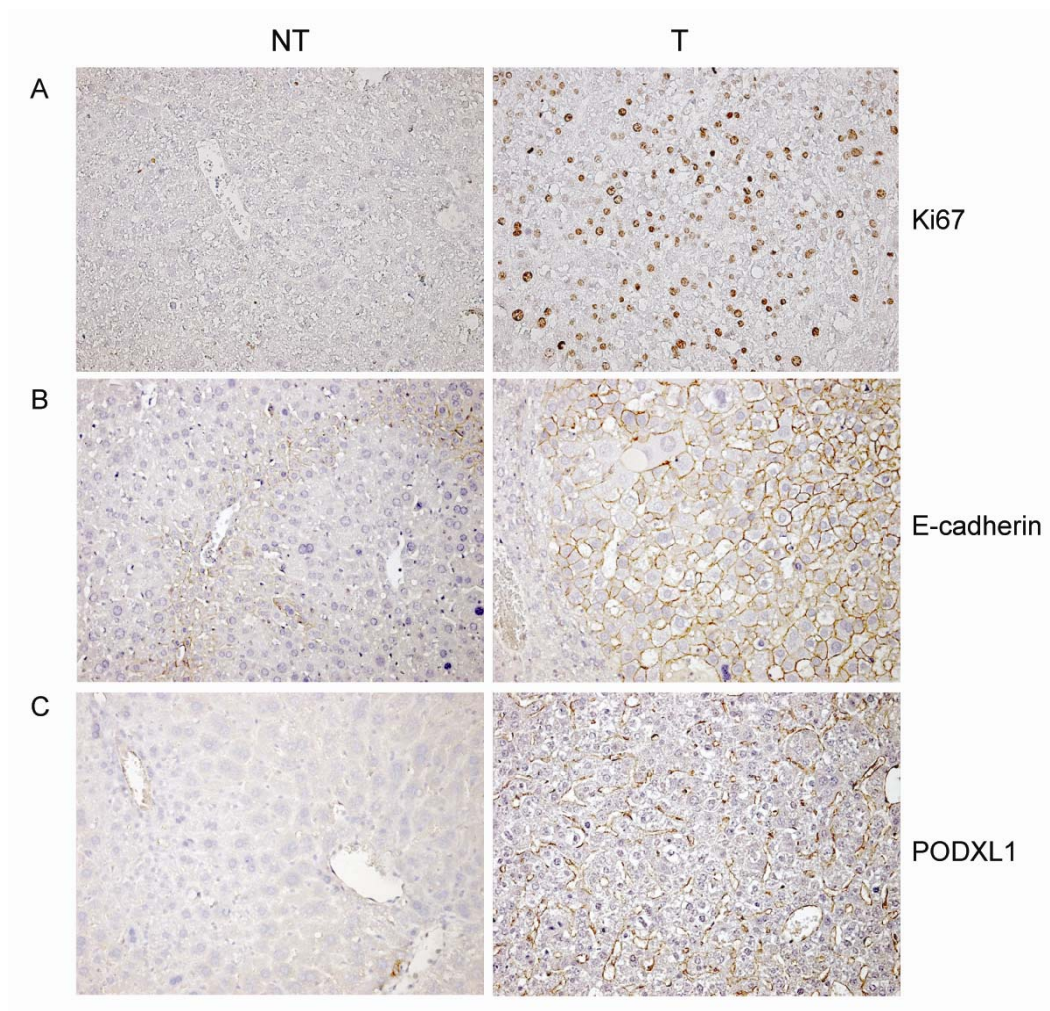


Figure 2.8 Immunohistochemical staining of liver tumor cells (T) and surrounding non-tumor cells (NT) for (A) Ki67, (B) E-cadherin and (C) PODXL1. Original magnifications, x200.

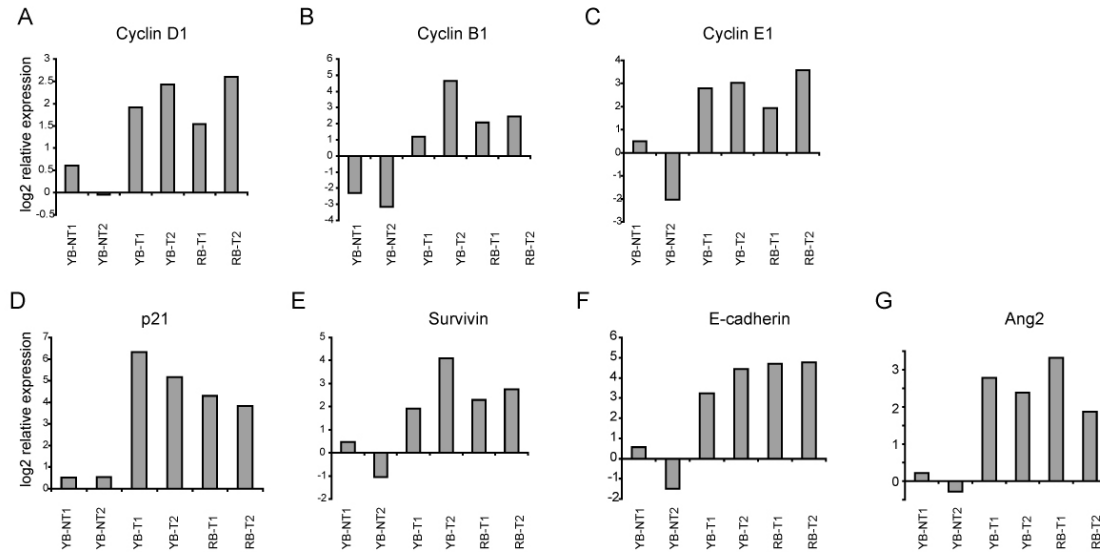


Figure 2.9 Real-time RT-PCR analysis of gene expression in normal liver (n=2), non-tumor liver tissues (n=2), HCCs from Spry2Y55F/ Δ N90- β -catenin injected mice (n=2), and RasV12/ Δ N90- β -catenin injected mice (n=2). Expression of each gene was calculated relative to rRNA and the expression values of two normal liver tissues were averaged, set to 1 and used to normalize all the rest of the samples. YB-NT: non-tumor liver tissues from Spry2Y55F/ Δ N90- β -catenin injected mice; YB-T: tumor liver tissues from Spry2Y55F/ Δ N90- β -catenin injected mice; and RB-T: tumor liver tissues from RasV12/ Δ N90- β -catenin injected mice.

Discussion

In this study, we identified 76 candidate oncogenes and 37 candidate tumor suppressor genes by correlating expression arrays and array CGH data. Although the majority of the genes are not well characterized, some of these genes have been implicated in tumorigenesis. For example, MEF2D was identified as a candidate oncogene in two murine retroviral insertional mutagenesis studies [33, 34]. Strikingly, 3

transcriptional coactivators are identified as candidate oncogenes in our study: transcriptional intermediary factor (TIF1), nuclear receptor coactivator 2 (NCOA2), and nuclear receptor coactivator 3 (NCOA3). These transcriptional coactivators are involved in regulating estrogen or androgen signaling. In humans, liver cancer occurs more frequently in males than females. The identification of co-activators involved in estrogen/androgen pathways as candidate oncogenes for human HCCs may provide clues to how these hormonal factors influence liver tumor development.

Although recent genomic studies have identified large numbers of genes whose expression levels are deregulated in human tumor samples, a major challenge remains as how to effectively study the functions of these genes in tumor development, especially *in vivo*. The most common method is to study the individual gene *in vitro* using tumor cell lines. These studies have limited value since tumor cell lines cultured *in vitro* have distinct properties from normal or neoplastic cells *in vivo*. In addition, these studies do not account for the tumor microenvironment. Mouse models are critical tools in dissecting signaling pathways and genetic events that are important for tumor development. However, the development of mouse models for human cancers is hindered by the fact that generating transgenic or knockout mouse lines are both expensive and time consuming. In this manuscript, we present evidence that hydrodynamic transfection is an efficient and flexible method which can be integrated into genomic studies for initial characterization of target genes' function *in vivo*. As an *in vivo* screening technique, this will allow us to efficiently and rapidly identify the meaningful genetic interactions during hepatic tumorigenesis.

Almost all reports of Spry2 in tumor pathogenesis are *in vitro* or xenograft studies. However, whether Spry2 can function as a tumor suppressor and whether loss of Spry2 expression is directly involved in tumor development *in vivo* remains unclear. In a recent study, it was found that the knockdown of Spry2 expression using small interfering RNA accelerates Ras-induced lung cancer development in mice [35]. In our study, we demonstrated that blocking Spry2 function using a dominant negative form of Spry2 cooperates with activated β -catenin signaling to induce liver cancer formation in mice. Our data provide compelling evidence that blocking Spry2 activity can directly participate in liver tumor development *in vivo*. Our results support a possible important mechanism of propagating Ras/ERK signaling in the absence of Ras mutations via loss of Spry2. Because Spry2 is down-regulated in other tumor types, this may also be a common approach for tumor cells to activate the ERK pathway.

Epidermal growth factor (EGFR) is a well characterized target of activated β -catenin in liver [36]. Consistently, EGFR mRNA expression is elevated in HCC samples from Spry2Y55F/ Δ N90- β -catenin mice (Fig. 2.10). Because no tumors were observed in mice injected with activated β -catenin alone, it suggests that up-regulation of EGFR by β -catenin is not sufficient to promote tumor development. However, when Spry2Y55F is co-expressed in these cells, Spry2Y55F may further propagate the increased EGFR signaling and eventually lead to tumor development. If this hypothesis is correct, one might expect that the tumors induced by Spry2Y55F/ Δ N90- β -catenin are dependent on EGFR expression. Further experiments treating Spry2Y55F/ Δ N90- β -catenin mice with EGFR inhibitors will assist to test this hypothesis.

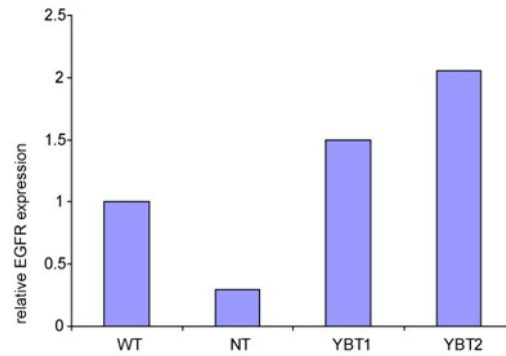


Figure 2.10 Real-time RT-PCR analysis for EGFR expression in wildtype liver (WT), non-tumor liver (NT) and Spry2^{Y55F/ΔN90}-β-catenin tumor samples (YBT1 or YBT2). Expression of each gene was calculated relative to rRNA and the expression value of the normal liver tissues was set to 1 and used to normalize all the rest of the samples.

Whether activation of Ras/ERK signaling is the major pathway that promotes HCC pathogenesis remains to be further investigated. Experiments using RNA interference to silence MEK or ERK expression *in vivo* or treatment of tumor cells with MEK inhibitors will clarify the roles of Ras/ERK in transducing Spry2 signaling in our mouse models. In addition, Spry2 has been shown to interact with other signaling molecules, including caveolin, FRS2 and PTP1B. Further biochemical characterization is required to determine the proteins that interact with Spry2 in mouse hepatocytes. Together these studies will provide novel insight into the molecular mechanisms of Spry2 in promoting HCC development.

There are multiple Spry family proteins expressed in liver. Our dominant negative Spry2 construct may interfere with functions of other Spry family members. To definitively test whether loss of Spry2 is sufficient to cooperate with activated β-catenin

to induce liver cancer, a conditional Spry2 knockout mice could be used in our system. This can be achieved by generating albumin-cre;Spry2^{flox/flox} mice and then expressing Δ N90- β -catenin in these mice. These experiments will provide additional information as to whether Spry2 functions as a tumor suppressor, or whether multiple Spry proteins have to be eliminated to cooperate with β -catenin to induce liver cancer *in vivo*.

References:

1. Parkin, D.M., *Global cancer statistics in the year 2000*. Lancet Oncol, 2001. **2**(9): 533-43.
2. Feitelson, M.A., B. Sun, N.L. Satiroglu Tufan, J. Liu, J. Pan, and Z. Lian, *Genetic mechanisms of hepatocarcinogenesis*. Oncogene, 2002. **21**(16): p. 2593-604.
3. Hsu, H.C., Y.M. Jeng, T.L. Mao, J.S. Chu, P.L. Lai, and S.Y. Peng, *Beta-catenin mutations are associated with a subset of low-stage hepatocellular carcinoma negative for hepatitis B virus and with favorable prognosis*. Am J Pathol, 2000. **157**(3): 763-70.
4. Taniguchi, K., L.R. Roberts, I.N. Aderca, X. Dong, C. Qian, L.M. Murphy, D.M. Nagorney, L.J. Burgart, P.C. Roche, D.I. Smith, J.A. Ross, and W. Liu, *Mutational spectrum of beta-catenin, AXIN1, and AXIN2 in hepatocellular carcinomas and hepatoblastomas*. Oncogene, 2002. **21**(31): 4863-71.
5. Harada, N., H. Miyoshi, N. Murai, H. Oshima, Y. Tamai, M. Oshima, and M.M. Taketo, *Lack of tumorigenesis in the mouse liver after adenovirus-mediated expression of a dominant stable mutant of beta-catenin*. Cancer Res, 2002. **62**(7): 1971-7.
6. Harada, N., H. Oshima, M. Katoh, Y. Tamai, M. Oshima, and M.M. Taketo, *Hepatocarcinogenesis in mice with beta-catenin and Ha-ras gene mutations*. Cancer Res, 2004. **64**(1): 48-54.
7. Calvisi, D.F., S. Ladu, A. Gorden, M. Farina, E.A. Conner, J.S. Lee, V.M. Factor, and S.S. Thorgeirsson, *Ubiquitous activation of Ras and Jak/Stat pathways in human HCC*. Gastroenterology, 2006. **130**(4): 1117-28.
8. Tsuda, H., S. Hirohashi, Y. Shimosato, Y. Ino, T. Yoshida, and M. Terada, *Low incidence of point mutation of c-Ki-ras and N-ras oncogenes in human hepatocellular carcinoma*. Jpn J Cancer Res, 1989. **80**(3): 196-9.
9. Challen, C., K. Guo, J.D. Collier, D. Cavanagh, and M.F. Bassendine, *Infrequent point mutations in codons 12 and 61 of ras oncogenes in human hepatocellular carcinomas*. J Hepatol, 1992. **14**(2-3): 342-6.
10. Fong, C.W., M.S. Chua, A.B. McKie, S.H. Ling, V. Mason, R. Li, P. Yusoff, T.L. Lo, H.Y. Leung, S.K. So, and G.R. Guy, *Sprouty 2, an inhibitor of mitogen-activated protein kinase signaling, is down-regulated in hepatocellular carcinoma*. Cancer Res, 2006. **66**(4): 2048-58.
11. Kim, H.J. and D. Bar-Sagi, *Modulation of signalling by Sprouty: a developing story*. Nat Rev Mol Cell Biol, 2004. **5**(6): 441-50.
12. Lo, T.L., C.W. Fong, P. Yusoff, A.B. McKie, M.S. Chua, H.Y. Leung, and G.R. Guy, *Sprouty and cancer: the first terms report*. Cancer Lett, 2006. **242**(2): 141-50.
13. Mason, J.M., D.J. Morrison, M.A. Basson, and J.D. Licht, *Sprouty proteins: multifaceted negative-feedback regulators of receptor tyrosine kinase signaling*. Trends Cell Biol, 2006. **16**(1): 45-54.
14. Sasaki, A., T. Taketomi, T. Wakioka, R. Kato, and A. Yoshimura, *Identification of a dominant negative mutant of Sprouty that potentiates fibroblast growth*

- factor- but not epidermal growth factor-induced ERK activation.* J Biol Chem, 2001. **276**(39): 36804-8.
15. Mason, J.M., D.J. Morrison, B. Bassit, M. Dimri, H. Band, J.D. Licht, and I. Gross, *Tyrosine phosphorylation of Sprouty proteins regulates their ability to inhibit growth factor signaling: a dual feedback loop.* Mol Biol Cell, 2004. **15**(5): 2176-88.
 16. Lo, T.L., P. Yusoff, C.W. Fong, K. Guo, B.J. McCaw, W.A. Phillips, H. Yang, E.S. Wong, H.F. Leong, Q. Zeng, T.C. Putti, and G.R. Guy, *The ras/mitogen-activated protein kinase pathway inhibitor and likely tumor suppressor proteins, sprouty 1 and sprouty 2 are deregulated in breast cancer.* Cancer Res, 2004. **64**(17): 6127-36.
 17. McKie, A.B., D.A. Douglas, S. Olijslagers, J. Graham, M.M. Omar, R. Heer, V.J. Gnanapragasam, C.N. Robson, and H.Y. Leung, *Epigenetic inactivation of the human sprouty2 (hSPRY2) homologue in prostate cancer.* Oncogene, 2005. **24**(13): 2166-74.
 18. Chen, X., S.T. Cheung, S. So, S.T. Fan, C. Barry, J. Higgins, K.M. Lai, J. Ji, S. Dudoit, I.O. Ng, M. Van De Rijn, D. Botstein, and P.O. Brown, *Gene expression patterns in human liver cancers.* Mol Biol Cell, 2002. **13**(6): 1929-39.
 19. Ye, Q.H., L.X. Qin, M. Forgues, P. He, J.W. Kim, A.C. Peng, R. Simon, Y. Li, A.I. Robles, Y. Chen, Z.C. Ma, Z.Q. Wu, S.L. Ye, Y.K. Liu, Z.Y. Tang, and X.W. Wang, *Predicting hepatitis B virus-positive metastatic hepatocellular carcinomas using gene expression profiling and supervised machine learning.* Nat Med, 2003. **9**(4): 416-23.
 20. Lee, J.S., I.S. Chu, J. Heo, D.F. Calvisi, Z. Sun, T. Roskams, A. Durnez, A.J. Demetris, and S.S. Thorgeirsson, *Classification and prediction of survival in hepatocellular carcinoma by gene expression profiling.* Hepatology, 2004. **40**(3): 667-76.
 21. Nam, S.W., J.Y. Park, A. Ramasamy, S. Shevade, A. Islam, P.M. Long, C.K. Park, S.E. Park, S.Y. Kim, S.H. Lee, W.S. Park, N.J. Yoo, E.T. Liu, L.D. Miller, and J.Y. Lee, *Molecular changes from dysplastic nodule to hepatocellular carcinoma through gene expression profiling.* Hepatology, 2005. **42**(4): 809-18.
 22. Patil, M.A., I. Gutgemann, J. Zhang, C. Ho, S.T. Cheung, D. Ginzinger, R. Li, K.J. Dykema, S. So, S.T. Fan, S. Kakar, K.A. Furge, R. Buttner, and X. Chen, *Array-based comparative genomic hybridization reveals recurrent chromosomal aberrations and Jab1 as a potential target for 8q gain in hepatocellular carcinoma.* Carcinogenesis, 2005. **26**(12): 2050-7.
 23. Carlson, C.M., J.L. Frandsen, N. Kirchhof, R.S. McIvor, and D.A. Largaespada, *Somatic integration of an oncogene-harboring Sleeping Beauty transposon models liver tumor development in the mouse.* Proc Natl Acad Sci U S A, 2005. **102**(47): 17059-64.
 24. Tward, A.D., K.D. Jones, S. Yant, S.T. Cheung, S.T. Fan, X. Chen, M.A. Kay, R. Wang, and J.M. Bishop, *Distinct pathways of genomic progression to benign and malignant tumors of the liver.* Proc Natl Acad Sci U S A, 2007.
 25. Patil, M.A., M.S. Chua, K.H. Pan, R. Lin, C.J. Lih, S.T. Cheung, C. Ho, R. Li, S.T. Fan, S.N. Cohen, X. Chen, and S. So, *An integrated data analysis approach*

- to characterize genes highly expressed in hepatocellular carcinoma. *Oncogene*, 2005. **24**(23): 3737-47.
26. Shim, K., G. Minowada, D.E. Coling, and G.R. Martin, *Sprouty2, a mouse deafness gene, regulates cell fate decisions in the auditory sensory epithelium by antagonizing FGF signaling*. *Dev Cell*, 2005. **8**(4): 553-64.
 27. Yant, S.R., L. Meuse, W. Chiu, Z. Ivics, Z. Izsvak, and M.A. Kay, *Somatic integration and long-term transgene expression in normal and haemophilic mice using a DNA transposon system*. *Nat Genet*, 2000. **25**(1): 35-41.
 28. Qin, L.F. and I.O. Ng, *Expression of p27(KIP1) and p21(WAF1/CIP1) in primary hepatocellular carcinoma: clinicopathologic correlation and survival analysis*. *Hum Pathol*, 2001. **32**(8): 778-84.
 29. Fields, A.C., G. Cotsonis, D. Sexton, R. Santoianni, and C. Cohen, *Survivin expression in hepatocellular carcinoma: correlation with proliferation, prognostic parameters, and outcome*. *Mod Pathol*, 2004. **17**(11): 1378-85.
 30. Calvisi, D.F., S. Ladu, E.A. Conner, V.M. Factor, and S.S. Thorgeirsson, *Disregulation of E-cadherin in transgenic mouse models of liver cancer*. *Lab Invest*, 2004. **84**(9): 1137-47.
 31. Chen, X., J. Higgins, S.T. Cheung, R. Li, V. Mason, K. Montgomery, S.T. Fan, M. Rijn Mv, and S. So, *Novel endothelial cell markers in hepatocellular carcinoma*. *Mod Pathol*, 2004.
 32. Mitsushashi, N., H. Shimizu, M. Ohtsuka, Y. Wakabayashi, H. Ito, F. Kimura, H. Yoshidome, A. Kato, Y. Nukui, and M. Miyazaki, *Angiopoietins and Tie-2 expression in angiogenesis and proliferation of human hepatocellular carcinoma*. *Hepatology*, 2003. **37**(5): 1105-13.
 33. Lund, A.H., G. Turner, A. Trubetskoy, E. Verhoeven, E. Wientjens, D. Hulsman, R. Russell, R.A. DePinho, J. Lenz, and M. van Lohuizen, *Genome-wide retroviral insertional tagging of genes involved in cancer in Cdkn2a-deficient mice*. *Nat Genet*, 2002. **32**(1): 160-5.
 34. Suzuki, T., H. Shen, K. Akagi, H.C. Morse, J.D. Malley, D.Q. Naiman, N.A. Jenkins, and N.G. Copeland, *New genes involved in cancer identified by retroviral tagging*. *Nat Genet*, 2002. **32**(1): 166-74.
 35. Shaw, A.T., A. Meissner, J.A. Dowdle, D. Crowley, M. Magendantz, C. Ouyang, T. Parisi, J. Rajagopal, L.J. Blank, R.T. Bronson, J.R. Stone, D.A. Tuveson, R. Jaenisch, and T. Jacks, *Sprouty-2 regulates oncogenic K-ras in lung development and tumorigenesis*. *Genes Dev*, 2007. **21**(6): 694-707.
 36. Tan, X., U. Apte, A. Micsenyi, E. Kotsagrellos, J.H. Luo, S. Ranganathan, D.K. Monga, A. Bell, G.K. Michalopoulos, and S.P. Monga, *Epidermal growth factor receptor: a novel target of the Wnt/beta-catenin pathway in liver*. *Gastroenterology*, 2005. **129**(1): 285-302.

Chapter 3

Suppression of Spry2 promotes unrestrained activation of c-Met signaling during hepatocarcinogenesis

Introduction

Hepatocarcinogenesis is considered to be a multiphase process involving the deregulation of various genetic pathways [1]. In particular, activation of the Ras/MAPK pathway has been detected in all human HCC samples [2]. The importance of Ras/MAPK signaling in hepatocarcinogenesis is further supported by the approval of Raf inhibitor Sorafenib, which has been found to significantly prolong the survival of HCC patients [3]. Ras/MAPK signaling is triggered when growth factors bind to receptor tyrosine kinases (RTK), recruit and activate guanine nucleotide exchange factors such as Sos, which then induces the formation of Ras-GTP (Ch.1, Fig. 1.1). Activated Ras in turn stimulates the Raf-MEK-MAPK cascade, which leads to the regulation of various cellular responses, including proliferation, survival, and differentiation. Mutations of Ras or its downstream effector, B-Raf, are the most common targets for somatic gain-of-function mutations in human cancers [4]. However, Ras family members and B-Raf are rarely mutated in human HCC [5, 6]. Thus, it remains unclear how Ras/MAPK signaling becomes activated during hepatocarcinogenesis in the presence of wild-type Ras and B-Raf. Over-expression of the protooncogene c-Met and loss of Spry2 have both been implicated as possible mechanisms leading to unconstrained activation of the Ras/MAPK pathway in the absence of Ras mutations [1, 2].

The *c-Met* protooncogene encodes the receptor tyrosine kinase for hepatocyte growth factor (HGF) and scatter factor (SF) [7, 8]. This multifunctional kinase has been shown to be involved in a variety of cellular responses, including proliferation, survival, migration, tumor development, and metastasis [9, 10]. Activation of c-Met signaling occurs in multiple tumor types, including human HCC. Indeed, c-Met mRNA and protein levels are frequently over-expressed in human liver cancer, and c-Met upregulation is associated with patients' poor prognosis [11, 12]. Accordingly, genomic studies identified a c-Met regulated gene expression signature that defines an aggressive biologic phenotype in human HCC [13]. Furthermore, over-expression of human c-Met in mouse hepatocytes promotes liver malignant transformation [14].

Sprouty (Spry)/Sprouty-related EVH1 domain containing protein (Spred) family proteins are evolutionarily conserved inhibitors of RTKs [15, 16]. Mounting evidence indicates that Spry proteins can be induced by the Ras/MAPK signaling pathway, and function as negative inhibitors of Ras/MAPK activation by disrupting growth-factor-receptor bound-2 (GRB2)-SOS complex and/or inhibiting Raf [15, 16]. There are four mammalian homologs for Spry (Spry1 to 4). Among them, Spry2 has been found to be down-regulated in multiple tumor types [17]. Both *in vitro* and *in vivo* studies have suggested that loss of Spry2 expression may contribute to abnormal activation of Ras/MAPK signaling in cancer [17]. Previous reports show that Spry2 expression is frequently downregulated in human HCC, presumably due to promoter hypermethylation and loss of DNA copy number at 13q31, and that its inactivation triggers elevated MAPK signaling in HCC.[17] In mouse models, it was recently demonstrated that inactivation of Spry2 using the dominant negative Spry2 (Spry2Y55F) construct cooperates with

activated β -catenin to promote hepatocarcinogenesis *in vivo*, strengthening the hypothesis that Spry2 is a *bona fide* tumor suppressor in the liver [18].

Many studies on the functional role of Spry2 have focused on its regulation over FGF and EGF signaling so far, while the biochemical and genetic interactions between c-Met activation and Spry2 downregulation have been poorly characterized. To date, only one paper has reported that over-expression of Spry2 inhibits HGF-mediated cell growth in SK-LMS-1 human leiomyosarcoma cells [19].

Current clinical data indicates that Spry2 function is impaired in human HCC via multiple mechanisms, including gene promoter hypermethylation, loss of heterozygosity, and inactivation via TESK1, substantiating the assumption that Spry2 is a key oncosuppressor in liver cancer (Calvisi et al, unpublished data). Furthermore, the overexpression of Spry2 inhibits c-Met-induced HCC cell proliferation, whereas c-Met signaling is activated following Spry2 silencing (Calvisi et al, unpublished data). However, the relationship between Spry2 and c-Met during hepatocarcinogenesis has not been examined *in vivo*. In this chapter, we demonstrate that a dominant negative Spry2 form (Spry2Y55F) cooperates with c-Met to induce hepatocarcinogenesis in Ink4A/Arf null mice by promoting proliferation and angiogenesis. Furthermore, the co-expression of Spry2Y55F and c-Met resulted in the over-activation of both Ras/MAPK and Akt signaling during liver tumorigenesis. Thus, our study provides substantial *in vivo* evidence that disruption of Spry2 and c-Met balance might be a dominant oncogenic event responsible for uncontrolled activation of the Ras/MAPK and AKT cascades in the presence of wild-type Ras genes in liver cancer.

Materials and Methods

Hydrodynamic Injection and Mice Monitoring

Ink4A/Arf ^{-/-} mice were obtained from Mouse Model of Human Cancer Consortium (NCI). Hydrodynamic injection was performed as described [20]. The constructs used for injections, pT3-EF1 α -hMet and pCMV/SB, were as previously described [20]. Spry2Y55F was generated as described [18]. Spry2Y55F (with C-terminal HA tag) was then cloned into pT3-EF1 α via the Gateway PCR cloning strategy (Invitrogen). All injected mice were monitored weekly and sacrificed at appropriate time points or when they developed a visibly enlarged abdomen or became moribund. All mice were housed, fed, and treated in accordance with protocols approved by the committee for animal research at the University of California, San Francisco (UCSF).

Histology, Immunohistochemistry and Immunofluorescence

Livers were fixed in 4% paraformaldehyde and then processed for paraffin embedding. Sections were done at 5 μ m in thickness. Immunohistochemistry was performed with anti-HA (1:100, Santa Cruz Biotechnology), anti-V5 (1:1000, Invitrogen), anti-Ki67 (1:150, Lab Vision), rabbit polyclonal anti-PCNA (1:5000, Santa Cruz Biotechnology), anti-PODXL1 (1:800, Applied Genomics), and anti-p-S6 Ribosomal Protein (1:75, Cell Signaling) antibodies as described. Immunofluorescence for anti-HA and anti-V5 antibodies were done using the same dilutions, followed by incubation with either FITC (Jackson ImmunoResearch) or Alexa 594 (Molecular Probes) labeled secondary antibodies.

Proliferation and apoptotic indices

Proliferation and apoptotic indices were determined in Spry2Y55F/c-Met tumors (hepatocellular adenoma and hepatocellular carcinoma) from Ink4A/ARF null mice by counting PCNA-positive cells and apoptotic figures stained with the ApoTag peroxidase in situ apoptosis kit (Millipore, Billerica, MA), respectively, on 3000 hepatocytes.

Real Time RT-PCR and Western Blot analysis

Syber-green-based real time reverse transcription (RT) PCR was carried out as described [18]. Ribosomal RNA was used as internal control. For western blotting and immunoprecipitation, samples were sonicated in lysis buffer containing M-PER Mammalian Protein Extraction Reagent (Thermo), proteinase inhibitor (Roche), and phosphatase inhibitor (Pierce). The following antibodies were used: anti-HA (1:1000) (Santa Cruz Biotechnology), anti-V5 (1:5000) (Invitrogen), anti-phospho-c-Met (1:1000), anti-phospho-ERK (1:1000), anti-ERK (1:1000), anti-phospho-Akt (1:1000), anti-Akt (1:1000), anti-phospho-PTEN (1:1000), anti-PTEN (1:1000), and anti- β -actin (1:10000, Sigma).

Statistical Analysis

Student's *t* and Tukey-Kramer tests were used to evaluate statistical significance. Values of $P < 0.05$ were considered significant. Data are expressed as means \pm SD.

Results

Loss of Spry2 Activity and Over-expression of c-Met Cooperate to Promote Hepatocarcinogenesis in Ink4A/ARF null mice

In order to determine whether the activation of c-Met and loss of Spry2 function has a synergistic role in hepatocarcinogenesis, we developed a mouse model to address this. However, we realized that activation of c-Met and loss of Spry2 activity may not be able to induce liver tumor formation *in vivo*, since we and others have demonstrated that activation of the Ras/MAPK signaling alone is not sufficient for hepatocarcinogenesis using mouse models [18, 21]. Therefore, we chose to add another genetic alteration in our model, namely the loss of the Ink4A/Arf locus. Indeed, preliminary data from our laboratory indicate that over-expression of an activated form of N-Ras drives hepatocarcinogenesis in Ink4A/Arf null mice (Lee SA, unpublished data). Additionally, epigenetic and genetic alternations of either Ink4A or Arf genes have been implicated in human HCC [22]. Using *in vivo* transfection method that combines hydrodynamic injection and sleeping beauty mediate somatic integration, we stably expressed c-Met (V5-tagged) and/or a dominant negative mutant form of Spry2, Spry2Y55F (HA-tagged) into the hepatocytes of Ink4A/ARF null mice and monitored for liver tumor development.

Expression of Spry2Y55F alone did not induce histological abnormalities in the mouse liver, whereas over-expression of only c-Met resulted in the formation of clear-cell foci of altered hepatocytes (FAH), proven to be preneoplastic in various rodent models of hepatocarcinogenesis (Fig. 3.1) [22]. These lesions were often located in zone 3 of the liver acinus (Fig. 3.1B,C-E) and showed an excess in glycogen storage (Fig. 3.1A,D), resulting in enlargement and clear-cell phenotype of hepatocytes in H&E

staining (Fig. 3.1B,C). Moreover, these lesions were proliferating, as indicated by the expression of proliferation-associated marker PCNA (Fig. 3.1E) and the detection of occasional mitotic figures. However, no HCC or hepatocellular adenomas (HCA) were observed in c-Met over-expressing mice.

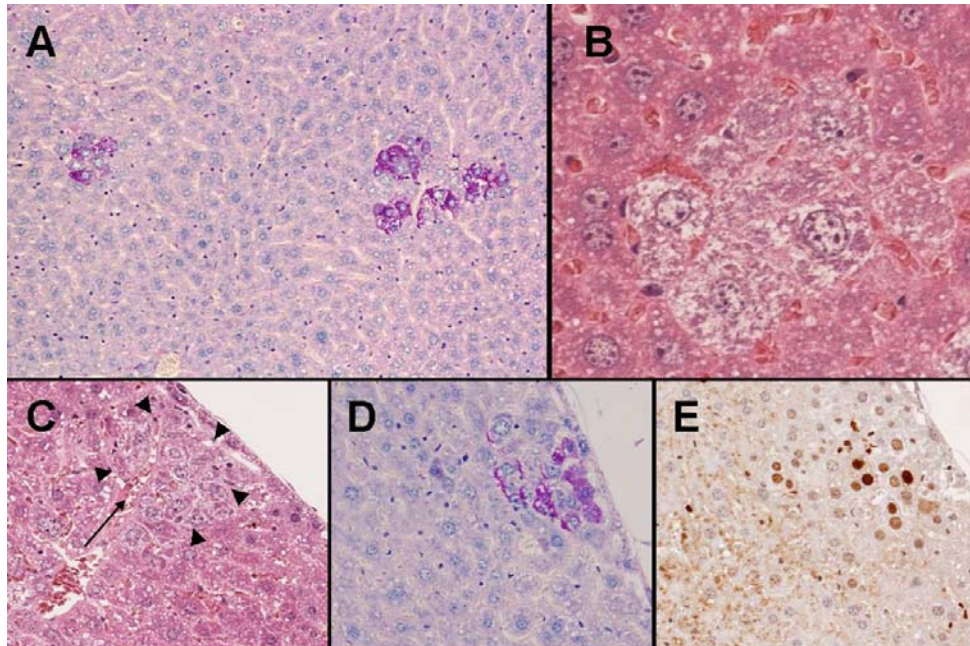


Figure 3.1. Over-expression of c-Met induces preneoplastic lesions. (A) Several small preneoplastic lesions are observed with the PAS reaction in c-Met overexpressing mice. The group of altered hepatocytes in the right part of the picture is located around a small hepatic vein (arrow). (B) The hepatocytes following c-Met overexpression are enlarged due to an excess in glycogen storage. (C-E) Serial sections of a small clear-cell focus of altered hepatocytes in a c-Met over-expressing mouse, as detected by H&E stain (C) and PAS reaction (D), located beneath the liver surface. Again, note the close vicinity to a hepatic vein in the H&E stain. (E) Strong proliferative activity in c-Met induced preneoplastic lesions is shown by the PCNA stain

In striking contrast, approximately 53% of co-transfected c-Met/Spry2Y55F mice in the Ink4A/Arf null background developed numerous liver tumors between 14 and 20 weeks post injection (Fig. 3.2A-C). The tumors varied in size and histopathologic features, and were classified as HCA or HCC according to the criteria by Frith and Ward (Fig 3.2C and D) [22]. Liver tumors were characterized by the presence of a trabecular or pseudo-glandular pattern. Small tumors usually consisted exclusively of the clear-cell phenotype (Fig 3.2C), thus retaining the morphology of the preneoplastic lesions in the model with exclusive over-expression of c-met (Fig. 3.1). However, with increasing tumor size, particularly in large HCCs, some tumor cells lost their glycogen content and transformed into mitotically more active glycogen-poor, basophilic hepatocytes, recapitulating the usual sequence of morphological progression in the clear-cell type of rodent hepatocarcinogenesis (Fig. 3.2D) [22]. Corresponding to their hepatocellular origin, the tumors showed typical high RNA expression levels of α -feto-protein (AFP; Fig 3.2E). The two co-transfected genes, c-Met and Spry2Y55F, were detected in the tumors by immunohistochemistry, immunofluorescence and Western blotting with antibodies against their respective epitope tags (Fig. 3.3). Sporadic expression of the injected genes was observed in the surrounding non-tumor liver as well (Fig 3.3A). In addition to validating the expression of the transfected genes, Western blotting also detected the presence of activated (phosphorylated) c-Met in the tumor cells (Fig 3.3C). Altogether, our observations indicate that co-expression of Spry2Y55F and c-Met promotes hepatocarcinogenesis in Ink4A/Arf null mice.

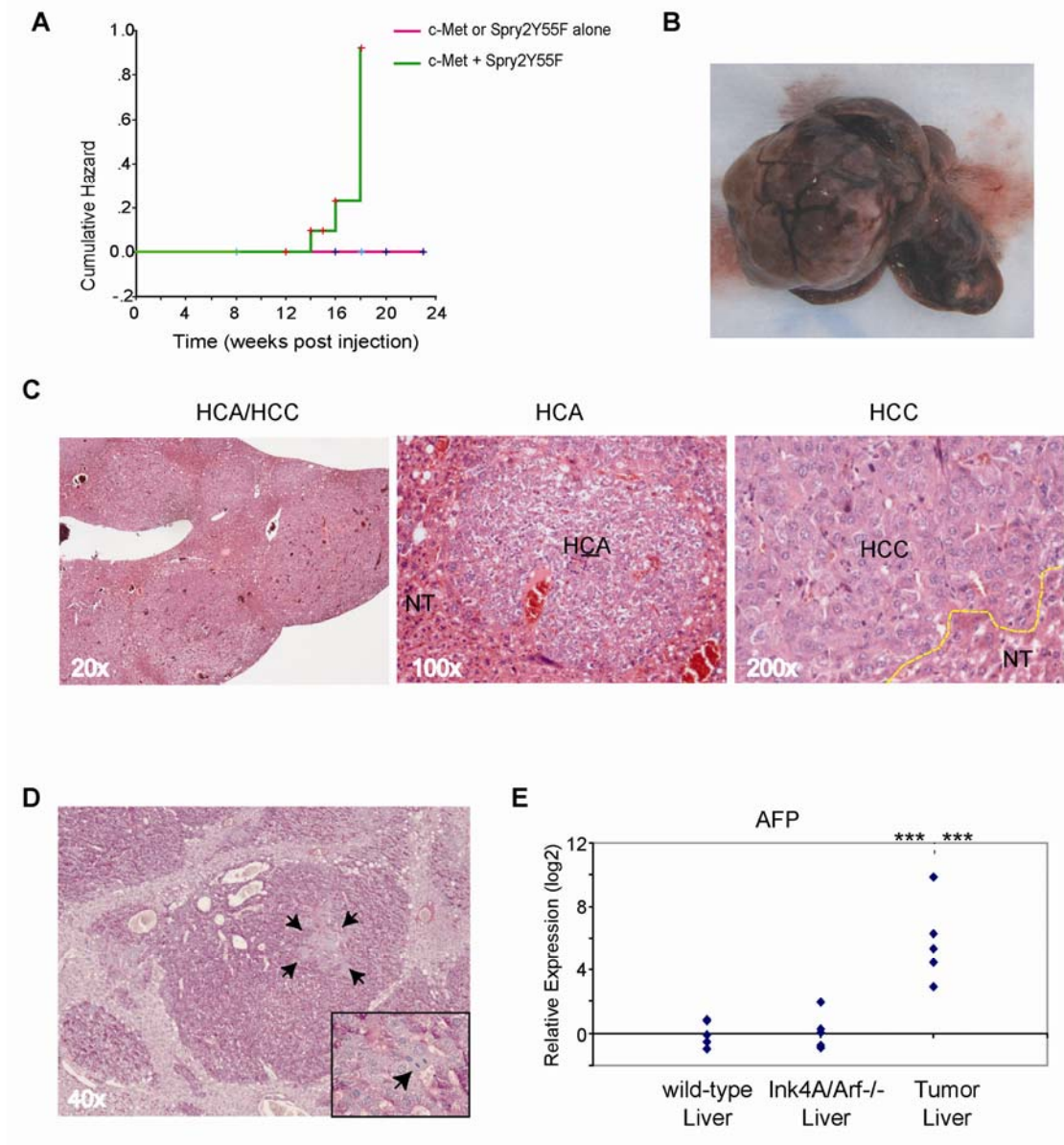


Figure 3.2. Over-expression of c-Met and dominant-negative form of Spry2 (Spry2Y55F) cooperates with the loss of Ink4A/Arf to induce liver carcinogenesis *in vivo*. (A) Cumulative hazard curve, which represents the relative probability of tumor development in mice injected with c-Met, Spry2Y55F, or both. (B) Gross image of a large liver tumor from c-Met/Spry2Y55F injected Ink4A/Arf null mice. (C) Histology of liver tumors induced by c-Met/Spry2Y55F; Left, H&E staining overview of the liver at

low magnification, showing numerous tumors of different sizes, corresponding to several HCA and HCC. Middle and right: H&E staining of sections from a small clear-cell HCA (middle) and part of a HCC (right) of c-Met/Spry2Y55F tumors. (D) PAS staining of this HCC shows a subpopulation of PAS-negative basophilic (glycogen-poor) tumor cells - marked by arrowheads – that transformed from the surrounding PAS-positive glycogen-rich hepatocytes. These basophilic cells are generally more mitotically active (Inset with mitotic figure). (E) Real-time PCR analysis of AFP expression in normal wild-type liver (n=5), Ink4A/Arf null liver (n=5), and liver tumors (n=5). Stars on the top represent P values comparing tumor samples vs. wild-type liver (left) and tumor samples vs. Ink4A/Arf null liver (right) using the Tukey-Kramer Multiple Comparisons Test. ***: P <0.001.

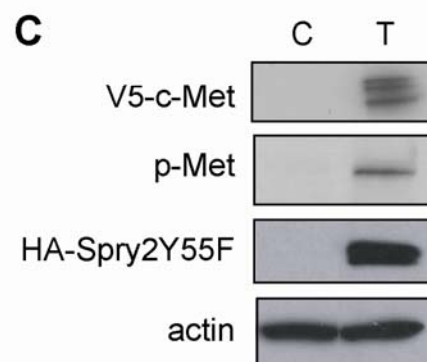
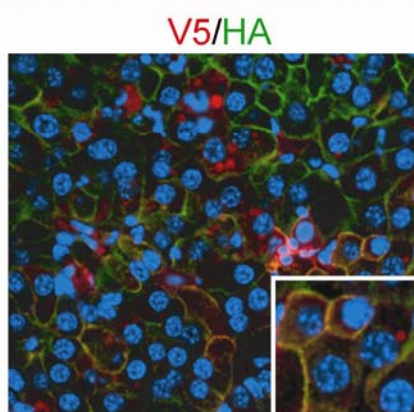
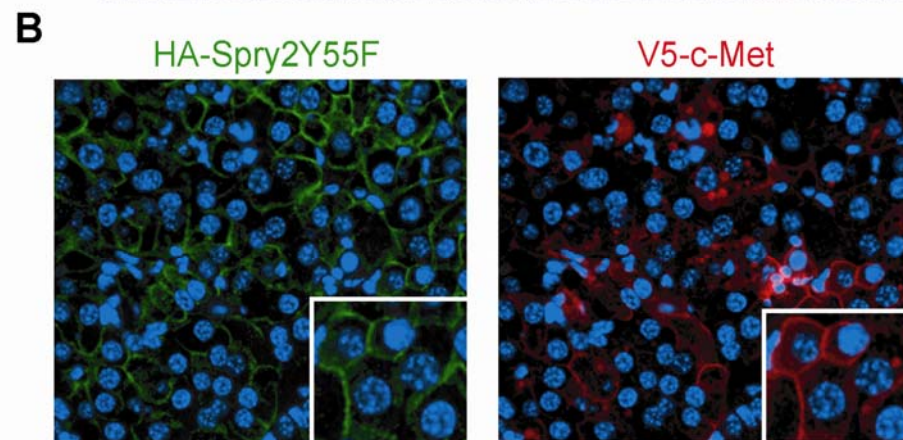
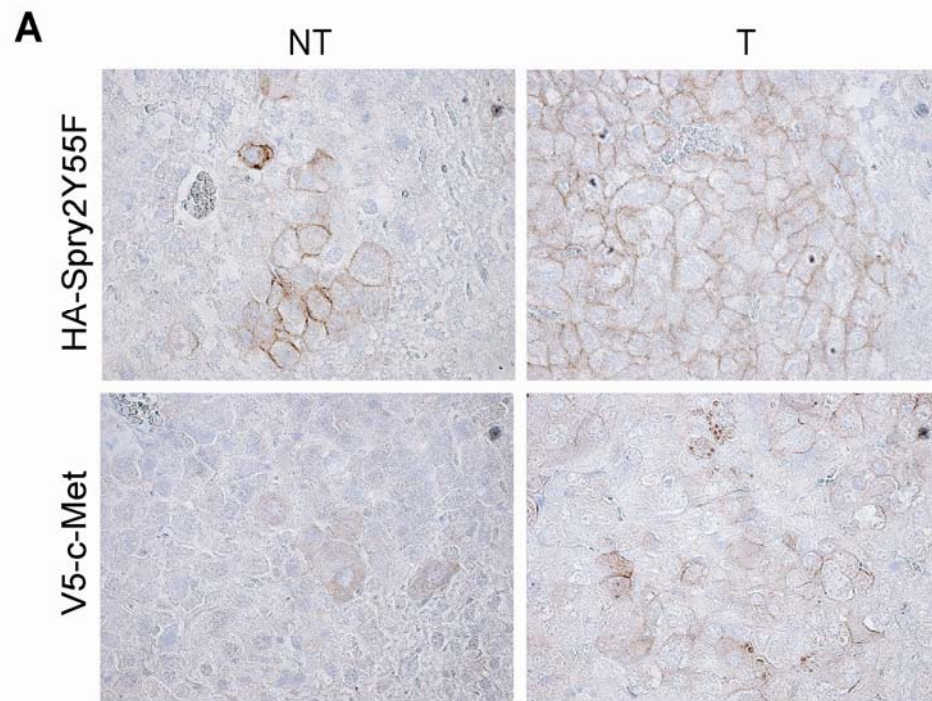


Figure 3.3. Co-expression of c-Met and Spry2Y55F in mouse liver tumors. (A) Immunohistochemical staining of c-Met and Spry2Y55F in non-tumorous (NT) and tumorous (T) liver; magnification, 200x. (B) Localization of c-Met (red) and/or Spry2Y55F (green) in liver tumors developed in c-Met/Spry2Y55F mice by immunofluorescence; magnification, 200x. Insets are close-up of the images. (C) Representative Western blot analysis of uninjected Ink4A/Arf null liver (C) and c-Met/Spry2Y55F tumor (T) for expression of c-Met, phospho-c-Met, and Spry2Y55F. Actin was used as a loading control.

Next, we determined how cellular processes were affected during c-Met/Spry2Y55F-driven hepatocarcinogenesis. c-Met/Spry2Y55F liver tumors were characterized by a gradual increase in proliferation, as shown by positive staining for the proliferation marker, PCNA (Fig. 3.4A). Accordingly, mRNA levels of cell cycle positive regulators, cyclin B1, E1, and CDC20, were upregulated in tumors (Fig 3.4D). In HCC, apoptosis was also induced, as indicated by TUNEL staining (Fig 3.4B). However, the mean apoptotic index was remarkably lower than the proliferation index in c-Met/Spry2Y55F tumors (4.4 ± 2.2 vs. 20.8 ± 3.8 , respectively; $n = 18$), indicating the prevalence of growth over death stimuli. Tumor samples were then assayed for angiogenesis by immunohistochemistry for the liver tumor endothelial marker PODXL1. Positive PODXL1 immunolabeling was detected only in neoplastic liver lesions from c-Met/Spry2Y55F mice, implying the presence of neovasculature in these lesions (Fig 3.4C). In addition, c-Met/Spry2Y55F tumors displayed a rise in mRNA levels of angiogenic markers, Angiogenin 1 and 2, and VEGF receptor-1 (Fig 3.4D). In summary,

the present data indicate that c-Met/Spry2Y55F co-expression promotes hepatocarcinogenesis by inducing cell proliferation and angiogenesis.

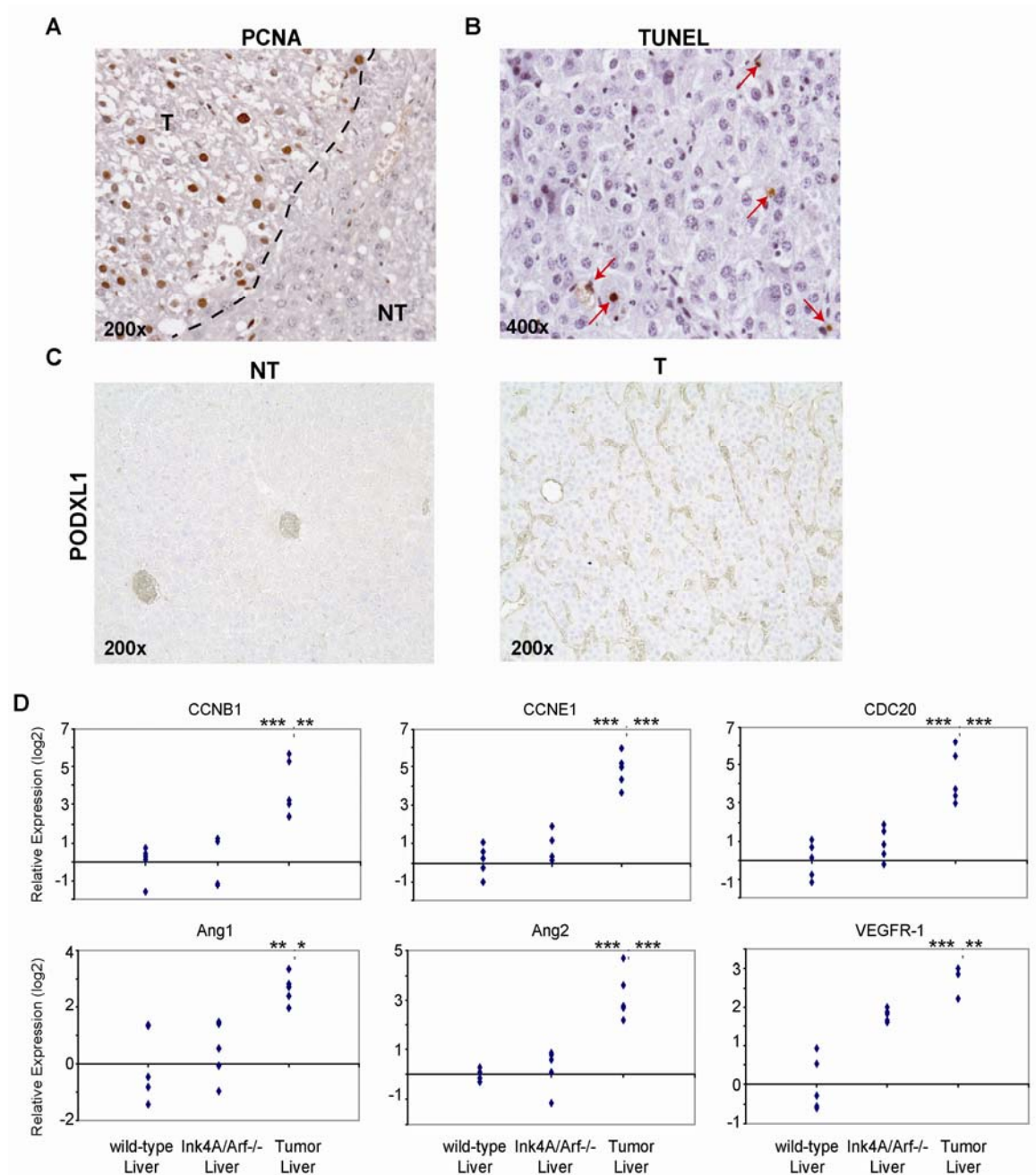


Figure 3.4. Overview of cell proliferation, apoptosis, and angiogenesis in c-Met/Spry2Y55F tumors. (A) PCNA immunostaining showing strong proliferation in a HCA when compared with non-neoplastic surrounding tissue; (B) Apoptotic bodies (indicated by arrows) in a well-differentiated HCC; (C) Immunohistochemical staining of tumor vessel marker, PODXL1, in non-tumorous (NT) and tumorous (T) liver. (D) Real-time PCR analysis of the expression levels of proliferation markers (Cyclin B1, Cyclin E1, and CDC20) and angiogenic factors (Ang1, Ang2 and VEGFR1) in normal wild-type liver (n=5), Ink4A/Arf null liver (n=5), and c-Met/Spry2Y55F liver tumors (n=5). Stars on the top represent *P* values comparing tumor samples versus wild-type liver (left) and tumor samples vs. Ink4A/Arf null liver (right) using the Tukey-Kramer Multiple Comparisons Test. ***: *P* <0.001; **: *P* <0.01; and *: *P* <0.05

Upregulation of MAPK and AKT Signaling in c-Met/Spry2Y55F Tumors

Since both Spry2 and c-Met are important regulators of the Ras pathway, we investigated whether simultaneous over-expression of c-Met and Spry2Y55F results in upregulation of Ras effectors, namely the MAPK and AKT cascades during hepatocarcinogenesis. Western blotting showed that c-Met/Spry2Y55F tumors from Ink4A/Arf null mice exhibited high levels of activated ERK and AKT proteins (Figure 3.5). Intriguingly, the phosphorylation of AKT was only noted at Ser473, but not at the Thr308 site. However, activation at Ser473 has been found to be sufficient in the propagation of AKT signaling pathway [23]. This is further supported by an increase of immunostaining for phospho-S6 Ribosomal Protein, a downstream target of the AKT pathway in c-Met/Spry2Y55F tumor samples (Figure 3.5B). The mechanism by which

Spry2 regulates AKT signaling is not clearly understood. A previous study demonstrated that Spry2-mediated inhibition of the AKT pathway requires tumor suppressor PTEN [24]. Since PTEN activity is altered by its phosphorylation, we assessed the samples for phospho-PTEN and PTEN levels. Western blotting showed no changes in the expressions of phospho-PTEN and PTEN in both tumor and normal liver (Figure 3.5A). In summary, our data indicate that over-expression of c-Met and Spry2Y55F leads to activation of MAPK and AKT signaling cascades during liver tumorigenesis. However, upregulation of AKT cascade in c-Met/SpryY55F does not depend on perturbation in the levels of PTEN.

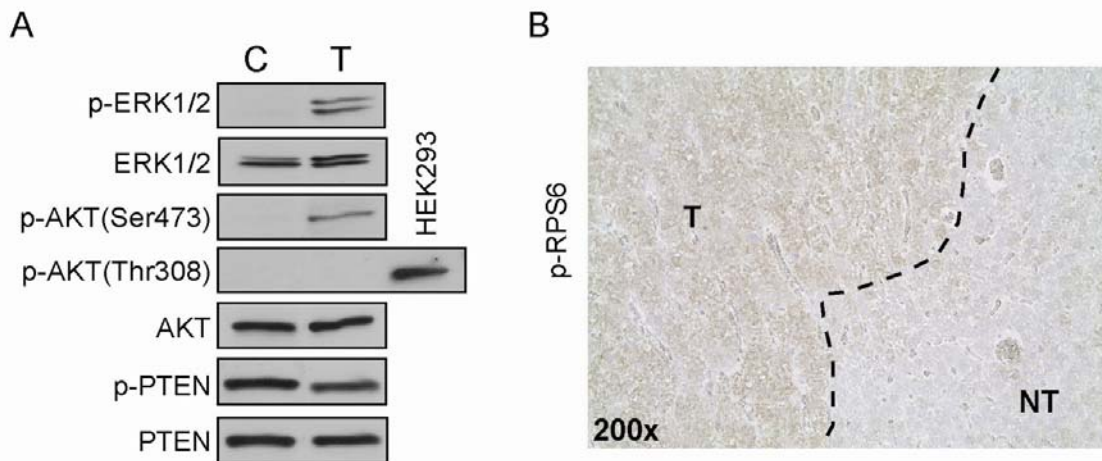


Figure 3.5. Activation of ERK and AKT signaling in c-Met/Spry2Y55F tumors. (A) Western blot analysis of total and phosphorylated AKT (detection of phosphorylation at Ser473 & Thr308), ERK, and Pten expression in uninjected Ink4A/Arf null liver (C) and c-Met/Spry2Y55F tumor (T) tissues. HEK293 cell lysate was used as a positive control for phospho-AKT (Thr308). (B) Immunohistochemical staining of phospho-S6 Ribosomal Protein in a c-Met/Spry2Y55F liver tumor.

Discussion

Activation of the Ras/MAPK pathway has been considered to be a key genetic event in carcinogenesis. In many tumor types, such as pancreatic cancer, colorectal cancer, and melanoma, oncogenic activating mutations of Ras or B-Raf are frequently observed [4]. However, such mutations are rare in other tumor types, including HCC [2,4-6]. Previous studies showed that Ras/MAPK pathway is upregulated by multiple factors in cancer, including down-regulation of Ras inhibitor RASSF1A [2] or loss of the Erk inhibitor DUSP1 [25]. Here, we demonstrated that loss of *Spry2*, *in vivo*, propagates the activation of Erk and AKT signaling initiated by c-Met, and cooperates with loss of Ink4A/Arf to promote hepatocarcinogenesis. Therefore, the study provides evidence that the coordinated deregulation of *Spry2* and c-Met signaling may be an important mechanism for the uncontrolled activation of Ras/MAPK signaling in the absence of Ras or B-Raf mutations.

Sprouty/Spred gene family members are feedback inhibitors of the receptor tyrosine kinase signaling [15, 16]. Both biochemical and genetic evidence supports that loss of Sprouty/Spred can lead to abnormal activation of the Ras/MAPK pathway. Recent genetic studies demonstrate that germline loss-of-function of the *Spred1* gene results in neurofibromatosis 1 like syndrome, which is phenotypically similar to other genetic disorders caused by mutations of genes encoding key components of the RAS-MAPK pathway [26]. Loss of expression of Sprouty/Spred gene family members has been reported in multiple tumor types [17]. Intriguingly, the tumor types showing frequent downregulation of *Spry* expression include breast cancer, prostate cancer, and HCC, which are all characterized by relatively low frequencies of mutations of Ras or B-Raf

genes [17]. Conversely, our analysis of previous microarray studies performed in tumor types with frequent Ras or B-Raf mutations, including pancreatic and colorectal cancer, revealed no significant downregulation of Spry/SpreD family members (Chen X et al., unpublished observation). Thus, this body of evidence suggests that downregulation of members of the Spry family may be a key and alternative mechanism leading to the propagation of the Ras/MAPK signaling in a context of wild-type Ras and B-Raf genes.

Previous studies in humans and rodents have demonstrated the oncogenic role of c-Met and the tumor suppressor role of Spry2, separately, in hepatocarcinogenesis [11, 12, 14, 18]. Although the regulation of c-Met signaling by Spry2 has been observed in cells, the functional interaction between these two factors during tumorigenesis has never been examined *in vivo* [19]. In the present investigation, we demonstrated that co-expression of c-Met and Spry2Y55F promotes liver tumorigenesis in Ink4A/Arf null mice, providing strong genetic evidence that deregulation of c-Met and Spry activity may have a pivotal role in HCC. Interestingly, over-expression of only Spry2Y55F did not alter liver morphology, whereas hepatic preneoplastic lesions developed following over-expression of c-Met alone. Similar to our data, previous findings showed that c-Met over-expression in FVB mouse livers resulted in the appearance of dysplastic, but not neoplastic lesions [20]. In many rodent models, hepatocarcinogenesis is defined by the emergence of glycogen-rich preneoplastic lesions, followed by progression through mixed-cell to predominantly glycogen-poor (basophilic) cell foci [27]. In accordance with the latter models, our present findings suggest that c-Met over-expression is sufficient for the appearance of glycogen-rich preneoplastic lesions in the mouse liver, whereas Spry2 disruption (Spry2Y55F) is necessary for full malignant transformation of

the liver, as indicated by the presence of both glycogen-rich and glycogen-poor cells in Spry2Y55F/c-Met HCC. Furthermore, we cannot exclude that loss of Ink4A/Arf contributes both to c-Met-induced preneoplasia and to Spry2Y55F/c-Met-induced tumorigenesis in this mouse model. Additional studies are required to define the role of Ink4A/Arf loss in hepatocarcinogenesis and the eventual crosstalk of the Ink4A/Arf locus with Spry2 and/or c-Met in our HCC model.

Although the mechanisms of Spry2-mediated inhibition of Ras/MAPK signaling have been clarified, its mode of repression of AKT activity remains unknown. A negative regulator of AKT signaling, PTEN, has been identified to be a necessary for suppression of AKT pathway by Spry2 [24]. However, loss of Spry2 function had no effect on PTEN activity during c-Met/Spry2Y55F-driven hepatocarcinogenesis, suggesting that the mechanisms of Spry2-mediated regulation on AKT signaling may be different depending on the cell type. In our model, AKT activation is more likely to be due to the upregulation of c-Met signaling, as the induction of AKT pathway by c-Met has been documented [9]. Since Spry2 can regulate c-Met signaling, it is probable that unrestrained c-Met signaling enhanced by the loss of Spry2 function triggers AKT pathway activation. Interestingly, a previous HCC mouse model characterized by the co-expression of Spry2Y55F and constitutively activated β -catenin did not show evidence of AKT signaling activation [18]. Thus, AKT activation by Spry2Y55F seems to specifically occur in the presence of c-Met activation during hepatocarcinogenesis. Further studies are needed to define the relationship between Spry2 and the AKT pathway during HCC pathogenesis.

In summary, our c-Met/Spry2Y55F model is a valuable *in vivo* system to address the functional role of a subset of genetic alterations occurring during human HCC development and progression. Furthermore, this mouse model could be extremely useful to study *in vivo* the pharmacological responsiveness of liver tumor cells to chemotherapeutic agents aimed at inhibiting the Ras/MAPK and AKT cascades.

References:

1. Aravalli, R.N., C.J. Steer, and E.N. Cressman, *Molecular mechanisms of hepatocellular carcinoma*. Hepatology, 2008. **48**(6): p. 2047-63.
2. Calvisi, D.F., S. Ladu, A. Gorden, M. Farina, E.A. Conner, J.S. Lee, V.M. Factor, and S.S. Thorgeirsson, *Ubiquitous activation of Ras and Jak/Stat pathways in human HCC*. Gastroenterology, 2006. **130**(4): p. 1117-28.
3. Spangenberg, H.C., R. Thimme, and H.E. Blum, *Targeted therapy for hepatocellular carcinoma*. Nat Rev Gastroenterol Hepatol, 2009.
4. Schubbert, S., K. Shannon, and G. Bollag, *Hyperactive Ras in developmental disorders and cancer*. Nat Rev Cancer, 2007. **7**(4): p. 295-308.
5. Tsuda, H., S. Hirohashi, Y. Shimosato, Y. Ino, T. Yoshida, and M. Terada, *Low incidence of point mutation of c-Ki-ras and N-ras oncogenes in human hepatocellular carcinoma*. Jpn J Cancer Res, 1989. **80**(3): p. 196-9.
6. Challen, C., K. Guo, J.D. Collier, D. Cavanagh, and M.F. Bassendine, *Infrequent point mutations in codons 12 and 61 of ras oncogenes in human hepatocellular carcinomas*. J Hepatol, 1992. **14**(2-3): p. 342-6.
7. Rubin, J.S., D.P. Bottaro, and S.A. Aaronson, *Hepatocyte growth factor/scatter factor and its receptor, the c-met proto-oncogene product*. Biochim Biophys Acta, 1993. **1155**(3): p. 357-71.
8. Bottaro, D.P., J.S. Rubin, D.L. Faletto, A.M. Chan, T.E. Kmiecik, G.F. Vande Woude, and S.A. Aaronson, *Identification of the hepatocyte growth factor receptor as the c-met proto-oncogene product*. Science, 1991. **251**(4995): p. 802-4.
9. Birchmeier, C., W. Birchmeier, E. Gherardi, and G.F. Vande Woude, *Met, metastasis, motility and more*. Nat Rev Mol Cell Biol, 2003. **4**(12): p. 915-25.
10. Gao, C.F. and G.F. Vande Woude, *HGF/SF-Met signaling in tumor progression*. Cell Res, 2005. **15**(1): p. 49-51.
11. Ueki, T., J. Fujimoto, T. Suzuki, H. Yamamoto, and E. Okamoto, *Expression of hepatocyte growth factor and its receptor, the c-met proto-oncogene, in hepatocellular carcinoma*. Hepatology, 1997. **25**(3): p. 619-23.
12. Taviani, D., G. De Petro, A. Benetti, N. Portolani, S.M. Giuliani, and S. Barlati, *u-PA and c-MET mRNA expression is co-ordinately enhanced while hepatocyte growth factor mRNA is down-regulated in human hepatocellular carcinoma*. Int J Cancer, 2000. **87**(5): p. 644-9.
13. Kaposi-Novak, P., J.S. Lee, L. Gomez-Quiroz, C. Coulouarn, V.M. Factor, and S.S. Thorgeirsson, *Met-regulated expression signature defines a subset of human hepatocellular carcinomas with poor prognosis and aggressive phenotype*. J Clin Invest, 2006. **116**(6): p. 1582-95.
14. Wang, R., L.D. Ferrell, S. Faouzi, J.J. Maher, and J.M. Bishop, *Activation of the Met receptor by cell attachment induces and sustains hepatocellular carcinomas in transgenic mice*. J Cell Biol, 2001. **153**(5): p. 1023-34.
15. Kim, H.J. and D. Bar-Sagi, *Modulation of signalling by Sprouty: a developing story*. Nat Rev Mol Cell Biol, 2004. **5**(6): p. 441-50.

16. Mason, J.M., D.J. Morrison, M.A. Basson, and J.D. Licht, *Sprouty proteins: multifaceted negative-feedback regulators of receptor tyrosine kinase signaling*. Trends Cell Biol, 2006. **16**(1): p. 45-54.
17. Lo, T.L., C.W. Fong, P. Yusoff, A.B. McKie, M.S. Chua, H.Y. Leung, and G.R. Guy, *Sprouty and cancer: the first terms report*. Cancer Lett, 2006. **242**(2): p. 141-50.
18. Lee, S.A., C. Ho, R. Roy, C. Kosinski, M.A. Patil, A.D. Tward, J. Fridlyand, and X. Chen, *Integration of genomic analysis and in vivo transfection to identify sprouty 2 as a candidate tumor suppressor in liver cancer*. Hepatology, 2008. **47**(4): p. 1200-10.
19. Lee, C.C., A.J. Putnam, C.K. Miranti, M. Gustafson, L.M. Wang, G.F. Vande Woude, and C.F. Gao, *Overexpression of sprouty 2 inhibits HGF/SF-mediated cell growth, invasion, migration, and cytokinesis*. Oncogene, 2004. **23**(30): p. 5193-202.
20. Tward, A.D., K.D. Jones, S. Yant, S.T. Cheung, S.T. Fan, X. Chen, M.A. Kay, R. Wang, and J.M. Bishop, *Distinct pathways of genomic progression to benign and malignant tumors of the liver*. Proc Natl Acad Sci U S A, 2007.
21. Harada, N., H. Oshima, M. Katoh, Y. Tamai, M. Oshima, and M.M. Taketo, *Hepatocarcinogenesis in mice with beta-catenin and Ha-ras gene mutations*. Cancer Res, 2004. **64**(1): p. 48-54.
22. Tannapfel, A., C. Busse, L. Weinans, M. Benicke, A. Katalinic, F. Geissler, J. Hauss, and C. Wittekind, *INK4a-ARF alterations and p53 mutations in hepatocellular carcinomas*. Oncogene, 2001. **20**(48): p. 7104-9.
23. Alessi, D.R., M. Andjelkovic, B. Caudwell, P. Cron, N. Morrice, P. Cohen, and B.A. Hemmings, *Mechanism of activation of protein kinase B by insulin and IGF-I*. Embo J, 1996. **15**(23): p. 6541-51.
24. Edwin, F., R. Singh, R. Endersby, S.J. Baker, and T.B. Patel, *The tumor suppressor PTEN is necessary for human Sprouty 2-mediated inhibition of cell proliferation*. J Biol Chem, 2006. **281**(8): p. 4816-22.
25. Calvisi, D.F., F. Pinna, F. Meloni, S. Ladu, R. Pellegrino, M. Sini, L. Daino, M.M. Simile, M.R. De Miglio, P. Virdis, M. Frau, M.L. Tomasi, M.A. Seddaiu, M.R. Muroli, F. Feo, and R.M. Pascale, *Dual-specificity phosphatase 1 ubiquitination in extracellular signal-regulated kinase-mediated control of growth in human hepatocellular carcinoma*. Cancer Res, 2008. **68**(11): p. 4192-200.
26. Brems, H., M. Chmara, M. Sahbatou, E. Denayer, K. Taniguchi, R. Kato, R. Somers, L. Messiaen, S. De Schepper, J.P. Fryns, J. Cools, P. Marynen, G. Thomas, A. Yoshimura, and E. Legius, *Germline loss-of-function mutations in SPRED1 cause a neurofibromatosis 1-like phenotype*. Nat Genet, 2007. **39**(9): p. 1120-6.
27. Bannasch, P., D. Mayer, and H.J. Hacker, *Hepatocellular glycogenosis and hepatocarcinogenesis*. Biochim Biophys Acta, 1980. **605**(2): p. 217-45.

Chapter 4

Role of Cyclin D1 as a Mediator of c-Met and β -Catenin Induced Hepatocarcinogenesis¹

Introduction

HCC progression is known to ensue a stepwise sequence of events [1]. Separate genetic or epigenetic aberrations are thought to be involved in each step during hepatic carcinogenesis. These changes include alterations in the expression or assembly of an oncogene or a tumor suppressor gene. Over-expression of the proto-oncogene c-Met is a common perturbation known to occur in HCC [2, 3]. c-Met encodes a receptor tyrosine kinase, which becomes activated upon binding to ligand hepatocyte growth factor (HGF) or scatter factor (SF). When stimulated, c-Met becomes phosphorylated, and triggers MAPK signaling through the Ras-Raf-Mek pathway [4]. It has been demonstrated that activation of c-Met can promote liver cancer development in mouse models [5].

Another pathway frequently mutated and activated is the wnt/ β -catenin signaling pathway. Wnt signals by binding to the frizzled family of receptors, which initiates a

¹ This chapter was published in a manuscript entitled: Role of cyclin D1 as a mediator of c-Met- and beta-catenin-induced hepatocarcinogenesis; Patil, M.A., Lee, S.A., Macias, E, Lam, E.T., Xu, C, Jones, K.D., Ho, C, Rodriguez-Puebla, M, Chen, X.; *Cancer Research*, 2009, 69(1):253-61. I thank the co-author and all other authors who contributed to this work.

First co-authors, Susie Lee and Mohini Patil contributed equally to this work.

signaling cascade involving dishevelled, GSK3, Axin, APC, and regulates the nuclear localization and activation of β -catenin [6, 7]. β -catenin subsequently binds to TCF-4, a member of the TCF/LEF family of transcriptional factors, and induces downstream gene expression. Multiple targets have been identified for activated β -catenin, many of which appear to be tissue specific [6, 7]. One of the well-characterized targets for activated β -catenin is cyclin D1 (CCND1) [8, 9].

CCND1 is a member of the D-type cyclin group, which also includes cyclin D2 (CCND2) and D3 (CCND3). This cyclin interacts with cyclin-dependent kinase (Cdk) 4/6 to phosphorylate the retinoblastoma (Rb) protein, which results in the transition from the G₁ to S phase of the cell cycle [10, 11]. However, CCND1 has been demonstrated to transform cells in combination with oncogenes, such as Ras, Src, and E1A [12-14]. Furthermore, over-expression of this cyclin promotes hepatocarcinogenesis, albeit at a low frequency (20-30%) and long latency (17 months), in transgenic mice [15, 16]. These findings suggest that CCND1, by itself, may not be sufficient to induce carcinogenesis. However, the expression of this cyclin in combination with another oncogenic factor may be able to promote liver tumorigenesis. CCND1 null mice have been generated and analyzed [17, 18]. While 75% of the homozygous mice are fertile and have a similar lifespan to that of wildtype mice, they are smaller in size and have developmental defects in the retinas and mammary glands [17, 18]. The use of these mice in cancer model studies has demonstrated that the effect of CCND1 expression on tumorigenesis induced by different oncogenes varies. In breast cancer, CCND1 is required for mammary tumorigenesis induced by oncogenic Ras and Her2, but not by Myc or β -catenin [19]. This cyclin has also been demonstrated to act as a modifier and be required for the

development of intestinal adenoma in APC mutant colon cancer models [20-22]. Interestingly, the absence of CCND1 enhanced β -catenin induced breast cancer [23]. However, the role of CCND1 in combination with other oncogenes during the development of liver cancer remains unknown.

In a recent study, tumors induced by human c-Met (hMet) in a mouse model were found to harbor β -catenin mutations [24]. We found that these mutations are the second hit during malignant transformation, and the constitutively active β -catenin mutants are required to cooperate with hMet to promote hepatic carcinogenesis [24]. In this report, we confirmed CCND1 expression is up-regulated in liver tumor samples induced by hMet and β -catenin. We therefore assessed the role of CCND1 in hepatocarcinogenesis induced by hMet and β -catenin using murine models. Our results provide novel insight into how D-type cyclins function to promote liver cancer development *in vivo*.

Material and Methods

Constructs and reagents

The pT3-EF1 α vector contains duplicated inverted repeats (IR) for sleeping beauty mediated integration and the EF1 α promoter (pT3-EF1 α) [24]. The pT3-EF1 α -hMet and pT3-EF1 α - Δ N90- β -catenin, as well as pCMV/SB (the hyperactive sleeping beauty expression vector) constructs used for animal injections were previously described [24]. Human cyclin D1 was cloned into pT3-EF1 α via the Gateway PCR cloning strategy

(Invitrogen). All plasmids were purified using the endotoxin free maxi prep kit (Sigma, St. Louis) before being injected into the mice.

Mice breeding, genotyping and hydrodynamic injections

Wildtype FVB/N mice were obtained from Charles River, and cyclin D1^{+/-} mice (in FVB/N background) were obtained from the Jackson Laboratory. CCND1^{+/-} mice were bred together to obtain CCND1^{-/-} mice, and the genotyping procedure was as described [18]. The hydrodynamic injection procedures were as previously described [24]. The injected mice were monitored weekly, and sacrificed when appropriate or when they showed visibly enlarged livers or became moribund. All mice were housed, fed and treated in accordance with protocols approved by the committee for animal research at the University of California, San Francisco.

Hepatocyte isolation and transfection

Primary mouse hepatocyte isolation was performed using standard collagenase perfusion method as described [25]. The hepatocytes were transfected with plasmids using Targefect-Hepatocyte (Targeting Systems) according to the manufacturer's instructions.

Histology

Animals were euthanized and their livers removed and rinsed in PBS. Samples collected from the livers were either immediately frozen for RNA and protein extraction or fixed overnight in freshly prepared cold 4% paraformaldehyde. Fixed tissue samples were embedded in paraffin. Five micron sections were placed on slides and stained with hematoxylin and eosin to observe morphology of the cells.

Immunohistochemistry and Immunofluorescence

Immunohistochemical staining was performed using avidin-biotin complex kit (Vector Laboratories) as previously described [24]. Immunofluorescence was performed in the similar manner, except that the appropriate Alexa labeled secondary antibody (Invitrogen) was applied following incubation with the primary antibody. Antibody dilutions were as follows: anti- β -catenin, (1:200), anti-E-cadherin, (1:1000) and anti-GS, (1:500; BD Bioscience); anti-Ki67, (1:150) and anti-CCND1 (SP4; 1:75; Lab vision).

Real-time RT-PCR

Total RNA was extracted from frozen liver tissues or primary hepatocytes using Trizol (Invitrogen) and digested with DNase I to remove genomic DNA contamination. Sybergreen based real-time RT-PCR was carried out as described [26] and rRNA was used as an internal control. Transcript quantification was performed in triplicate for

every sample and reported relative to rRNA. The primer pair sequences are as described previously [26].

Preparation of lysates and western blotting

Liver tumors were frozen on dry ice upon harvesting, and homogenates were sonicated in lysis buffer (150 mM NaCl, 1.0% IGEPAL, 0.5% DOC, 0.1% SDS, 50 mM Tris (pH 8.0)) and centrifuged at 14,000 rpm at 4°C. Supernatant were boiled in Laemlli sample buffer for western blot analysis. The antibodies used are as follows: anti-Cyclin D1 (Ab3, 1:1000, Lab Vision, or C-20, 1:500, Santa Cruz Biotech); anti-Cyclin D2 (M-20, 1:500, Santa Cruz Biotech); anti-Cyclin D3 (C-16, 1:300, Santa Cruz Biotech.); anti-Cdk4 (C-22, 1:500, Santa Cruz Biotech); anti-Cdk6 (1:300, Santa Cruz Biotech.); anti-Cdk2 (M-2, 1:500, Santa Cruz Biotech); anti-GS, (1:1000); anti-actin (1:5000; Sigma); anti-Erk, (1:1000); anti-phospho-Erk (1:1000); anti-phospho-Met (1:1000; Cell signaling); and anti-V5 (1:5000; Invitrogen). Western blots were quantified using the ImageJ software [4].

Array based comparative genomic hybridization (aCGH)

Mouse CGH arrays were obtained from the UCSF Cancer Center Array Core. The arrays contained 2,896 BAC clones spotted in triplicate, with an average spacing between clones of ~1MB. Array hybridization and data analyses were the same as previously described [27].

Results

Cyclin D1 is induced in hMet/ β -catenin tumors

In a recent study, we characterized a unique and efficient HCC mouse model, driven by the inducible expression of the human receptor tyrosine kinase c-Met (hMet). Tumors arise sporadically in livers of such mice and all show mutation and activation of β -catenin [24]. Using hydrodynamic transfection, we demonstrated that while neither hMet or activated β -catenin alone is able to promote HCC development, the cooperation between aberrant β -catenin signaling and activated Met is required for genesis of HCC in the mouse model [24].

To determine the molecular mechanisms of how activated β -catenin contributes to hepatic carcinogenesis, we searched for genes that are de-regulated by activated β -catenin in the mouse HCC samples. We determined the expression levels of candidate β -catenin targets: Axin 2, glutamine synthetase (GS), CCND1, and c-myc, by quantitative real time RT-PCR in 5 paired HCC and non-tumor liver tissues from hMet transgenic mice (Fig. 4.1A). We chose to use the liver samples from hMet transgenic mice instead of those from hMet and β -catenin injected mice because in hMet transgenic mice, non-tumor liver tissues also overexpress hMet. Therefore, genes that are up-regulated in tumors versus non-tumor tissues are most likely due to β -catenin activation. As expected, both Axin2 and GS were upregulated; their expressions were approximately 23 and 38-fold higher in HCC samples than in surrounding non-tumor liver tissue. CCND1 was also found to be expressed 7-fold higher in HCC than in non-tumor liver tissue. However, c-Myc expression levels did not show significant differences (Fig. 4.1A).

To further validate our observations, we assayed the protein expression of CCND1 and GS. Immunohistochemical staining of liver tumor tissues revealed nuclear staining of β -catenin in HCC lesions, indicating the activation of β -catenin (Fig. 4.1C). In normal liver, GS was found to be only expressed in hepatocytes immediately adjacent to the central vein. In contrast, in HCC, GS expression was detected in virtually all malignant hepatocytes (Fig. 4.1C). Analysis of CCND1 expression revealed there was weak expression of CCND1 in normal mouse liver cells. However, strong nuclear staining of CCND1 was apparent in the tumor samples (Fig. 4.1C). The expression patterns of these genes are similar for all tumors from hMet transgenic mice and hMet/ β -catenin injected mice (Fig. 4.1C). The up-regulation of CCND1 and GS in tumor tissues was also confirmed by Western blotting (Fig. 4.1B).

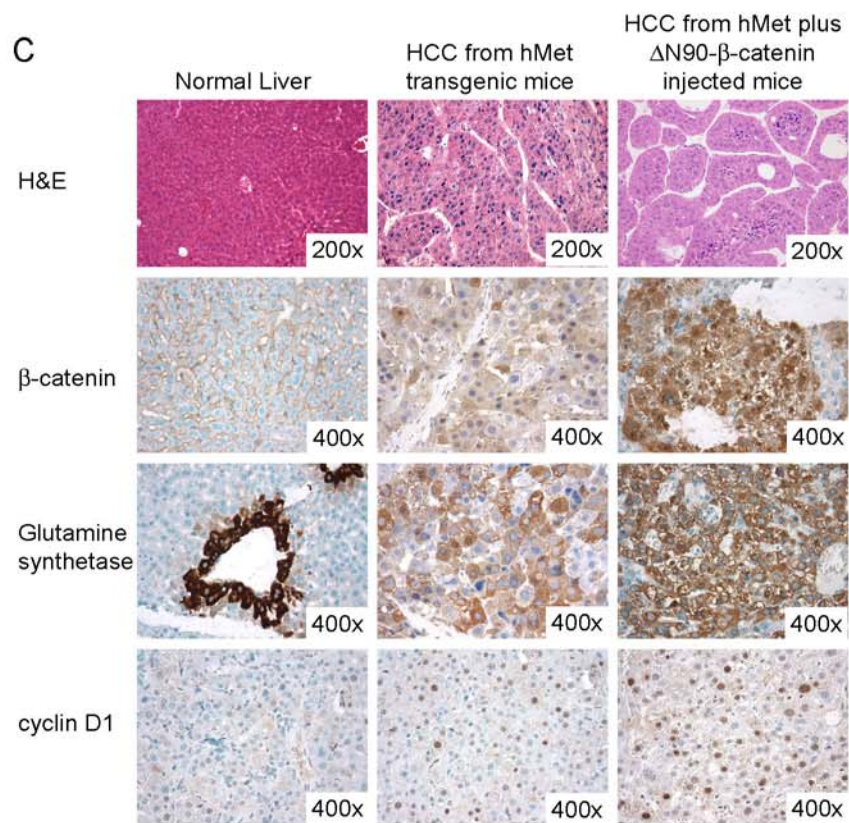
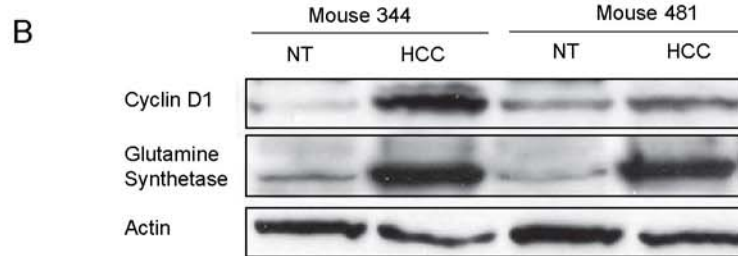
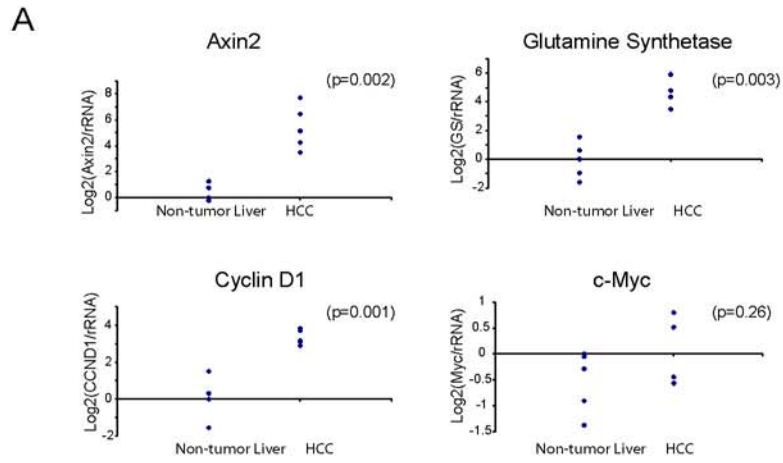


Figure 4.1: Cyclin D1 is induced in hMet/ β -catenin tumors. (A) Quantitative real-time RT-PCR analyses of β -catenin candidate target genes Axin2, GS, CCND1, and c-Myc in 5 paired HCC and non-tumor liver tissues from hMet transgenic mice. Values are displayed as log₂ ratio of tumor versus non-tumor liver. (B) Representative Western blots showing GS and CCND1 expression in two paired tumor and non-tumor liver samples of hMet transgenic mice. Actin was used as the loading control. (C) Immunohistochemical staining in normal (left), HCC from hMet transgenic (middle) or HCC from hydrodynamic co-transfection of hMet and Δ N90- β -catenin (right). First row: H&E staining; Second row: β -catenin; Third row: glutamine synthetase (GS); and Fourth row: CCND1.

Our data suggest that CCND1 expression is induced by β -catenin during hepatic carcinogenesis. We next examined if this occurrence also takes place in normal hepatocytes. To assess the induction of CCND1 by β -catenin, we expressed an activated form of β -catenin, Δ N90- β -catenin, into mice using hydrodynamic transfection. CCND1 and Δ N90- β -catenin expression were analyzed by immunofluorescent staining. We found that while sporadic activated β -catenin staining could be visualized in normal hepatocytes, no CCND1 expression was detected in the same cells (Fig. 4.2A). Consistent with our previous results, we observed co-localization of β -catenin and CCND1 in tumor cells induced by c-Met/ Δ N90- β -catenin (Fig. 4.2A). To confirm our findings, we transfected primary mouse hepatocytes with Δ N90- β -catenin (Fig. 4.2B). Although we detected strong expression of the β -catenin target gene Axin2, no up-regulation of CCND1 was observed (Fig. 4.2C). These experiments suggest that although CCND1 is

not a direct target for β -catenin in normal hepatocytes, its expression is induced during hepatic carcinogenesis.

In conclusion, we found that CCND1 expression is up-regulated in mouse liver tumors induced by hMet and β -catenin. Consistent with our observation, over-expression of CCND1, but not c-Myc, has been reported in two HCC mouse models involving the activation of β -catenin: conditional APC knockout mice and RasV12 and β -catenin double conditional transgenic mice [28, 29]. Since CCND1 is an important factor in the regulation of cell cycle progression, we hypothesized that CCND1 may be a key mediator of β -catenin in promoting hepatic carcinogenesis.

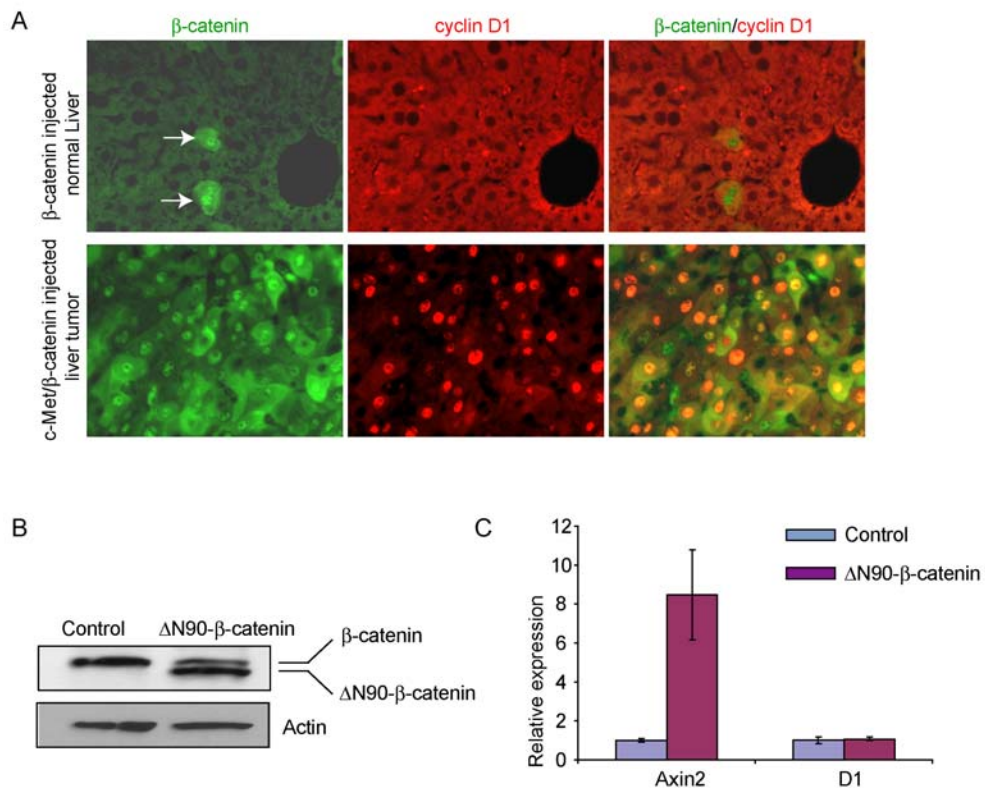


Figure 4.2: Cyclin D1 is not a direct target of activated β -catenin in normal hepatocytes. (A) Immunofluorescent staining of β -catenin (green) and CCND1 (red) in normal liver injected with Δ N90- β -catenin (upper row), and in liver tumor induced by c-Met and β -catenin (lower row). White arrows indicate Δ N90- β -catenin stably expressed cells in normal liver; (B) Western blotting showing the expression of a truncated and activated form of β -catenin after transfection of primary mouse hepatocytes with Δ N90- β -catenin; (C) Real-time RT-PCR analysis of Axin2 and CCND1 expression in control and Δ N90- β -catenin transfected primary mouse hepatocytes.

Cyclin D1 cooperates with hMet to induce HCC in mice

To test whether CCND1 is a mediator of activated β -catenin signaling during hepatic carcinogenesis, we investigated whether over-expression of this cyclin can substitute for activated β -catenin and cooperate with hMet to induce HCC in mice. We used hydrodynamic transfection to co-express CCND1 and hMet in the mouse liver. Histological examination revealed that none of the nine mice injected with hMet/CCND1 showed any signs of tumor development between 11 to 22 weeks post injection (Fig 4.3). Tumor formation was first observed in these mice at 25 weeks post injection. In total, 6 of the 19 mice injected with CCND1 and hMet developed liver tumors within 29 weeks post injection (Fig 4.3). Gross examination of livers from these mice also showed multiple small lesions scattered throughout the surface of the liver (Fig. 4.4). In contrast, mice expressing only hMet (n=9) or CCND1 alone (n=10) failed to develop liver cancer during this time period (Fig 4.3). The fact that tumors were only observed when CCND1

and hMet are co-expressed suggests that over-expression of CCND1 cooperates with hMet to promote liver cancer formation.

We found that co-expression of hMet and Δ N90- β -catenin induces HCC in 12 out of 15 mice within 17 weeks post injection (Fig 4.3), much earlier than mice injected with CCND1 and hMet. We also observed that the frequency of tumor development in hMet and Δ N90- β -catenin (80%) was higher than that of hMet and CCND1 injected mice (32%) (Fig 4.3). Together the data suggest that tumor initiation is likely to be much later in hMet/CCND1 injected mice compared with hMet/ β -catenin injected mice.

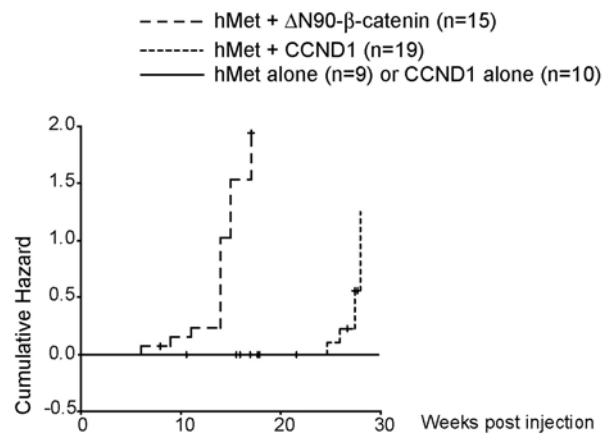


Figure 4.3: Cyclin D1 cooperates with hMet to induce HCC in mice. Cumulative hazard curve comparing the latency and frequency of tumor development in hMet alone, CCND1 alone, hMet/CCND1, and hMet/ Δ N90- β -catenin injected mice. The cumulative hazard represents the relative probability of tumor development in each condition.

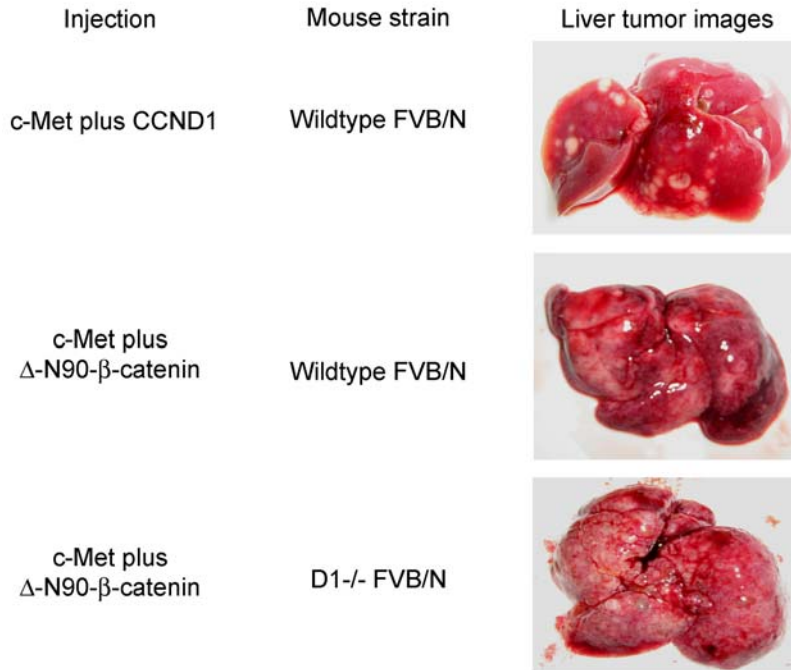


Figure 4.4: Gross images of liver tumors.

Molecular features of liver tumors induced by CCND1/ hMet

To gain further insight into the molecular features of liver tumors induced by hMet/CCND1, we examined tumor samples using histological analysis and quantitative RT-PCR. We found up-regulation of liver tumor specific marker α -fetoprotein (AFP) in hMet/CCND1 tumor samples (Fig. 4.5C), confirming the neoplastic nature of these cells. Histological examination of liver tissue from hMet/CCND1 injected mice revealed that the majority of the tumors appeared to be adenoma that compressed the surrounding non-tumorous liver parenchyma (Fig. 4.5A). Increased plate thickness and trabecular disorganization were rarely observed in these tumors (Fig. 4.5A). This is distinct from tumors found in hMet transgenic mice or mice injected with hMet/ Δ N90- β -catenin,

where a majority of the tumors display features consistent with malignant HCC (Fig. 4.1B). Nuclear staining of CCND1 was observed, revealing the presence of CCND1 in neoplastic hepatocytes, but rarely in non-tumor liver tissues (Fig. 4.5A). The level of CCND1 expression in hMet/CCND1 tumor cells is similar to what we observed in tumors from hMet/ Δ N90- β -catenin injected mice. Over-expression of hMet (with c-terminal V5 tag) was confirmed by Western blotting using the V5 antibody (Fig. 4.5B); and the activation of hMet as illustrated by the high levels of phospho-Met and phospho-Erk in hMet/CCND1 tumor cells (Fig. 4.5B). To rule out the possibility that the tumors induced by hMet/CCND1 were due to endogenous mutations of β -catenin, we analyzed β -catenin and its target gene expression in tumor samples. We found no evidence of activation of β -catenin signaling in tumor cells, as only membrane β -catenin staining was observed (Fig. 4.5A), and no up-regulation of β -catenin target genes Axin2 and GS was detected by real-time RT-PCR (Fig 4.5C and data not shown). Altogether, these analyses support our hypothesis that hMet and cyclin D1 together promote liver adenoma formation in mice.

Next, we examined the genes involved in cell cycle, apoptosis and cell adhesion in CCND1/hMet tumor samples. We observed an increase in the proliferation of tumor cells as indicated by positive staining for the proliferative marker, Ki67 (Fig. 4.5A). This observation is also confirmed by the high expression of cell cycle regulatory genes, *cyclins B1* and *E1*, as well as Cdk inhibitor p21Cip1 in the tumors (Fig. 4.5C). In addition, tumor cells expressed high levels of the anti-apoptotic protein, survivin, as well as the angiogenic gene, *Ang2* (Fig. 4.5C). Immunostaining revealed that tumor cells are positive for the cell-cell adhesion molecule, E-cadherin (data not shown). This

observation is confirmed by up-regulation of E-cadherin as indicated by real-time PCR analysis (Fig. 4.5C). While there are striking differences in tumor latency and incidence between the hMet/ Δ N90- β -catenin and hMet/CCND1 injected mice, molecular features of both tumors are similar to a certain extent. For example, elevated expressions of cyclins, survivin, Ang2, E-cadherin, and p21Cip1 were observed in all tumor samples examined (Fig. 4.5C).

In conclusion, our study demonstrates that over-expression of CCND1 can cooperate with hMet to promote liver cancer formation, supporting the hypothesis that CCND1 is a critical downstream signaling molecule of activated β -catenin. However, the differences between tumors induced by hMet/CCND1 and hMet/ Δ N90- β -catenin indicate that other factors, in addition to CCND1, may be required to fully transduce the signaling generated by aberrant β -catenin.

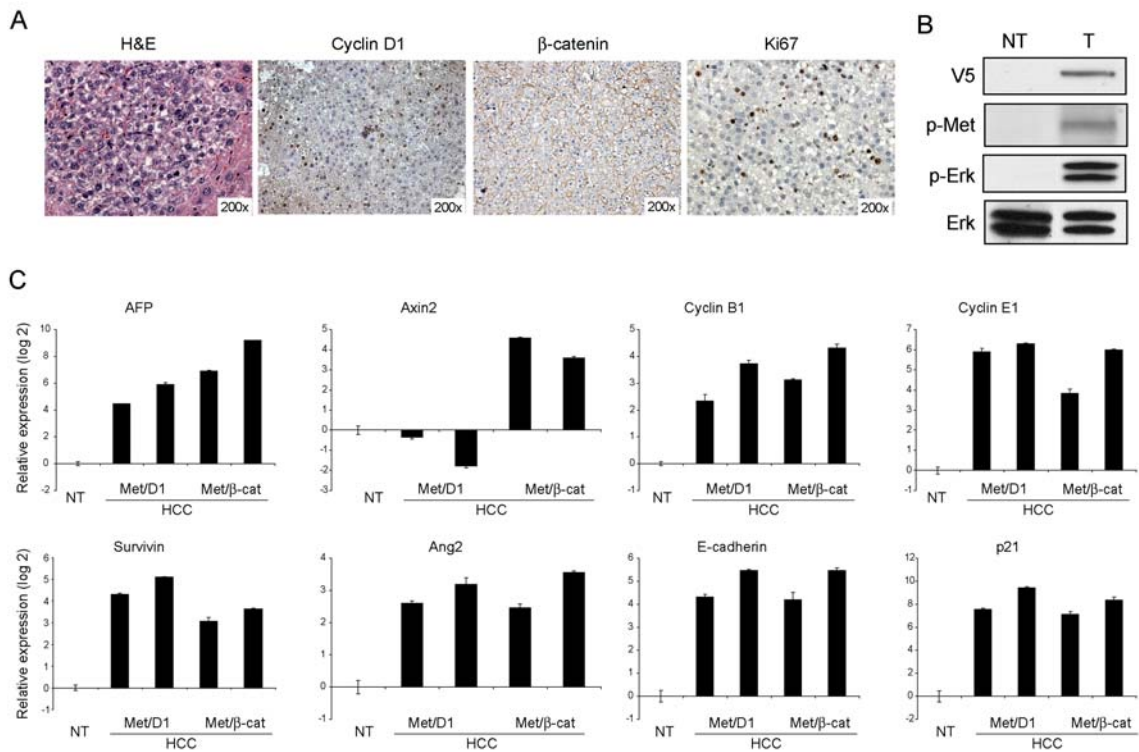


Figure 4.5: Molecular features of liver tumors induced by hMet/CCND1. (A) Immunohistochemical staining of liver tumor tissues from hMet/CCND1 mice: H&E, CCND1, β -catenin and Ki67 staining (left to right). (B) Western blot analyses showing the expression of V5 tagged hMet, activation of hMet (phospho-Met) and elevated MAPK signaling (phospho-Erk) in hMet/CCND1 tumor cells; (C) Quantitative real time-PCR analyses of liver tumor markers in normal liver (NT), hMet/CCND1 tumors and hMet/ Δ N90- β -catenin tumor samples. In all cases, the expression in normal liver was set to 1 and used to normalize all the other samples.

CCND1 expression is not required for tumor development induced by activated β -catenin plus hMet

Since CCND1 expression is induced by hMet and β -catenin in liver tumors, we next determined whether the expression of CCND1 is required for activated β -catenin and hMet to promote HCC development *in vivo*. Towards this aim, we generated CCND1 knockout mice in the FVB/N background. These CCND1 null mice show similar phenotypes as described in the C57/BL6 background [17, 18]. Liver tissues appeared to be normal in these mice. Δ N90- β -catenin and hMet were co-injected into CCND1^{+/-} and CCND1^{-/-} mice, and tumor development was monitored. Mice were sacrificed if they became moribund or if there was noticeable enlargement of their abdomen.

We found that hMet and Δ N90- β -catenin could induce liver cancer development independent of the CCND1 genotype. In particular, we observed 7 out of 8 CCND1^{-/-} mice developed tumors within 11 weeks post injection; 8 out of 10 CCND1^{+/-} mice

developed tumors 14 weeks post injection, and 12 out of 15 wild type mice developed tumors 17 weeks post injection (Fig. 4.6). Intriguingly, we noticed that the CCND1 gene dosage affected the onset and progress of hepatocarcinogenesis: tumors progressed earlier with lower CCND1 gene doses, i.e., CCND1^{-/-} mice demonstrated the fastest tumor progression, whereas wild type mice showed the longest latency time for tumor development (Fig. 4.6). Tumors from CCND1^{-/-} or CCND1^{+/-} mice are multi-focal and scattered around the liver, similar to what has been observed in wild type FVB/N mice (Fig. 4.4).

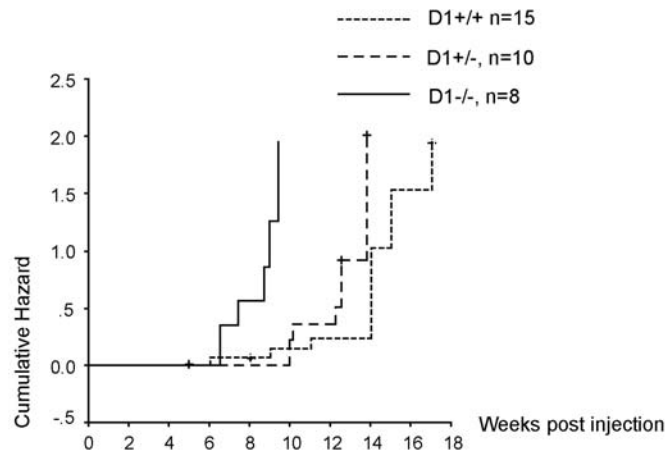


Figure 4.6: Accelerated tumor development induced by hMet/ Δ N90- β -catenin in cyclin D1 knockout mice. Cumulative hazard curve comparing the latency and frequency of tumor development induced by hMet/ Δ N90- β -catenin in wildtype, CCND1^{+/-} or CCND1^{-/-} mice. The cumulative hazard represents the relative probability of tumor development in each condition.

Histological analyses revealed tumor lesions from CCND1^{+/-} and CCND1^{-/-} mice emerge as hepatocellular carcinoma with cytological atypia and frequent trabecular disorganization (Fig. 4.7A and data not shown). This is further verified by high expression levels of AFP in these tumor samples (Fig. 4.7D). Ectopic expression of β -catenin is validated by nuclear and cytoplasmic staining in tumor cells (Fig. 4.7A). Expression of hMet in tumor samples is indicated by the presence of the V5 marker. The activation of hMet signaling is confirmed by an increase in the expression of phospho-Met and phospho-Erk (Fig. 4.7C). CCND1 expression was not detected in tumors from CCND1^{-/-} mice by immunohistochemical staining or Western blotting (Fig. 4.7A and Fig. 4.9A).

We further assayed the molecular signatures of tumors from different CCND1 genetic backgrounds. Increased cell proliferation was detected in tumors from CCND1^{-/-} mice, as indicated by positive Ki67 staining (Fig. 4.7A). The over-expression of cyclin B1, E1, and Cdk inhibitor p21Cip1 in tumors from CCND1^{-/-} as well as CCND1^{+/-} and wildtype mice further verify this observation (Fig. 4.7D). The anti-apoptotic gene *survivin* is also found to be over-expressed in all tumor samples (Fig. 4.7D).

We next examined the expression of the cell-cell adhesion molecule, E-cadherin. In the normal liver, hepatocytes show weak staining of E-cadherin around the periportal area (Fig. 4.7B) [30]. Tumors induced by hMet and β -catenin in wild type mice displayed ubiquitous expression of E-cadherin in all tumor cells (Fig. 4.7B). In contrast, there appeared to be a heterogeneous pattern of E-cadherin expression in tumors from CCND1^{-/-} mice: while some tumor nodules retained E-cadherin staining, others showed

no expression (Fig. 4.7B). Because loss of E-cadherin has been linked with malignant phenotype, our data indicates that tumors from cyclin D1 null mice show moderate accelerated tumor growth and increased malignancy.

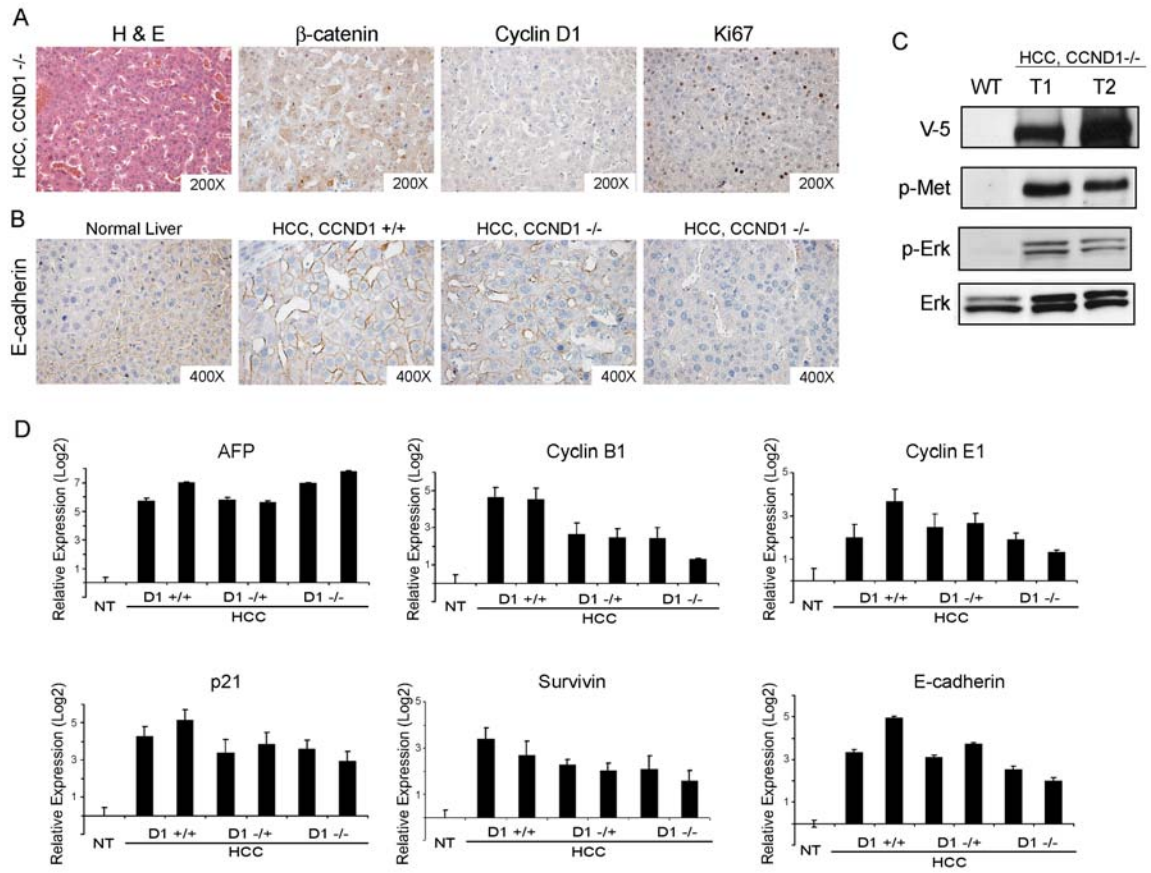


Figure 4.7: Molecular features of liver tumors induced by hMet/ Δ N90- β -catenin in different Cyclin D1 genetic backgrounds. (A) Immunohistochemical staining of liver tumor tissues from hMet/ Δ N90- β -catenin injected CCND1^{-/-} mice: H&E, β -catenin, CCND1, and Ki67 staining (left to right). (B) Immunohistochemical staining of E-cadherin expression in normal liver, liver tumors from wildtype or CCND1^{-/-} mice; (C) Western blot analyses showing the expression of V5 tagged hMet, activation of hMet (phospho-Met), and elevated MAPK signaling (phospho-Erk) in hMet/ Δ N90- β -

catenin;CCND1^{-/-} tumor cells (D) Quantitative real time-PCR analyses of tumor markers in normal liver, liver tumors from wildtype, CCND1^{+/-} or CCND1^{-/-} mice. In all cases, the expression in normal liver was set to 1 and used to normalize all the other samples.

A study by Calvisi *et. al.* demonstrated that mouse liver tumors with β -catenin activation have a stable genome [31]. Consistent with this observation, we found that tumors induced by hMet and Δ N90- β -catenin also have a stable genome, with no abnormal chromosomal gains or losses (Fig. 4.8 (labeled as Supplementary Figure 4): <http://cancerres.aacrjournals.org/cgi/content/full/69/1/253/DC1>). We examined genomic instability in tumor samples from CCND1^{-/-} mice using array based comparative genomic hybridization. Similar to what we observed in wildtype mice, liver tumors induced by hMet and Δ N90- β -catenin in CCND1^{-/-} mice have no genomic instabilities (Fig. 4.8: see link above). The study therefore suggests that the accelerated tumor growth in CCND1^{-/-} mice is not due to the increased genomic instability of these tumor samples.

Up-regulation of CCND2 in CCND1 null liver and liver tumor samples

Our preliminary studies demonstrate that mRNA of all three members of the D-type cyclin family is expressed in the mouse liver (data not shown). To determine whether the loss of CCND1 was compensated by the two other D-type cyclins, we assayed for the protein expression of cyclin D2 and D3 in tumor tissues from wildtype, CCND1^{+/-} and CCND1^{-/-} mice. Strikingly we observed that while CCND2 is expressed

at very low levels in wildtype tumor samples, its expression is significantly up-regulated in tumors from CCND1^{+/-} and CCND1^{-/-} mice (Fig. 4.9A). The expression of CCND3 remains the same in all tumor samples. We further examined the expression of the D-type cyclin partners, Cdk4 and Cdk6, as well as Cdk2, which binds to cyclin E and A. We found the expression of Cdk2 and Cdk6 to be independent of tumor genotypes. However, the expression of Cdk4, a major signaling partner of CCND1, in CCND1^{-/-} mice tumors is significantly decreased by 60% in comparison to tumors from wildtype mice (Fig. 4.9A and Fig. 4.10).

We next determined whether the up-regulation of CCND2 also compensates for the loss of CCND1 during normal liver development, or occurs only during tumorigenesis. We assayed the expression of CCND1 and CCND2 in normal wildtype liver and in the liver of CCND1 null mice. We found that CCND2 expression is increased in normal liver samples compared to CCND1^{+/-} and CCND1^{-/-} mice (Fig. 4.8B). The results suggest that CCND2 replaces CCND1 function when the CCND1 gene is deleted in the liver and the CCND2/Cdk6 complex replaces the CCND1/Cdk4 complex during hepatic carcinogenesis.

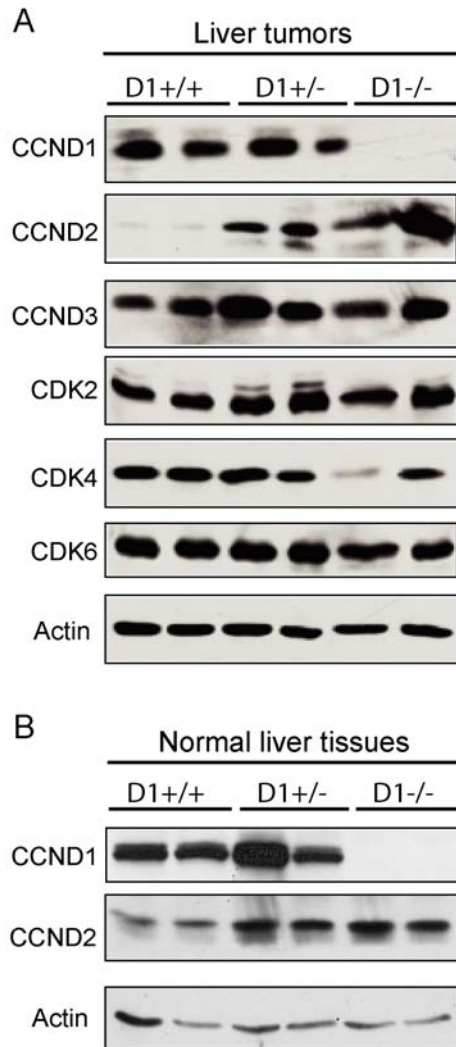


Figure 4.9: Expression in D-type cyclins and Cdk6 in mouse liver tissues. (A) Western blotting analysis of the expression of CCND1, CCND2, CCND3, Cdk2, Cdk4 and Cdk6 in liver tumor samples with different CCND1 genetic backgrounds. (B) Expression of CCND1 and CCND2 in normal liver tissues from mice with different CCND1 genetic backgrounds. Actin was used as the loading control.

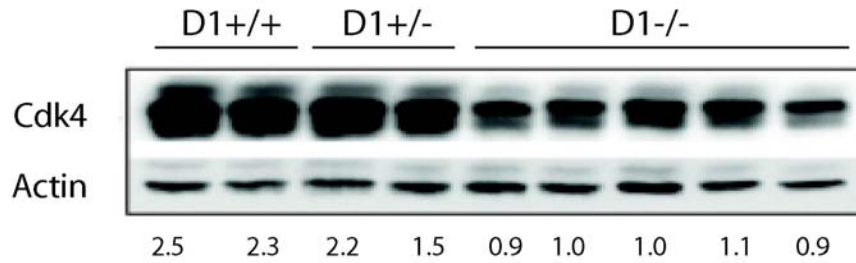


Figure 4.10: Decreased expression of Cdk4 in liver tumors induced by c-Met and β -catenin from mice with different CCND1 genetic backgrounds. Five more tumors samples from CCND1 null mice are shown here in addition to what is shown in Figure 4.8A; and the numbers at the bottom of the figure are relative ratio of Cdk4 expression after normalization.

Discussion

We found that CCND1 expression is elevated in hMet/ β -catenin induced liver tumors. However, this cyclin does not appear to be a direct target of activated β -catenin in normal mouse hepatocytes, as indicated by our findings and studies from Cadoret A. and colleagues [32]. This is in contrast to studies that have shown there to be a correlation between the over-expression of CCND1 and β -catenin activation in mouse liver tumor models [28, 29, 33]. Zeng G. *et. al.* recently reported that CCND1 expression is decreased in response to RNA-mediated β -catenin knockdown in human HCC cells carrying activated β -catenin mutations [34]. Altogether, the data suggest that CCND1 is likely to be induced by activated β -catenin during hepatic carcinogenesis. Our experiments demonstrate that CCND1 can partially substitute activated β -catenin and

cooperate with hMet to induce liver cancer formation *in vivo*, thus providing additional evidence of CCND1 as a target of β -catenin during malignant transformation.

Although co-expression of CCND1 and hMet can induce liver cancer formation in mice, we found that these tumors form at a longer latency and lower frequency as well as appear to be more benign in comparison with tumors induced by β -catenin/hMet. These observations indicate that other factors, in addition to CCND1, may be required to fully transduce the aberrant β -catenin signaling. The long latency of CCND1/hMet tumors suggests that other mutations, albeit unknown to us at this point, may occur during the tumorigenic process and cooperate with CCND1 and hMet to promote hepatic carcinogenesis. Other targets of β -catenin, Tbx3 [35] and Gpr49 [36], were found to be up-regulated in liver tumors induced by hMet/ β -catenin (Patil M.A. *et al.*, unpublished results). Tbx3, a member of the T-box transcriptional repressor family, has been found to be over-expressed in melanoma, breast cancer, and ovarian cancer [37-39]. In addition, Tbx3 has been shown to be a potent inhibitor of p19Arf and hence, a regulator of the p19Arf-MDM2-p53 pathway [40]. Thus, Tbx3 may provide a novel link between activated β -catenin and p19Arf tumor suppressor pathways. Gpr49, also known as Lgr5, is an orphan G protein-coupled receptor. Gpr49 has been found to be over-expressed in human colon and ovarian tumors and is proven to be a marker for intestinal stem cells [41, 42]. Altogether, it would be of great importance to elucidate how Tbx3, Gpr49, and CCND1 function together and mimic the activity of β -catenin in cooperation with c-Met to induce liver cancer.

We have shown that, although CCND1 expression is up-regulated in liver cancer cells, this cyclin appears to be dispensable for c-Met and β -catenin's induced liver tumor development. Our study therefore adds to the intricate picture of CCND1 requirement for oncogene induced tumor development. The expression of this cyclin, for instance, is required for ErbB2 or Ras induced, but not for Wnt-1 or c-Myc induced mammary tumors [19]. In colon cancer models, CCND1 appears to function as a modifier for disease severity [20-22]. In addition, loss of CCND1 has been found to reduce Ras dependent papilloma development [13]. Unexpectedly, we observed that hMet and Δ N90- β -catenin induced tumor development was accelerated by the loss of CCND1. Tumor cells appeared to be more aggressive, with frequent E-cadherin negative tumors present in the HCCs of CCND1^{-/-} mice. Interestingly, increased breast tumorigenesis has also been observed in CCND1^{-/-} mice when they were crossed with mice specifically expressing activated β -catenin in the mammary gland [23]. Our study provides additional evidence that CCND1 plays divergent roles under different oncogenic signals and in diverse cell types. For each specific oncogenic signal and cell type, one has to assay for the tumorigenic activity of the oncogene in a CCND1 null background in order to elucidate the requirements of this cyclin in the specific circumstance.

What are the molecular mechanisms for the accelerated and more aggressive phenotype observed in CCND1 knockout mice? One possible clue comes from our investigation of the expression of other D-type cyclins and Cdks in the CCND1^{-/-} tumor samples. Increased expression of CCND2 in CCND1^{+/-} and CCND1^{-/-} tumors strongly suggests that this cyclin can replace CCND1. In addition, lack of CCND1 seems to decrease the Cdk4 protein level, likely through reduced stability of free Cdk4. Whether

CCND2/Cdk6 is more efficient in the phosphorylation of Rb than CCND1/Cdk4 during liver tumor development warrants further investigation, and may provide functional roles for CCND2 in hepatic carcinogenesis. A recent study supports a positive role for CCND2 in tumorigenesis, where CCND2 transgenic mice are more susceptible to developing skin tumors, a characteristic that is not shared by cyclin D1 and D3 transgenic mice generated under the same promoter [43, 44]. In addition, D-type cyclins play Cdk-independent roles in certain cell types. D-type cyclins, for instance, has been demonstrated to bind to nuclear receptors such as androgen, estrogen, and vitamin D receptors, thus regulating the expression of several genes in prostate, mammary gland and skin keratinocytes [45, 46]. While the interaction of D-type cyclins with nuclear receptors has not been described in liver, whether CCND1 acts through this pathway during liver tumorigenesis clearly needs to be evaluated. A third possibility is that D-type cyclins play tumor promoting roles in cell types other than hepatocytes. That is, D type cyclins may be important in regulating tumor immunity or angiogenesis. The more rapid tumor growth in CCND1 null mice may be due to the reduced immune response or more robust angiogenesis since CCND1 is deleted in all cell types in these mice. This hypothesis can be tested by generating hepatocyte specific deletion of CCND1 in mice using the albumin Cre system. If we fail to observe this accelerated tumor growth phenotype in these mice, the result will support an additional non-hepatocyte role of D type cyclins during HCC pathogenesis.

It has been speculated that small molecules targeted against CCND1/Cdk4 may be useful as therapeutic reagents against human tumors. However, our study and that by Rowlands et al suggest that we need to be cautious about such treatments, since it could lead to unfavorable consequences under certain conditions. For example, CCND1/Cdk4

inhibitors may not be suitable for patients who have chronic HBV or HCV infection, as these patients are at a greater risk of developing HCC, and loss of CCND1/CDK4 activity may accelerate the progression of this malignancy.

References:

1. Feitelson, M.A., B. Sun, N.L. Satiroglu Tufan, J. Liu, J. Pan, and Z. Lian, *Genetic mechanisms of hepatocarcinogenesis*. *Oncogene*, 2002. **21**(16): p. 2593-604.
2. Ueki, T., J. Fujimoto, T. Suzuki, H. Yamamoto, and E. Okamoto, *Expression of hepatocyte growth factor and its receptor, the c-met proto-oncogene, in hepatocellular carcinoma*. *Hepatology*, 1997. **25**(3): p. 619-23.
3. Kaposi-Novak, P., J.S. Lee, L. Gomez-Quiroz, C. Coulouarn, V.M. Factor, and S.S. Thorgeirsson, *Met-regulated expression signature defines a subset of human hepatocellular carcinomas with poor prognosis and aggressive phenotype*. *J Clin Invest*, 2006. **116**(6): p. 1582-95.
4. Birchmeier, C., W. Birchmeier, E. Gherardi, and G.F. Vande Woude, *Met, metastasis, motility and more*. *Nat Rev Mol Cell Biol*, 2003. **4**(12): p. 915-25.
5. Wang, R., L.D. Ferrell, S. Faouzi, J.J. Maher, and J.M. Bishop, *Activation of the Met receptor by cell attachment induces and sustains hepatocellular carcinomas in transgenic mice*. *J Cell Biol*, 2001. **153**(5): p. 1023-34.
6. Cadigan, K.M., *Wnt signaling--20 years and counting*. *Trends Genet*, 2002. **18**(7): p. 340-2.
7. Clevers, H., *Wnt/beta-catenin signaling in development and disease*. *Cell*, 2006. **127**(3): p. 469-80.
8. Tetsu, O. and F. McCormick, *Beta-catenin regulates expression of cyclin D1 in colon carcinoma cells*. *Nature*, 1999. **398**(6726): p. 422-6.
9. Shtutman, M., J. Zhurinsky, I. Simcha, C. Albanese, M. D'Amico, R. Pestell, and A. Ben-Ze'ev, *The cyclin D1 gene is a target of the beta-catenin/LEF-1 pathway*. *Proc Natl Acad Sci U S A*, 1999. **96**(10): p. 5522-7.
10. Fu, M., C. Wang, Z. Li, T. Sakamaki, and R.G. Pestell, *Minireview: Cyclin D1: normal and abnormal functions*. *Endocrinology*, 2004. **145**(12): p. 5439-47.
11. Ewen, M.E. and J. Lamb, *The activities of cyclin D1 that drive tumorigenesis*. *Trends Mol Med*, 2004. **10**(4): p. 158-62.
12. Lee, R.J., C. Albanese, R.J. Stenger, G. Watanabe, G. Inghirami, G.K. Haines, 3rd, M. Webster, W.J. Muller, J.S. Brugge, R.J. Davis, and R.G. Pestell, *pp60(v-src) induction of cyclin D1 requires collaborative interactions between the extracellular signal-regulated kinase, p38, and Jun kinase pathways. A role for cAMP response element-binding protein and activating transcription factor-2 in pp60(v-src) signaling in breast cancer cells*. *J Biol Chem*, 1999. **274**(11): p. 7341-50.
13. Robles, A.I., M.L. Rodriguez-Puebla, A.B. Glick, C. Trempus, L. Hansen, P. Sicinski, R.W. Tennant, R.A. Weinberg, S.H. Yuspa, and C.J. Conti, *Reduced skin tumor development in cyclin D1-deficient mice highlights the oncogenic ras pathway in vivo*. *Genes Dev*, 1998. **12**(16): p. 2469-74.
14. Lovec, H., A. Sewing, F.C. Lucibello, R. Muller, and T. Moroy, *Oncogenic activity of cyclin D1 revealed through cooperation with Ha-ras: link between cell cycle control and malignant transformation*. *Oncogene*, 1994. **9**(1): p. 323-6.
15. Deane, N.G., M.A. Parker, R. Aramandla, L. Diehl, W.J. Lee, M.K. Washington, L.B. Nannay, Y. Shyr, and R.D. Beauchamp, *Hepatocellular carcinoma results*

- from chronic cyclin D1 overexpression in transgenic mice.* Cancer Res, 2001. **61**(14): p. 5389-95.
16. Deane, N.G., H. Lee, J. Hamaamen, A. Ruley, M.K. Washington, B. LaFleur, S.S. Thorgeirsson, R. Price, and R.D. Beauchamp, *Enhanced tumor formation in cyclin D1 x transforming growth factor beta1 double transgenic mice with characterization by magnetic resonance imaging.* Cancer Res, 2004. **64**(4): p. 1315-22.
 17. Sicinski, P., J.L. Donaher, S.B. Parker, T. Li, A. Fazeli, H. Gardner, S.Z. Haslam, R.T. Bronson, S.J. Elledge, and R.A. Weinberg, *Cyclin D1 provides a link between development and oncogenesis in the retina and breast.* Cell, 1995. **82**(4): p. 621-30.
 18. Fantl, V., G. Stamp, A. Andrews, I. Rosewell, and C. Dickson, *Mice lacking cyclin D1 are small and show defects in eye and mammary gland development.* Genes Dev, 1995. **9**(19): p. 2364-72.
 19. Yu, Q., Y. Geng, and P. Sicinski, *Specific protection against breast cancers by cyclin D1 ablation.* Nature, 2001. **411**(6841): p. 1017-21.
 20. Wilding, J., J. Straub, J. Bee, M. Churchman, W. Bodmer, C. Dickson, I. Tomlinson, and M. Ilyas, *Cyclin D1 is not an essential target of beta-catenin signaling during intestinal tumorigenesis, but it may act as a modifier of disease severity in multiple intestinal neoplasia (Min) mice.* Cancer Res, 2002. **62**(16): p. 4562-5.
 21. Hulit, J., C. Wang, Z. Li, C. Albanese, M. Rao, D. Di Vizio, S. Shah, S.W. Byers, R. Mahmood, L.H. Augenlicht, R. Russell, and R.G. Pestell, *Cyclin D1 genetic heterozygosity regulates colonic epithelial cell differentiation and tumor number in ApcMin mice.* Mol Cell Biol, 2004. **24**(17): p. 7598-611.
 22. Sansom, O.J., K.R. Reed, M. van de Wetering, V. Muncan, D.J. Winton, H. Clevers, and A.R. Clarke, *Cyclin D1 is not an immediate target of beta-catenin following Apc loss in the intestine.* J Biol Chem, 2005. **280**(31): p. 28463-7.
 23. Rowlands, T.M., I.V. Pechenkina, S.J. Hatsell, R.G. Pestell, and P. Cowin, *Dissecting the roles of beta-catenin and cyclin D1 during mammary development and neoplasia.* Proc Natl Acad Sci U S A, 2003. **100**(20): p. 11400-5.
 24. Tward, A.D., K.D. Jones, S. Yant, S.T. Cheung, S.T. Fan, X. Chen, M.A. Kay, R. Wang, and J.M. Bishop, *Distinct pathways of genomic progression to benign and malignant tumors of the liver.* Proc Natl Acad Sci U S A, 2007.
 25. Nelsen, C.J., D.G. Rickheim, M.M. Tucker, L.K. Hansen, and J.H. Albrecht, *Evidence that cyclin D1 mediates both growth and proliferation downstream of TOR in hepatocytes.* J Biol Chem, 2003. **278**(6): p. 3656-63.
 26. Lee, S.A., C. Ho, R. Roy, C. Kosinski, M.A. Patil, A.D. Tward, J. Fridlyand, and X. Chen, *Integration of genomic analysis and in vivo transfection to identify sprouty 2 as a candidate tumor suppressor in liver cancer.* Hepatology, 2007.
 27. Patil, M.A., M.S. Chua, K.H. Pan, R. Lin, C.J. Lih, S.T. Cheung, C. Ho, R. Li, S.T. Fan, S.N. Cohen, X. Chen, and S. So, *An integrated data analysis approach to characterize genes highly expressed in hepatocellular carcinoma.* Oncogene, 2005. **24**(23): p. 3737-47.

28. Harada, N., H. Oshima, M. Katoh, Y. Tamai, M. Oshima, and M.M. Taketo, *Hepatocarcinogenesis in mice with beta-catenin and Ha-ras gene mutations*. *Cancer Res*, 2004. **64**(1): p. 48-54.
29. Colnot, S., T. Decaens, M. Niwa-Kawakita, C. Godard, G. Hamard, A. Kahn, M. Giovannini, and C. Perret, *Liver-targeted disruption of Apc in mice activates beta-catenin signaling and leads to hepatocellular carcinomas*. *Proc Natl Acad Sci U S A*, 2004. **101**(49): p. 17216-21.
30. Hailfinger, S., M. Jaworski, A. Braeuning, A. Buchmann, and M. Schwarz, *Zonal gene expression in murine liver: lessons from tumors*. *Hepatology*, 2006. **43**(3): p. 407-14.
31. Calvisi, D.F., V.M. Factor, S. Ladu, E.A. Conner, and S.S. Thorgeirsson, *Disruption of beta-catenin pathway or genomic instability define two distinct categories of liver cancer in transgenic mice*. *Gastroenterology*, 2004. **126**(5): p. 1374-86.
32. Cadoret, A., C. Ovejero, S. Saadi-Kheddouci, E. Souil, M. Fabre, B. Romagnolo, A. Kahn, and C. Perret, *Hepatomegaly in transgenic mice expressing an oncogenic form of beta-catenin*. *Cancer Res*, 2001. **61**(8): p. 3245-9.
33. Gotoh, J., M. Obata, M. Yoshie, S. Kasai, and K. Ogawa, *Cyclin D1 overexpression correlates with beta-catenin activation, but not with H-ras mutations, and phosphorylation of Akt, GSK3 beta and ERK1/2 in mouse hepatic carcinogenesis*. *Carcinogenesis*, 2003. **24**(3): p. 435-42.
34. Zeng, G., U. Apte, B. Cieply, S. Singh, and S.P. Monga, *siRNA-mediated beta-catenin knockdown in human hepatoma cells results in decreased growth and survival*. *Neoplasia*, 2007. **9**(11): p. 951-9.
35. Renard, C.A., C. Labalette, C. Armengol, D. Cougot, Y. Wei, S. Cairo, P. Pineau, C. Neuveut, A. de Reynies, A. Dejean, C. Perret, and M.A. Buendia, *Tbx3 is a downstream target of the Wnt/beta-catenin pathway and a critical mediator of beta-catenin survival functions in liver cancer*. *Cancer Res*, 2007. **67**(3): p. 901-10.
36. Yamamoto, Y., M. Sakamoto, G. Fujii, H. Tsuiji, K. Kenetaka, M. Asaka, and S. Hirohashi, *Overexpression of orphan G-protein-coupled receptor, Gpr49, in human hepatocellular carcinomas with beta-catenin mutations*. *Hepatology*, 2003. **37**(3): p. 528-33.
37. Fan, W., X. Huang, C. Chen, J. Gray, and T. Huang, *TBX3 and its isoform TBX3+2a are functionally distinctive in inhibition of senescence and are overexpressed in a subset of breast cancer cell lines*. *Cancer Res*, 2004. **64**(15): p. 5132-9.
38. Vance, K.W., S. Carreira, G. Brosch, and C.R. Goding, *Tbx2 is overexpressed and plays an important role in maintaining proliferation and suppression of senescence in melanomas*. *Cancer Res*, 2005. **65**(6): p. 2260-8.
39. Lomnytska, M., A. Dubrovskaya, U. Hellman, N. Volodko, and S. Souchelnytskyi, *Increased expression of cSHMT, Tbx3 and utrophin in plasma of ovarian and breast cancer patients*. *Int J Cancer*, 2006. **118**(2): p. 412-21.

40. Lingbeek, M.E., J.J. Jacobs, and M. van Lohuizen, *The T-box repressors TBX2 and TBX3 specifically regulate the tumor suppressor gene p14ARF via a variant T-site in the initiator*. J Biol Chem, 2002. **277**(29): p. 26120-7.
41. McClanahan, T., S. Koseoglu, K. Smith, J. Grein, E. Gustafson, S. Black, P. Kirschmeier, and A.A. Samatar, *Identification of overexpression of orphan G protein-coupled receptor GPR49 in human colon and ovarian primary tumors*. Cancer Biol Ther, 2006. **5**(4): p. 419-26.
42. Barker, N., J.H. van Es, J. Kuipers, P. Kujala, M. van den Born, M. Cozijnsen, A. Haegebarth, J. Korving, H. Begthel, P.J. Peters, and H. Clevers, *Identification of stem cells in small intestine and colon by marker gene Lgr5*. Nature, 2007. **449**(7165): p. 1003-7.
43. Rojas, P., M.B. Cadenas, P.C. Lin, F. Benavides, C.J. Conti, and M.L. Rodriguez-Puebla, *Cyclin D2 and cyclin D3 play opposite roles in mouse skin carcinogenesis*. Oncogene, 2007. **26**(12): p. 1723-30.
44. Rodriguez-Puebla, M.L., M. LaCava, and C.J. Conti, *Cyclin D1 overexpression in mouse epidermis increases cyclin-dependent kinase activity and cell proliferation in vivo but does not affect skin tumor development*. Cell Growth Differ, 1999. **10**(7): p. 467-72.
45. Jian, Y., J. Yan, H. Wang, C. Chen, M. Sun, J. Jiang, J. Lu, Y. Yang, and J. Gu, *Cyclin D3 interacts with vitamin D receptor and regulates its transcription activity*. Biochem Biophys Res Commun, 2005. **335**(3): p. 739-48.
46. Weigel, N.L. and N.L. Moore, *Cyclins, cyclin dependent kinases, and regulation of steroid receptor action*. Mol Cell Endocrinol, 2007. **265-266**: p. 157-61.

Chapter 5

Bmi1 Functions as an Oncogene Independent of Ink4A/Arf Repression in Hepatic Carcinogenesis¹

Introduction

Bmi1, a member of the mammalian polycomb group of multimeric transcriptional repressors, is involved in the regulation of development, stem cell self-renewal, cell cycle, and senescence [1]. Bmi1 was first identified as a *c-myc* cooperating oncogene in murine B-cell lymphomas [2]. Subsequent studies have revealed that Bmi1 is required by both normal and leukemic hematopoietic stem cells to maintain their proliferative capacity [3, 4]. In addition, Bmi1 has been shown to be important for self-renewal of neural stem cells [5], and its expression is essential for the tumorigenicity of MycN induced neuroblastoma [6]. Studies have found that Bmi1 induces telomerase activity and subsequently immortalizes mammary epithelial cells [7]. Perhaps the most prominent link between Bmi1 and tumor development is its inhibition of the *Ink4A/Arf* locus, which results in the regulation of cell senescence and proliferation [8, 9].

Deregulation of Bmi1 expression has been reported in multiple tumor types, including non-small cell lung carcinoma, colon carcinoma, medulloblastoma, metastatic melanoma, and nasopharyngeal carcinoma [10-14]. Up-regulation of Bmi1 in human

¹ This chapter was published in a manuscript entitled: Bmi1 functions as an Oncogene Independent of Ink4A/Arf Repression in Hepatic Carcinogenesis; Xu, C., Lee, S.A., Ho, C., Bommi, P., Huang, S., Cheung, S.T., Dimri, G.P., Chen, X.; accepted in *Molecular Cancer Research*; I thank the co-authors, Chuan-Rui Xu and Coral Ho, and all other authors who contributed to this work. First co-authors, Susie Lee, Chuan-Rui Xu, and Coral Ho contributed equally to this work.

hepatocellular carcinoma (HCC) has also been reported [15, 16]. In a recent study, Chiba *et al* showed that silencing Bmi1 expression decreased the side population (SP) cells in HCC cell lines [17]. These SP subpopulation cells are considered to harbor cancer stem cell like properties [18]. However, the exact role of Bmi1 during HCC pathogenesis remains unclear. There are currently no *in vivo* models, which show that Bmi1 functions as an oncogene and directly contributes to HCC pathogenesis.

In this article, we describe that Bmi1 is over-expressed in human HCC samples. Bmi1 expression is also required for HCC cell proliferation *in vitro*. Notably, we established a novel mouse model for Bmi1 and show that Bmi1 can cooperate with activated Ras signaling to promote hepatic carcinogenesis *in vivo*. However, expression analysis suggests that Bmi1 functions independent of its ability to repress Ink4A/Arf tumor suppressor genes. Our data therefore provide solid evidence for a functional role of Bmi1 in liver cancer pathogenesis.

Materials and Methods

Human tissue samples and RNA preparation

Samples of tumor and non-tumor liver tissues were collected from liver resections at The University of Hong Kong. Tissues were frozen in liquid nitrogen within 0.5 hour after they were resected. Total RNA was extracted using Trizol (Invitrogen). This study was approved by the Ethics Committee of the University of Hong Kong and the Internal Review Boards from UCSF.

Constructs and reagents

Two shRNA constructs targeting Bmi1: Bmi1/pLKO.1 #1 (TRCN0000020155, NM_005180.5-693s1c1) and Bmi1/pLKO.1 #2 (TRCN0000020156, NM_005180.5-1061s1c1), used to silence Bmi1 expression were obtained from OpenBiosystems. Control pLKO.1 (empty vector) or SC/PLKO.1 (with a scrambled sequence) plasmids were obtained from Addgene. The hyperactive sleeping beauty construct (pCMV/SB) was provided by Dr. Mark Kay of Stanford University; and pCaggs-RasV12 was provided by Dr. David Largaespada of University of Minnesota. The pT3-EF1 α vector containing duplicated inverted repeats (IR) for sleeping beauty mediated integration and EF1 α promoter (pT3-EF1 α) used for hydrodynamic injection was described by Tward A *et al* [45]. Human Bmi1 (with a C-terminal V5 tag) was cloned into pT3-EF1 α via the Gateway PCR cloning strategy (Invitrogen). All plasmids were purified using the Endotoxin free Maxi prep kit (Sigma) before injecting into mice.

Cell culture, lentiviral infection, cell proliferation, BrdU labeling, caspase-3 activity and cell cycle assays

All human HCC cell lines were purchased from ATCC except Huh7, which were kindly provided by Dr. Ben Yen of UCSF. The cells are cultured in DMEM plus 10% fetal bovine serum. Lentivirus was generated and used to infect HCC cells. Three days post infection, cells were expanded and selected with 1 μ g/ml puromycin for 3 days and harvested for protein or RNA analysis. To assay cell proliferation rate, equal number of cells were seeded in 6-well plates and counted 3 to 4 days post seeding. Cell cycle

analysis was performed by flow cytometry after propidium iodide (PI) staining, and the results were analyzed using FlowJo. BrdU labeling was as described [46] and Caspase-3 activity was measured using Caspase-Glo3/7 Assay kit (Promega).

Hepatocyte isolation, transfection, adenovirus infection, and cell senescence assay

Primary hepatocyte isolation was performed using standard collagenase perfusion method as described [47]. The hepatocytes were transfected with plasmids using Targefect-Hepatocyte reagents (Targeting Systems) per manufacturer's instruction. Ad-H-RasV12 was kindly provided by Dr. Judy Meinkoth of the University of Pennsylvania [48]. Adenovirus was amplified and titered by Vector Biolabs and used to infect primary hepatocytes at 50 MOI. Hepatocytes were harvested 30 hours post transfection or infection. Hepatocyte senescence was determined using senescence β -galactosidase staining kit (Cell Signaling Technology).

Mouse hydrodynamic transfection and monitoring

Wildtype FVB/N mice were used in this study. The hydrodynamic transfection procedure are as described previously [45]. The injected mice were monitored weekly and sacrificed between 14 to 30 weeks post injection. All mice were housed, fed, and treated in accordance with protocols approved by the committee for animal research at the University of California, San Francisco.

Histology and immunohistochemistry

Animals were euthanized and their livers were removed and rinsed in PBS. Samples

collected from the livers were either frozen in dry ice for RNA and protein extraction or fixed overnight in freshly prepared cold 4% paraformaldehyde. Fixed tissue samples were embedded in paraffin. Five-micron sections were placed on slides and stained with hematoxylin and eosin. Immunohistochemistry was performed as described [28]. Antibodies and dilutions were as follows: anti-V5, 1:1000 (Invitrogen); anti-phospho-ERK, 1:100 (Cell Signalling Technology); anti-PODXL1, 1:200 (Applied Genomics, Burlingame, CA); and anti-Ki67, 1:150 (Lab vision).

Preparation of lysates and Western blotting

Liver tissues or cell lines were lysed in M-PER mammalian protein extraction buffer (Pierce) plus proteinase inhibitor cocktail (Roche) and Halt phosphatase inhibitor cocktail (Pierce). Protein content of the lysate was quantified using the BCA protein assay (Pierce). Western blotting was performed as described [45]. Antibodies were used as follows: anti-Bmi1, 1:1000 (Millipore) or 1:1000 (Invitrogen); anti-phospho-ERK, 1:1000; anti-ERK, 1:1000 (Cell Signaling Technology); anti-actin, 1:1000 (Sigma); anti-V5, 1:5000 (Invitrogen); anti-NRas, 1:1000; p16, 1:1000; and anti-HA, 1:1000 (Santa Cruz Biotechnology, Santa Cruz, CA)

Real-time RT-PCR

Total RNA was extracted from frozen liver tissues using Trizol (Invitrogen) and digested with DNase I to remove any genomic DNA contamination. Sybergreen-based real-time RT-PCR was carried out as described [21], and rRNA was used as internal control.

Transcript quantification was performed in triplicate for every sample and reported relative to rRNA. The primer pairs used are listed in Table 5.1.

		Forward	Reverse
Human primers	rRNA	CGG CTA CCA CAT CCA AGG AA-3'	GCT GGA ATT ACC GCG GCT-3'
	Bmi1	TGG ACT GAC AAA TGC TGG AGA-3'	GAA GAT TGG TGG TGG TTA CCG CTG-3'
	P21	CCT GTC ACT GTC TTG TAC CCT-3'	GCG TTT GGA GTG GTA GAA ATC T-3'
	P14	GTT CTT GGT GAC CCT CCG GAT T-3'	ATC AGC ACG AGG GCC ACA G-3'
	P16	GCC CAA CGC ACC GAA TAG TT -3'	GGG CAG TTG TGG CCC TGT AG-3'
	Mad2	AGC TAC GGT GAC ATT TCT GCC-3'	ATA AAC TGT GGT CCC GAC TCT-3'
	Cdc2	AAC TAC AGG TCA AGT GGT AGC C-3'	CTG GAA TCC TGC ATA AGC ACA-3'
	Cdc20	GAC CAC TCC TAG CAA ACC TGG-3'	GAG CCG AAG GAT CTT GGC TT-3'
	Bub1	CAC CCC GGA AAA TGT CCT TCA-3'	GAG GTC ACT GTT GTA CTC AGC-3'
	H-Ras	ACA ACA CCA AGT CTT TTG AGG AC-3'	GCC TGC CGA GAT TCC ACA G-3'
	RASSF1A	GGA GAC ACC TGA CCT TTC TCA-3'	CTG TTG ATC TGG GCA TTG TAC T-3'
	Mouse primers	Bmi1	CCA GGG CTT TTC AAA AAT GA-3'
P16		CGG TCG TAC CCC GAT TCA G-3'	GCA CCG TAG AGC AGA AGA G-3'
P19		AGA GGA TCT TGA GAA GAG GGC C-3'	GCA GTT CGA ATC TGC ACC G-3'
P21		CAC AGC GAT ATC CAG ACA TTC AG-3'	CGG AAC AGG TCG GAC ATC AC-3'
rRNA		CGG CTA CCA CAT CCA AGG AA-3'	GCT GGA ATT ACC GCG GCT-3'
E-cadherin		TGTGGGTCAGGAAATCACATCTT	CCAAATCCGATACGTGATCTTCT
cyclin D1		CGTGGCCTCTAAGATGAAGGA	CCTCGGGCCGGATAGAGTAG
cyclin E1		TGCCAAGATTGACAAGACTGTGA	TCCACGCATGCTGAATTATCA
Survivin		GCCACGCATCCCAGCTT	TTTAAAATACCACTGTCTCCTTCTC
Ang2		TTAGCACAAAGGATTCGGACAAT	TTTTGTGGGTAGTACTGTCCATTCA
AFP		TCTGCTGGCACGCAAGAAG	TCGGCAGGTTCTGGAAACTG

Table 5.1: Primers used for real-time RT-PCR.

Statistical analysis

The Pearson's correlation coefficient (R) was used to determine the correlations between gene expression values and p-value was determined using SPSS statistical program. Student's t test was used to evaluate statistical significance among experimental groups. Values of $P < 0.05$ were considered to be significant.

Results

Bmi1 is over-expressed in human HCC samples

In our previous studies, we used genomic approaches, including cDNA microarray and array-based comparative genomic hybridization, to characterize molecular variations in human HCC [19-21]. We identified 703 genes, which are highly expressed in human HCC [21]. One of these up-regulated genes is Bmi1. From this microarray study, Bmi1 expression is up-regulated in human HCC compared with non-tumor liver tissues ($p=2\times 10^{-6}$, after Bonferoni correction) (Fig. 5.1A). To verify this observation, we performed real-time RT-PCR analysis for Bmi1 expression in an independent liver tumor sample set which have not been previously assayed in microarray studies. Again, we observed up-regulation of Bmi1 in HCC samples ($p<0.001$, Fig. 5.1B). In two recent studies, the over-expression of Bmi1 in human HCC samples was shown at protein levels [15, 16].

Because p16Ink4A and p14Arf have been considered to be major targets of Bmi1 during tumor development, we investigated whether there is any correlation between Bmi1 and Ink4A/Arf expression in human HCC. On the cDNA microarrays, there was one probe corresponding to the COOH-terminal sequences of Ink4A/Arf, which hybridized to both p16Ink4A and p14Arf. Our analysis of this microarray data found no correlation between Bmi1 and total Ink4A/Arf expression ($R=-0.094$) (Fig. 5.1C). We next assayed the expression of Bmi1, p16Ink4A, and p14Arf individually using real-time RT-PCR in 19 human HCC and 4 non-tumor liver tissues. Again, we found no correlation between the expression values of Bmi1 and p16Ink4A or p14Arf (Fig. 5.1D and E).

Altogether, these data demonstrate that Bmi1 is up-regulated in human HCC, suggesting that Bmi1 may play a role in HCC pathogenesis. However, Bmi1 expression does not appear to be correlated with the expression of Ink4A/Arf tumor suppressor genes in human HCC samples.

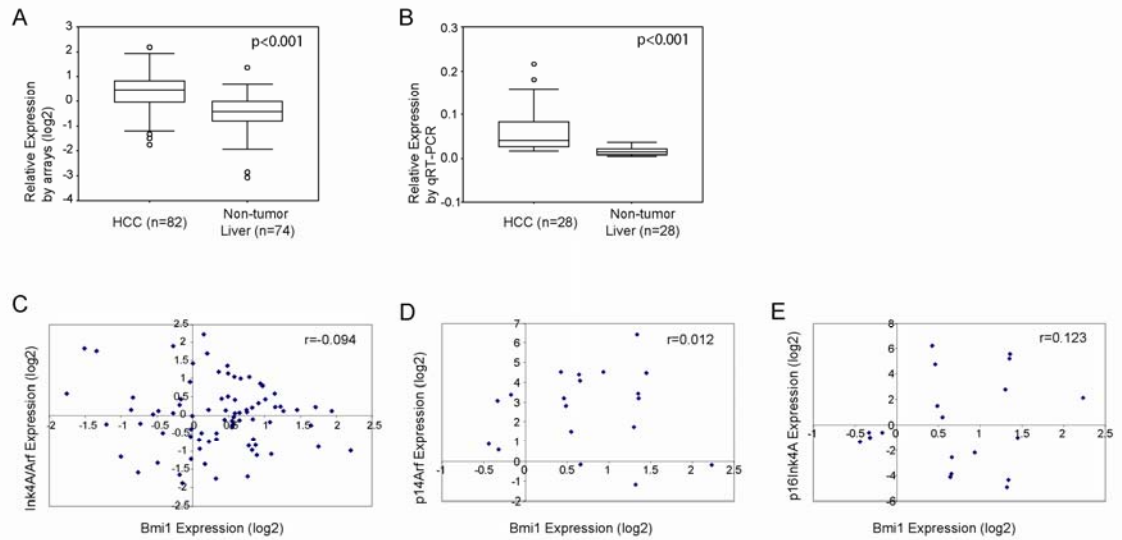


Figure 5.1: Bmi1 expression and its correlation with Ink4A/Arf expression in human HCC samples. (A) Bmi1 expression in non-tumor liver and HCC samples assayed by cDNA microarrays; (B) Bmi1 expression in an independent liver tissues set assayed by real-time RT-PCR; (C) Correlation between Bmi1 and Ink4A/Arf expression in human HCC samples assayed by cDNA microarrays; (D) and (E) Correlation between Bmi1 and p14Arf (D) or p16Ink4A (E) expression in human HCC samples assayed using real-time RT-PCR.

Stable shRNA-mediated knockdown of Bmi1 inhibits cancer cell growth *in vitro*

Our expression analysis suggests a potential role for Bmi1 during liver tumorigenesis. We therefore decided to study the functional significance of Bmi1 in hepatocarcinogenesis. We found that Bmi1 protein is highly expressed in human HCC cell lines (data not shown). To investigate whether Bmi1 is required during liver cancer development, we stably knocked down its expression using lentiviral shRNA in human HCC cell lines. To better study the relationship of Bmi1 expression and genetic alternations in human HCCs, we chose three HCC cell lines (SK-Hep1, Huh7, and Hep3B) with different genetic variations in α -fetoprotein, p53, p16Ink4A, and p14Arf (Table 5.2).

	SK-Hep1	Huh7	Hep3B
AFP	(-)	(+)	(+)
p16Ink4A	(-) Ink4A/Arf/-*	(-) promoter methylation	(+)
p14Arf	(-) Ink4A/Arf/-*	(+)	(+)
p53	WT	mutation (Y220C)	p53-/-

Table 5.2: Summary of the HCC cell lines used in the study

We infected these cells with lentivirus encoding empty vector pLKO.1, a vector with scrambled shRNA (SC/pLKO.1) or vectors against Bmi1, Bmi1/pLKO.1. Because similar results were obtained using pLKO.1 or SC/pLKO.1 as controls (data not shown), only the data with pLKO.1 and Bmi/pLKO.1 are shown here. To exclude non-specific RNAi-mediated effects, we tested two shRNA constructs which target different regions of Bmi1 sequences (Bmi1/pLKO.1 #1 and Bmi1/pLKO.1 #2). We found that both of Bmi1/pLKO.1 vectors efficiently silence Bmi1 expression in human HCC cell lines, as

confirmed by both real-time RT-PCR and Western blotting (Fig. 5.2, Fig. 5.3A and B). Therefore, only data from the Bmi1/pLKO.1 #1 studies are shown.

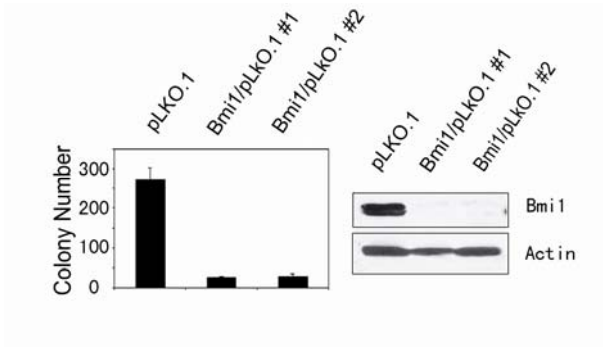


Figure 5.2: Cell growth inhibition in Hep3B cells when Bmi1 knock down was validated by a second shRNA construct.

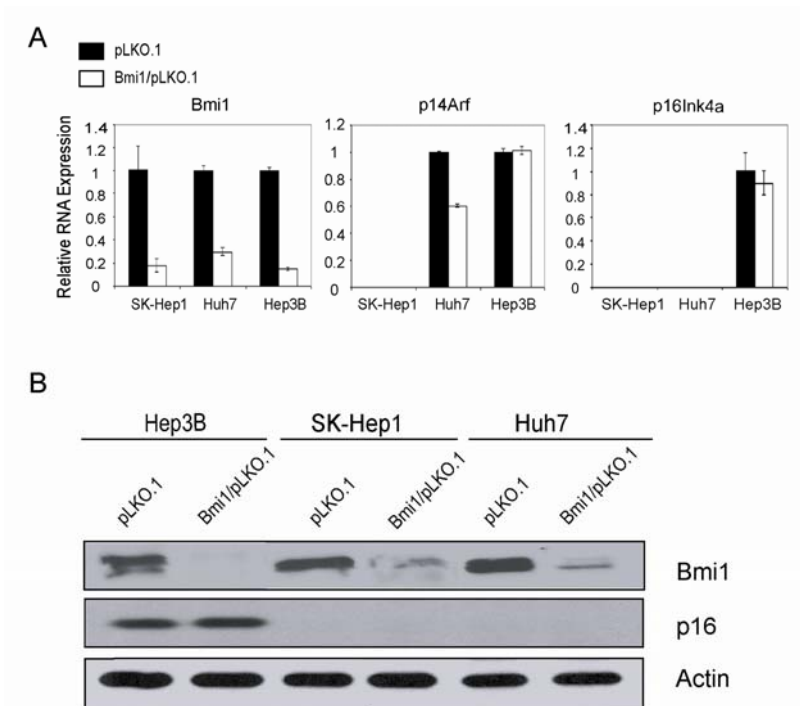


Figure 5.3: Down-regulation of Bmi1 and its effects on its target gene expression in human HCC cells. (A) Real-time RT-PCR analysis of Bmi1, p14Arf, p16Ink4A, and

p21 in pLKO.1 or Bmi1/pLKO.1 infected HCC cells; (B) Protein expression of Bmi1 and p16 in pLKO.1 or Bmi1/pLKO.1 infected HCC cells. Actin was used as loading control.

We found that despite different genetic backgrounds and Ink4A/Arf status, silencing of Bmi1 inhibits growth of all three HCC cell lines (Fig. 5.2 and Fig. 5.4A). Furthermore, the expression of cell cycle genes, such as *Cdc2*, *Cdc20*, and *Bub1* [22] are significantly down-regulated in Bmi1/pLKO.1 infected HCC cells (Fig. 5.4B and Fig. 5.5). In addition, BrdU labeling revealed a decreased proliferative rate (Fig. 5.4C and Fig. 5.6), whereas activated caspase 3 assay showed a slight increase in apoptosis when Bmi1 expression is silenced (data not shown). Finally, cell cycle analysis suggests that loss of Bmi1 perturbs cell cycle regulation and leads to G2/M accumulation (Fig. 5.4D, Fig. 5.7 and Table 5.3). There is also an increase of sub-G1 phase cells in Bmi1/pLKO.1 infected cells, providing further support of increased cell apoptosis when Bmi1 expression is silenced (Fig. 5.4D, Fig. 5.7 and Table 5.3).

In summary, the studies support that Bmi1 expression is required for *in vitro* growth of human HCC cell lines.

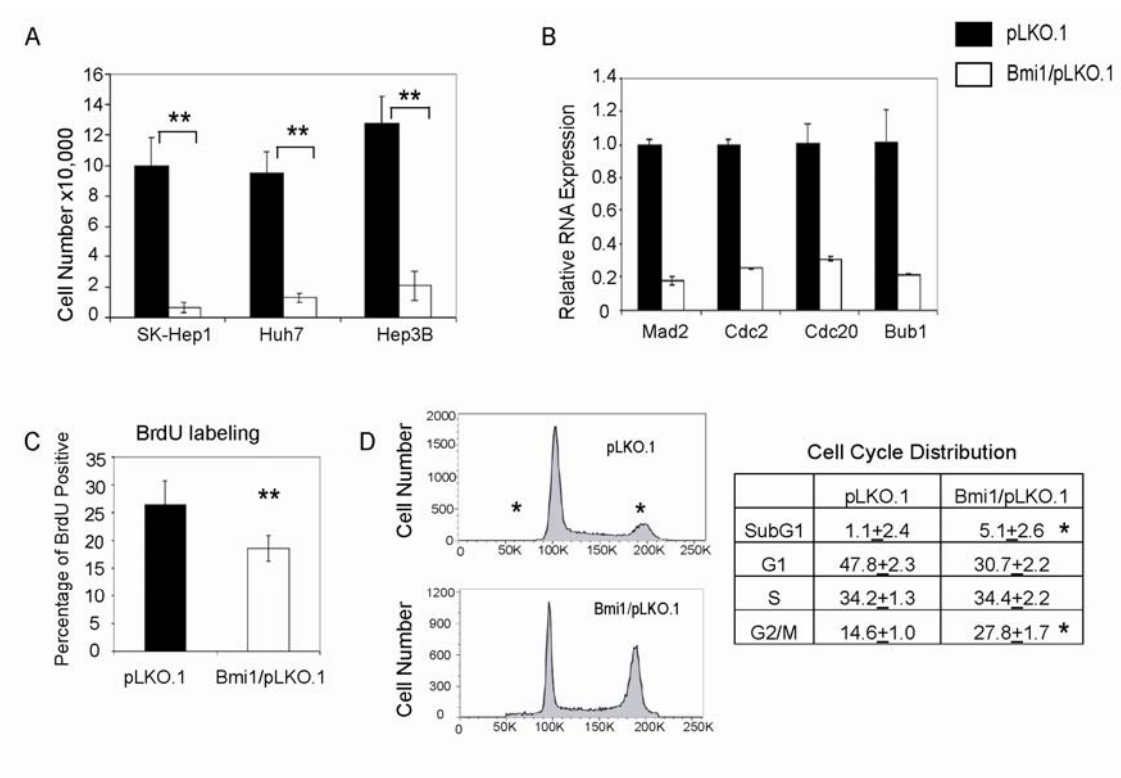


Figure 5.4: Silencing Bmi1 expression leads to decreased cell growth in human HCC cells. (A) Cell growth assays in three HCC cell lines infected with lentivirus encoding pLKO.1 or Bmi1/pLKO.1. Cell numbers were counted at day 3 post infection; (B) Down-regulation of cell cycle genes: Mad2, Cdc2, Cdc20, and Bub1 in Bmi1/pLKO.1 infected Huh7 cells; (C) BrdU labeling assays showing a decrease in cell proliferation in Bmi1/pLKO.1 infected Hep3B cells; (D) Representative images of cell cycle distribution of Hep3B cells infected with pLKO.1 or Bmi1/pLKO.1 measured by PI staining and FACS analysis. The percentage of cells in each cell cycle phase is listed on the right panel. **: $p < 0.01$; *: $p < 0.05$.

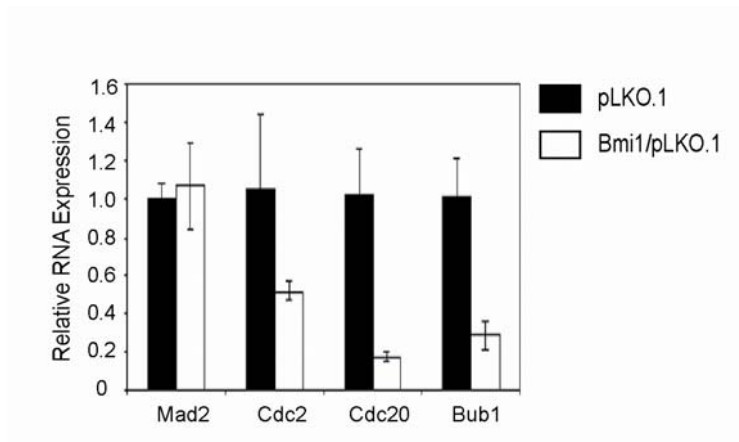


Figure 5.5: Cell cycle regulated genes expression decreased partly in Bmi1 knock down Hep3B cells.

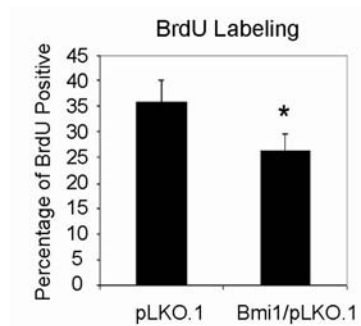


Figure 5.6: BrdU labeling assay showed decreased proliferation activity in Bmi1 knock down Huh7 cells. *: p < 0.05

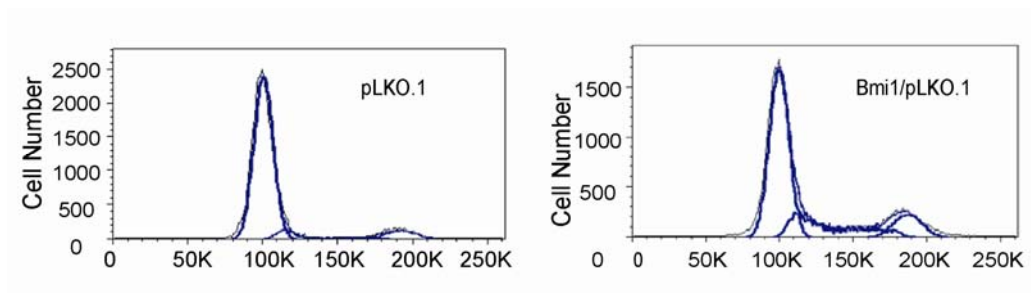


Figure 5.7: Bmi1 knock down in SK-Hep1 cells resulted in cell cycle blockages in S and G2/M phases.

	pLKO.1	Bmi1/pLKO.1
SubG1	0.86±0.32	1.77±0.27
G1	83.1±3.64	61.8±1.87
S	6.63±2.20	20.77±1.00
G2/M	7.26±0.10	13.47±0.70

Table 5.3: Cell cycle distribution of SK-Hep1 cells infected with pLKO.1 or Bmi1/pLKO.1.

Loss of Bmi1 does not lead to significant increased expression of p16Ink4A or p14Arf in HCC cell lines

One of the major mechanisms of Bmi1-induced tumor development is its function as a potent inhibitor of *CDKN2A* which encodes two major proteins: p16Ink4A and p14Arf (p19Arf in mice) [8, 23]. We first determined whether Bmi1 knockdown affects the mRNA expression of *CDKN2A* genes using real-time RT-PCR. SK-Hep1 cells have a deletion of *Ink4A/Arf* locus, whereas Huh7 cells have strong promoter methylation of *p16Ink4A*. Therefore, p16Ink4A expression is virtually undetectable in these two cell lines, regardless of whether Bmi1 is down-regulated (Fig. 5.3A). In addition, the loss of Bmi1 expression in transfected Hep3B cells does not appear to affect the expression of p16Ink4A. Likewise, we found that silencing Bmi1 expression does not lead to up-regulation of p14Arf in Huh7 and Hep3B cells, whereas p14Arf expression is absent in SK-Hep1 cells (Fig. 5.3A). We next assayed p16Ink4A protein expression in these HCC cell lines (Fig. 5.3B). Consistent with real-time RT-PCR results, p16Ink4A is undetectable in SK-Hep1 and Huh7 cells, whereas there is little change of p16Ink4A protein levels in Bmi1/pLKO.1 infected Hep3B cells (Fig. 5.3B).

In summary, our data showed that Bmi1 is required for HCC cell proliferation; however the effect of Bmi1 in promoting HCC cell growth is independent of Ink4A/Arf status.

Overexpression of Bmi1 cooperates with activated Ras to induce HCC in mice

We next determined whether Bmi1 can function as an oncogene by establishing a mouse model. We reasoned that it is unlikely Bmi1 alone is sufficient to induce liver cancer formation *in vivo*. Therefore, we searched for other signaling pathways that may be able to cooperate with Bmi1 to promote hepatic carcinogenesis. We chose activated Ras as the second signal, based on studies which have shown that Bmi1 is capable of cooperating with activated Ras to transform cells *in vitro* [24, 25]. In addition, Ras/MAPK signaling is known to be activated in all human HCC samples [26]. Therefore it represents a critical genetic alteration present in human HCC. Furthermore, studies from our and other labs have found that activated Ras alone is not sufficient to induce HCC formation in mice [27, 28].

We applied hydrodynamic transfection to stably express Bmi1 (with COOH-terminal V5 tag) and/or an activated form of N-ras (RasV12) into mouse hepatocytes. These animals were then monitored and sacrificed at specific time points or when moribund. We found that whereas over-expression of RasV12 (n=15) or Bmi1 (n=5) alone was not sufficient to promote liver tumor development, the co-expression of Bmi1 and RasV12 induced liver tumors in 78.6% (11/14) of the mice between 15 to 30 weeks post injection (Fig. 5.8A). Tumors tend to be multifocal, sometimes with over 100 tumor nodules scattered around the entire liver (Fig. 5.8B and data not shown).

Histological examination of liver tumor samples induced by Bmi1/RasV12 showed that tumors consisted of neoplastic cells with frequent trabecular disorganization, which are characteristic of HCC (Fig. 5.8D). In most cases, the tumor cells appear to be well differentiated. Real-time RT-PCR analysis revealed high expression of HCC specific marker α -fetoprotein (AFP) (Fig. 5.8C), further confirming the tumors to be of hepatocellular origin.

We next examined the tumor nodules for expression of injected Bmi1 (with a COOH-terminal V5 tag) and RasV12. Using anti-V5 antibody we observed that all tumor cells showed positive nuclear staining of Bmi1 (Fig. 5.8D). Sporadic expression of Bmi1 was also detected in the hepatocytes of surrounding non-tumor liver. RasV12 is indicated by elevated protein levels (Fig. 5.8E). Because activated Ras is a potent inducer of MAPK signaling, we investigated the activity of RasV12 by assaying for the presence of phospho-ERK. Both western blot and immunohistochemical analyses detected strong expression of phospho-ERK in the tumors (Fig. 5.8D & E).

Altogether, these results support that Bmi1 and RasV12 can cooperate to induce HCC *in vivo*.

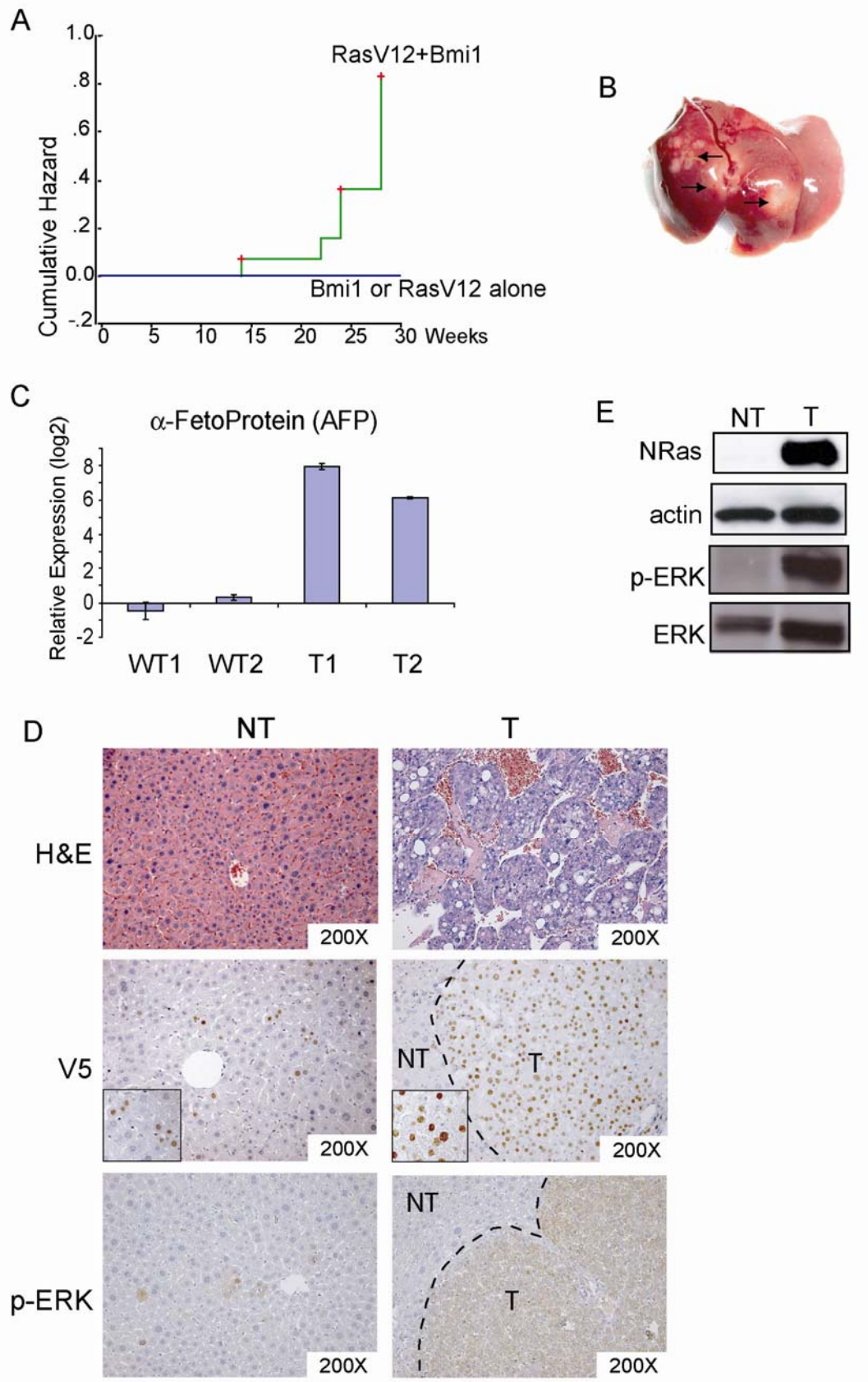


Figure 5.8: Bmi1 cooperates with activated Ras (RasV12) to promote hepatic carcinogenesis *in vivo*. (A) Tumor development incident curves in mice. The cumulative hazard represents the relative probability of tumor development in each condition; (B) Representative gross image of liver tumors induced by Bmi1/RasV12. Arrows indicate visible tumor nodules; (C) Quantitative RT-PCR analysis of AFP expression in normal liver and Bmi1/RasV12 tumor samples; (D) H&E staining of non-tumor liver (NT) and HCC (T) induced by Bmi1/RasV12 (top). Immunohistochemical staining with anti-V5 antibody showing staining of V5-tagged Bmi1 in HCC cells in a tumor nodule, with sporadic staining in non-tumor liver tissues (middle). Insets: expanded view showing specific nuclear staining of Bmi1 in non-tumor liver or HCC cells. Immunohistochemical staining of phospho-ERK in both NT and T samples (bottom); (E) Western blot analysis of N-Ras, phospho-ERK, and ERK expression. Actin was used as loading control.

Molecular characterization of Bmi1/RasV12 induced HCC

We then investigated the molecular features of Bmi1/RasV12 induced tumors in order to determine whether these traits resemble phenotypes observed in human HCC. We first assayed for cell proliferation in Bmi1/RasV12 tumor samples. Our detection of proliferative marker, Ki67, suggested the tumor cells to be highly proliferative (Fig. 5.9A). We also observed increased expression of cyclin E1 in liver tumor samples, whereas there is little variability in the expression of cell cycle regulator, cyclin D1 (Fig. 5.9B). In addition, we found that these tumors exhibited elevated levels of cell cycle inhibitor p21 (Fig. 5.9B), which is likely to be a feedback response to the activated Ras signaling. Furthermore, anti-apoptotic marker survivin and cell-cell adhesion marker E-

cadherin were also found to be up-regulated in liver tumor samples (Fig. 5.9B). The up-regulation of E-cadherin is consistent with the well-differentiated tumor histology, and is frequently observed in certain mouse models of HCCs [29, 30]. The occurrence of angiogenesis during liver carcinogenesis can be distinguished by the expression of endothelial markers, like PODXL1 [31]. Although PODXL1 is not typically expressed by normal liver sinusoidal endothelial cells, this marker is frequently present in the endothelial cells of liver tumors [31]. Therefore, we analyzed our samples for PODXL1 and observed that only endothelial cells within tumor nodules stained positive for this marker (Fig. 5.9A). Furthermore, these HCC samples also highly expressed angiogenic factor Ang2 (Fig. 5.9B).

Overall, our data suggests that Bmi1/RasV12 expressing tumors resemble a subset of human HCC characterized by the deregulation of factors involved in proliferation, apoptosis, and angiogenesis.

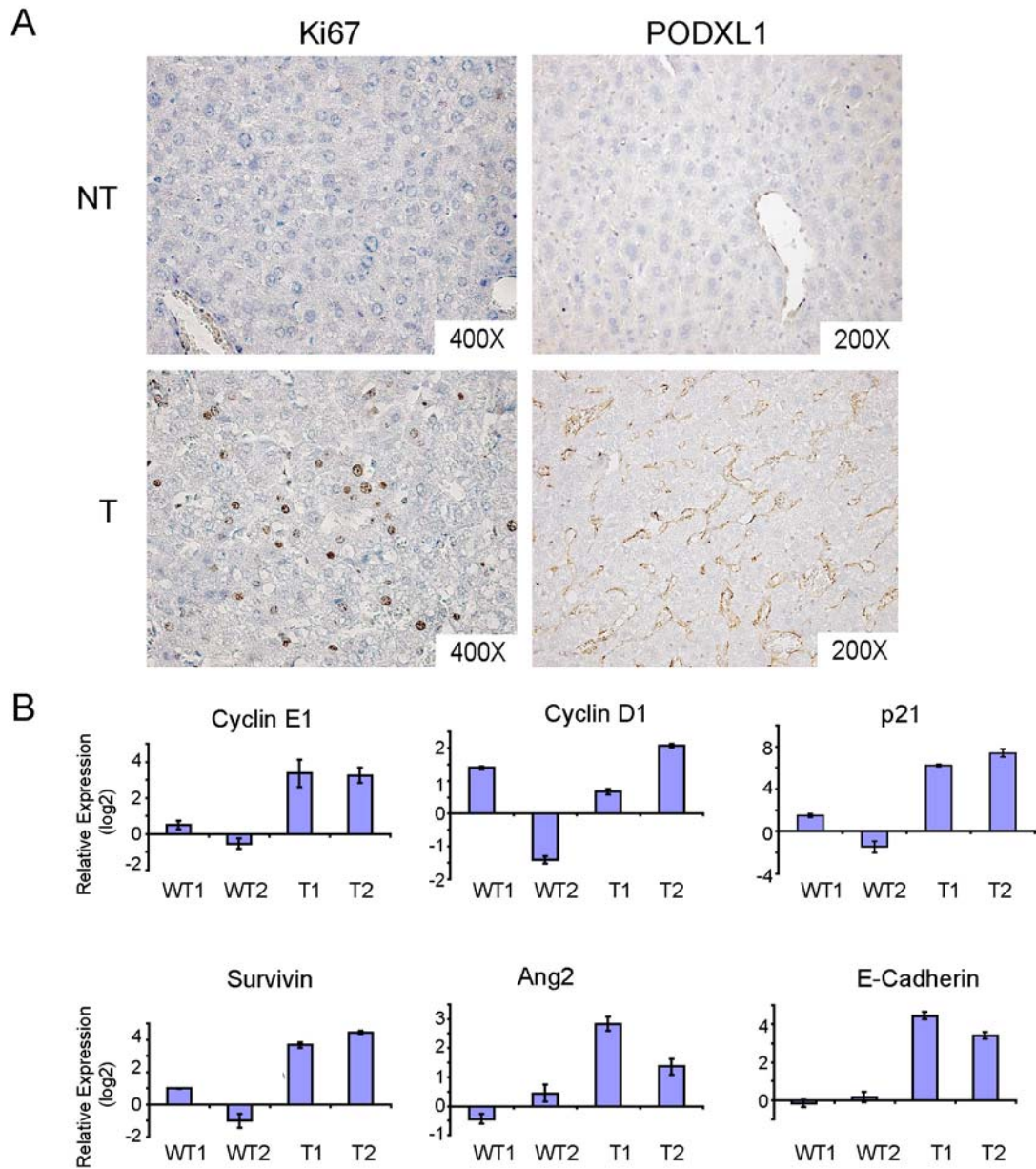


Figure 5.9: Characterization of liver tumors induced by Bmi1/RasV12. (A) Immunohistochemical staining of Ki67 and PODXL1 in non-tumor liver (NT) and tumor (T) tissues; (B) Quantitative RT-PCR analysis of genes in two wildtype (WT) liver tissues and two Bmi1/Ras liver tumors. In all cases, the expression values of the two wildtype samples were averaged, set to 1 and used to normalize liver tumor samples.

Up-regulation of p16Ink4A/p19Arf expression in Bmi1/RasV12 induced liver tumors

Bmi1 has been shown to cooperate with RasV12 to transform MEF cells via inhibition of *Ink4A/Arf* locus [24]. We therefore investigated whether this regulation is a mechanism by which Bmi1 and activated Ras promote tumorigenesis *in vivo*. We examined the expressions of p16Ink4A and p19Arf in our samples by quantitative RT-PCR. We have used multiple primers against p16Ink4A and p19ARF, and we found that in all cases, both p16Ink4A and p19ARF can only be detected after more than 30 cycles of PCR, indicating that p16Ink4A and p19ARF are expressed at very low levels in normal liver tissues. In contrast, p16Ink4A expression is up-regulated ~5 fold and p19Arf expression is up-regulated ~50 fold in Bmi1/RasV12 tumor samples (Fig. 5.10).

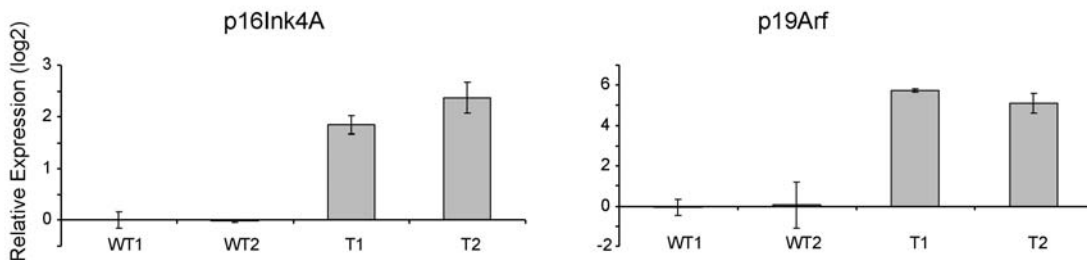


Figure 5.10: Up-regulation of p16Ink4A and p19Arf in liver tumor samples induced by Bmi1/RasV12. The relative expression of p16Ink4A and p19Arf of two wildtype liver tissues (WT) and two tumor samples (T) is shown.

Regulation of Ink4A/Arf expression by RasV12 and Bmi1 in mouse hepatocytes

The up-regulation of p16Ink4A and p19Arf in Bmi1/RasV12 tumor samples is quite surprising because Bmi1 is a known inhibitor of Ink4A/Arf locus. One of the

possibilities is that Ras is a potent inducer of p16Ink4A and p19Arf. The up-regulation of Ink4A/Arf may be why activated Ras alone is not sufficient to induce HCC formation *in vivo*. It is possible that the partial inhibition of Ras-induced Ink4A/Arf expression by Bmi1 is what eventually leads to hepatic carcinogenesis. If this is the case, it is likely that Bmi1/RasV12 tumor cells may have somewhat elevated expression of p16Ink4A and p19Arf than normal liver. However, this hypothesis is only possible if RasV12 can strongly induce p16Ink4A and p19Arf expression in hepatocytes. We therefore investigated the regulation of p16Ink4A and p19Arf by RasV12 or Bmi1 in normal mouse hepatocytes.

First, we generated adenovirus encoding activated Ras. Adenoviral infection has been shown to be able to transfect 100% of mouse hepatocytes at MOI of 10 [32]. We infected mouse primary hepatocytes with either control adenovirus encoding EGFP (AD-EGFP), or activated Ras (AD-RasV12-HA). Western blot analysis showed the expression of RasV12 in infected cells (Fig. 5.11A). Using quantitative RT-PCR, we found that p16Ink4A expression is repressed, whereas p19ARF expression remains unchanged in primary mouse hepatocytes after AD-RasV12-HA infection (Fig. 5.11A). Next we transfected primary mouse hepatocytes with plasmids encoding activated N-Ras (RasV12-HA) and/or Bmi1 (Bmi1-V5) using Targefect-Hepatocyte transfection reagents, which have a transfection efficiency of 50% for primary hepatocytes. The expression of RasV12 and Bmi1 are indicated by western blot analysis (Fig. 5.11B). We found that although the expression of p16Ink4A is down-regulated by RasV12 transfection, there is very little change in the expression of p19Arf. Bmi1 up-regulates p16Ink4A expression and inhibits p19Arf expression in this condition (Fig. 5.11B). Co-transfection with Bmi1

and RasV12 showed similar impact on p16Ink4A while having little effect on p19Arf (Fig. 5.11B). Next, we assayed p16Ink4A protein expression in these mouse hepatocytes. We found that p16Ink4A protein is undetectable in primary mouse hepatocytes in all these conditions (Fig.5.11A).

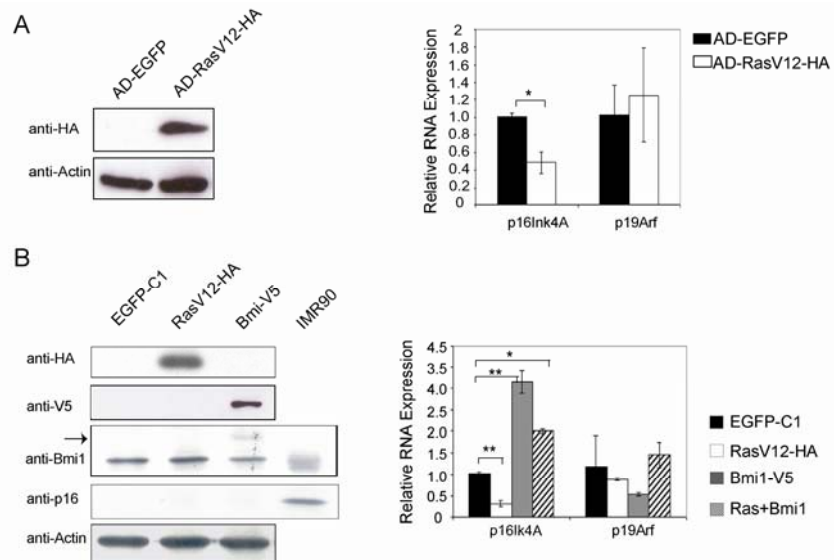


Figure 5.11: Regulation of p16Ink4A and p19Arf expression by RasV12 and/or Bmi1 in primary mouse hepatocytes. (A) Primary mouse hepatocytes were infected with adenovirus encoding EGFP or RasV12-HA. Western blotting shows the expression of HA-tagged RasV12 (left), and real-time RT-PCR shows the quantification of p16Ink4A and p19Arf expression in adenoviral infected primary hepatocytes (right); (B) Primary mouse hepatocytes were transfected with plasmids encoding EGFP, RasV12-HA and/or Bmi1-V5. Western blotting shows the expression of HA-tagged RasV12, V5-tagged Bmi1 and p16Ink4A (left). Arrow shows the ectopically expressed Bmi1-V5 that migrates higher than endogenous Bmi1 on gel. IMR90 cell lysate was used as positive control of p16Ink4A protein expression. Quantification of p16Ink4A and p19Arf mRNA

expression in transfected primary hepatocytes was performed using real-time RT-PCR (right). **: $p < 0.01$; *: $p < 0.05$.

Ras has been shown to induce cell senescence in certain cell types [33, 34], but the induction of cell senescence in hepatocytes by Ras has not been reported. It is possible that Bmi1 cooperates with RasV12 to promote HCC pathogenesis by overcoming Ras-mediated induction of senescence. We therefore investigated whether RasV12 or Bmi1 regulates cell senescence in primary hepatocytes. We transfected primary mouse hepatocytes with EGFP, RasV12, Bmi1, or RasV12 and Bmi1, and assayed for cell senescence. We found no evidence that either RasV12 or Bmi1 can modulate senescent status in primary hepatocytes (Fig. 5.12 and Table 5.4).

In summary, our data do not support activation of Ink4A/Arf by Ras or inhibition of Ink4A/Arf by Bmi1 overexpression in hepatocytes. The experiments therefore indicate that Bmi1 cooperates with RasV12 to promote HCC pathogenesis in an Ink4A/Arf-independent manner.

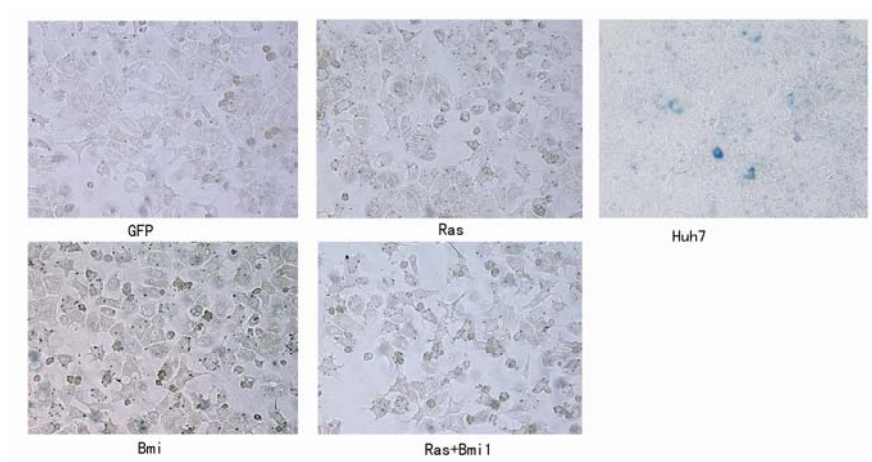


Figure 5.12: Ras does not induce senescence in mouse hepatocytes.

100 X Area	Area1	Area2	Area3	Area4	Average
GFP	1	3	3	0	1.75
Ras	1	2	1	0	1.00
Bmi1	1	1	1	2	1.25
Ras+Bmi1	2	0	1	1	1.25

Table 5.4: Statistics of positive stained cells for transfected hepatocytes.

DISCUSSION

There is increasing evidence supporting Bmi1 as an important oncogene in tumor development. Up-regulation of Bmi1 expression has been reported in multiple tumor types. Studies also showed that Bmi1 expression is required for *in vitro* cell proliferation in Ewing Sarcoma, lung cancer, and medulloblastoma cells [35-37], whereas over-expression of Bmi1 enhances cell survival in epidermis [38] and prostate cancer cells [39]. Using Bmi1 knockout mice, studies demonstrated that Bmi1 expression is required for the tumorigenesis of leukemia and lung cancer *in vivo* [4, 40]. However, there is still little evidence whether Bmi1 overexpression can directly contribute to carcinogenesis, especially in solid tumors. Proper mouse models need to be established to address this critical question. In our current study, we showed that Bmi1 is over-expressed in human HCC samples and required for HCC cell growth *in vitro*. More importantly, we established a novel mouse model which demonstrates that Bmi1 can cooperate with activated Ras to promote HCC pathogenesis in mice. Our study therefore provides pivotal data supporting Bmi1 as an oncogene and its role in hepatic carcinogenesis.

In this study, we used activated Ras to mimic the activation of Ras/MAPK pathway and in combination with Bmi1 to induce HCC in our mouse model. Although there is ubiquitous activation of Ras/MAPK signaling in human HCC, Ras mutations are,

in fact, very rare [41, 42]. De-regulation of other factors, including tumor suppressor genes *Spry2* and *RASSF1* as well as over expression of H-Ras, activation of receptor tyrosin kinases, such as EGFR and c-Met, have been implicated in human HCC, all of which result in up-regulation of this pathway [26]. Therefore, combination of these genetic alternations with Bmi1 overexpression in mouse models will provide additional *in vivo* models to mimic human HCC pathogenesis. We assayed the expressions of H-Ras and RASSF1A in human HCC samples, and found no correlation between the expression of these two genes with Bmi1 expression (Fig. 5.13). Clearly, further experiments will be needed to determine whether the expression of other factors involved in activation of Ras/MAPK pathways, such as c-Met or epidermal growth factor receptor, are associated with up-regulation of Bmi1 expression during HCC pathogenesis.

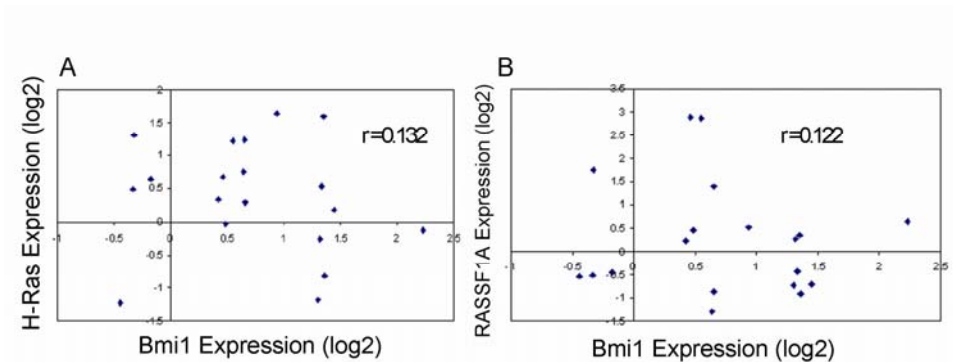


Figure 5.13: H-Ras and RASSF1A expression in HCC samples showed no correlation between Bmi1 and H-Ras, as well as Ras inhibitor RASSF1A.

An important implication of our study is that the tumorigenicity of Bmi1 during HCC pathogenesis is independent of its ability to repress Ink4A/Arf expression. First, we showed there is no correlation between the expressions of Bmi1 and p16Ink4A or p14Arf

in human HCC samples. Second, we found that the down-regulation of Bmi1 inhibits HCC cell growth independent of Ink4A/Arf status. Finally, we showed that in mouse tumor cells induced by Bmi1/RasV12, there is no down-regulation of p16Ink4A or p19Arf expression. Consistent with our observation, several recently published reports have revealed an Ink4A/Arf-independent role for Bmi1 during tumor pathogenesis. Bruggeman *et al*, for instance, showed that Bmi1 controls mouse glioma development in an Ink4a/Arf-independent manner [43]. Bmi1 knockdown significantly inhibits cell growth in both wildtype and p16Ink4A null Ewing Sarcoma [35], and medulloblastoma cell lines [37]. Thus, although inhibition of Ink4A/Arf tumor suppressor gene expression has been widely considered to be the key mechanism of the oncogenic activity of Bmi1, more recent data suggest a critical role of an Ink4A/Arf independent mechanism for Bmi1 during carcinogenesis.

Clearly, the next step in the characterization of molecular mechanisms of Bmi1 is to identify novel targets and/or pathways regulated by Bmi1 during HCC pathogenesis, and investigate how they cooperate with activated Ras/MAPK signaling to induce liver cancer formation. Some potential targets of Bmi1 have been identified in human cancer cell lines. For example, hTert is thought to be a major target in Bmi1 induced immortalization of mammary epithelial cells [7]. *NIDI*, a gene related to cell adhesion has been implicated as a Bmi1 target in Ewing Sarcoma cells [35]. Signaling molecules including BMP5, TGF- β 2, and Notch2 have been found to be regulated by Bmi1 in medulloblastoma cell lines [37]. It would be of interest to determine whether the expression of these factors is modulated by Bmi1 during HCC pathogenesis. A recent study indicated that the loss of Bmi1 results in the increase of reactive oxygen species

and subsequent stimulation of the DNA damage response pathway [44]. Activation of the DNA damage response pathway has been found to be an important barrier to tumorigenesis. In our recent studies, we observed up-regulation of mRNA of p53 and ATM genes in Bmi1/RasV12 induced liver tumor samples (Lee SA, unpublished observation). Clearly, it would be important to further characterize the expression of these genes in tumor samples at protein levels. Analysis of the regulation of this pathway by Bmi1 in liver may identify an additional function for Bmi1 during the development of HCC.

Reference:

1. Valk-Lingbeek, M.E., S.W. Bruggeman, and M. van Lohuizen, *Stem cells and cancer; the polycomb connection*. Cell, 2004. **118**(4): p. 409-18.
2. Haupt, Y., W.S. Alexander, G. Barri, S.P. Klinken, and J.M. Adams, *Novel zinc finger gene implicated as myc collaborator by retrovirally accelerated lymphomagenesis in E mu-myc transgenic mice*. Cell, 1991. **65**(5): p. 753-63.
3. Park, I.K., D. Qian, M. Kiel, M.W. Becker, M. Pihalja, I.L. Weissman, S.J. Morrison, and M.F. Clarke, *Bmi-1 is required for maintenance of adult self-renewing haematopoietic stem cells*. Nature, 2003. **423**(6937): p. 302-5.
4. Lessard, J. and G. Sauvageau, *Bmi-1 determines the proliferative capacity of normal and leukaemic stem cells*. Nature, 2003. **423**(6937): p. 255-60.
5. Molofsky, A.V., R. Pardal, T. Iwashita, I.K. Park, M.F. Clarke, and S.J. Morrison, *Bmi-1 dependence distinguishes neural stem cell self-renewal from progenitor proliferation*. Nature, 2003. **425**(6961): p. 962-7.
6. Cui, H., B. Hu, T. Li, J. Ma, G. Alam, W.T. Gunning, and H.F. Ding, *Bmi-1 is essential for the tumorigenicity of neuroblastoma cells*. Am J Pathol, 2007. **170**(4): p. 1370-8.
7. Dimri, G.P., J.L. Martinez, J.J. Jacobs, P. Keblusek, K. Itahana, M. Van Lohuizen, J. Campisi, D.E. Wazer, and V. Band, *The Bmi-1 oncogene induces telomerase activity and immortalizes human mammary epithelial cells*. Cancer Res, 2002. **62**(16): p. 4736-45.
8. Park, I.K., S.J. Morrison, and M.F. Clarke, *Bmi1, stem cells, and senescence regulation*. J Clin Invest, 2004. **113**(2): p. 175-9.
9. Lobo, N.A., Y. Shimono, D. Qian, and M.F. Clarke, *The biology of cancer stem cells*. Annu Rev Cell Dev Biol, 2007. **23**: p. 675-99.
10. Leung, C., M. Lingbeek, O. Shakhova, J. Liu, E. Tanger, P. Saremaslani, M. Van Lohuizen, and S. Marino, *Bmi1 is essential for cerebellar development and is overexpressed in human medulloblastomas*. Nature, 2004. **428**(6980): p. 337-41.
11. Vonlanthen, S., J. Heighway, H.J. Altermatt, M. Gugger, A. Kappeler, M.M. Borner, M. van Lohuizen, and D.C. Betticher, *The bmi-1 oncoprotein is differentially expressed in non-small cell lung cancer and correlates with INK4A-ARF locus expression*. Br J Cancer, 2001. **84**(10): p. 1372-6.
12. Kim, J.H., S.Y. Yoon, C.N. Kim, J.H. Joo, S.K. Moon, I.S. Choe, Y.K. Choe, and J.W. Kim, *The Bmi-1 oncoprotein is overexpressed in human colorectal cancer and correlates with the reduced p16INK4a/p14ARF proteins*. Cancer Lett, 2004. **203**(2): p. 217-24.
13. Mihic-Probst, D., A. Kuster, S. Kilgus, B. Bode-Lesniewska, B. Ingold-Heppner, C. Leung, M. Storz, B. Seifert, S. Marino, P. Schraml, R. Dummer, and H. Moch, *Consistent expression of the stem cell renewal factor BMI-1 in primary and metastatic melanoma*. Int J Cancer, 2007. **121**(8): p. 1764-70.
14. Sacchi, S., M. Federico, G. Dastoli, C. Fiorani, G. Vinci, V. Clo, and B. Casolari, *Treatment of B-cell non-Hodgkin's lymphoma with anti CD 20 monoclonal antibody Rituximab*. Crit Rev Oncol Hematol, 2001. **37**(1): p. 13-25.

15. Wang, H., K. Pan, H.K. Zhang, D.S. Weng, J. Zhou, J.J. Li, W. Huang, H.F. Song, M.S. Chen, and J.C. Xia, *Increased polycomb-group oncogene Bmi-1 expression correlates with poor prognosis in hepatocellular carcinoma*. *J Cancer Res Clin Oncol*, 2008. **134**(5): p. 535-41.
16. Sasaki, M., H. Ikeda, K. Itatsu, J. Yamaguchi, S. Sawada, H. Minato, T. Ohta, and Y. Nakanuma, *The overexpression of polycomb group proteins Bmi1 and EZH2 is associated with the progression and aggressive biological behavior of hepatocellular carcinoma*. *Lab Invest*, 2008.
17. Chiba, T., S. Miyagi, A. Saraya, R. Aoki, A. Seki, Y. Morita, Y. Yonemitsu, O. Yokosuka, H. Taniguchi, H. Nakauchi, and A. Iwama, *The polycomb gene product BMI1 contributes to the maintenance of tumor-initiating side population cells in hepatocellular carcinoma*. *Cancer Res*, 2008. **68**(19): p. 7742-9.
18. Chiba, T., K. Kita, Y.W. Zheng, O. Yokosuka, H. Saisho, A. Iwama, H. Nakauchi, and H. Taniguchi, *Side population purified from hepatocellular carcinoma cells harbors cancer stem cell-like properties*. *Hepatology*, 2006. **44**(1): p. 240-51.
19. Chen, X., S.T. Cheung, S. So, S.T. Fan, C. Barry, J. Higgins, K.M. Lai, J. Ji, S. Dudoit, I.O. Ng, M. Van De Rijn, D. Botstein, and P.O. Brown, *Gene expression patterns in human liver cancers*. *Mol Biol Cell*, 2002. **13**(6): p. 1929-39.
20. Patil, M.A., I. Gutgemann, J. Zhang, C. Ho, S.T. Cheung, D. Ginzinger, R. Li, K.J. Dykema, S. So, S.T. Fan, S. Kakar, K.A. Furge, R. Buttner, and X. Chen, *Array-based comparative genomic hybridization reveals recurrent chromosomal aberrations and Jab1 as a potential target for 8q gain in hepatocellular carcinoma*. *Carcinogenesis*, 2005. **26**(12): p. 2050-7.
21. Patil, M.A., M.S. Chua, K.H. Pan, R. Lin, C.J. Lih, S.T. Cheung, C. Ho, R. Li, S.T. Fan, S.N. Cohen, X. Chen, and S. So, *An integrated data analysis approach to characterize genes highly expressed in hepatocellular carcinoma*. *Oncogene*, 2005. **24**(23): p. 3737-47.
22. Whitfield, M.L., G. Sherlock, A.J. Saldanha, J.I. Murray, C.A. Ball, K.E. Alexander, J.C. Matese, C.M. Perou, M.M. Hurt, P.O. Brown, and D. Botstein, *Identification of genes periodically expressed in the human cell cycle and their expression in tumors*. *Mol Biol Cell*, 2002. **13**(6): p. 1977-2000.
23. Pardal, R., A.V. Molofsky, S. He, and S.J. Morrison, *Stem cell self-renewal and cancer cell proliferation are regulated by common networks that balance the activation of proto-oncogenes and tumor suppressors*. *Cold Spring Harb Symp Quant Biol*, 2005. **70**: p. 177-85.
24. Jacobs, J.J., K. Kieboom, S. Marino, R.A. DePinho, and M. van Lohuizen, *The oncogene and Polycomb-group gene bmi-1 regulates cell proliferation and senescence through the ink4a locus*. *Nature*, 1999. **397**(6715): p. 164-8.
25. Datta, S., M.J. Hoenerhoff, P. Bommi, R. Sainger, W.J. Guo, M. Dimri, H. Band, V. Band, J.E. Green, and G.P. Dimri, *Bmi-1 cooperates with H-Ras to transform human mammary epithelial cells via dysregulation of multiple growth-regulatory pathways*. *Cancer Res*, 2007. **67**(21): p. 10286-95.
26. Calvisi, D.F., S. Ladu, A. Gorden, M. Farina, E.A. Conner, J.S. Lee, V.M. Factor, and S.S. Thorgeirsson, *Ubiquitous activation of Ras and Jak/Stat pathways in human HCC*. *Gastroenterology*, 2006. **130**(4): p. 1117-28.

27. Harada, N., H. Oshima, M. Katoh, Y. Tamai, M. Oshima, and M.M. Taketo, *Hepatocarcinogenesis in mice with beta-catenin and Ha-ras gene mutations*. *Cancer Res*, 2004. **64**(1): p. 48-54.
28. Lee, S.A., C. Ho, R. Roy, C. Kosinski, M.A. Patil, A.D. Tward, J. Fridlyand, and X. Chen, *Integration of genomic analysis and in vivo transfection to identify sprouty 2 as a candidate tumor suppressor in liver cancer*. *Hepatology*, 2008. **47**(4): p. 1200-10.
29. Calvisi, D.F., S. Ladu, E.A. Conner, V.M. Factor, and S.S. Thorgeirsson, *Disregulation of E-cadherin in transgenic mouse models of liver cancer*. *Lab Invest*, 2004. **84**(9): p. 1137-47.
30. Wei, Y., J.T. Van Nhieu, S. Prigent, P. Srivatanakul, P. Tiollais, and M.A. Buendia, *Altered expression of E-cadherin in hepatocellular carcinoma: correlations with genetic alterations, beta-catenin expression, and clinical features*. *Hepatology*, 2002. **36**(3): p. 692-701.
31. Chen, X., J. Higgins, S.T. Cheung, R. Li, V. Mason, K. Montgomery, S.T. Fan, M. Rijn Mv, and S. So, *Novel endothelial cell markers in hepatocellular carcinoma*. *Mod Pathol*, 2004.
32. Prost, S., S. Sheahan, D. Rannie, and D.J. Harrison, *Adenovirus-mediated Cre deletion of floxed sequences in primary mouse cells is an efficient alternative for studies of gene deletion*. *Nucleic Acids Res*, 2001. **29**(16): p. E80.
33. Serrano, M., A.W. Lin, M.E. McCurrach, D. Beach, and S.W. Lowe, *Oncogenic ras provokes premature cell senescence associated with accumulation of p53 and p16INK4a*. *Cell*, 1997. **88**(5): p. 593-602.
34. Lin, A.W., M. Barradas, J.C. Stone, L. van Aelst, M. Serrano, and S.W. Lowe, *Premature senescence involving p53 and p16 is activated in response to constitutive MEK/MAPK mitogenic signaling*. *Genes Dev*, 1998. **12**(19): p. 3008-19.
35. Douglas, D., J.H. Hsu, L. Hung, A. Cooper, D. Abdueva, J. van Doorninck, G. Peng, H. Shimada, T.J. Triche, and E.R. Lawlor, *BMI-1 promotes ewing sarcoma tumorigenicity independent of CDKN2A repression*. *Cancer Res*, 2008. **68**(16): p. 6507-15.
36. Yu, Q., B. Su, D. Liu, B. Liu, Y. Fan, Y. Wang, and X. Meng, *Antisense RNA-mediated suppression of Bmi-1 gene expression inhibits the proliferation of lung cancer cell line A549*. *Oligonucleotides*, 2007. **17**(3): p. 327-35.
37. Wiederschain, D., L. Chen, B. Johnson, K. Bettano, D. Jackson, J. Taraszka, Y.K. Wang, M.D. Jones, M. Morrissey, J. Deeds, R. Mosher, P. Fordjour, C. Lengauer, and J.D. Benson, *Contribution of polycomb homologues Bmi-1 and Mel-18 to medulloblastoma pathogenesis*. *Mol Cell Biol*, 2007. **27**(13): p. 4968-79.
38. Lee, K., G. Adhikary, S. Balasubramanian, R. Gopalakrishnan, T. McCormick, G.P. Dimri, R.L. Eckert, and E.A. Rorke, *Expression of Bmi-1 in epidermis enhances cell survival by altering cell cycle regulatory protein expression and inhibiting apoptosis*. *J Invest Dermatol*, 2008. **128**(1): p. 9-17.
39. Fan, C., L. He, A. Kapoor, A. Gillis, A.P. Rybak, J.C. Cutz, and D. Tang, *Bmi1 promotes prostate tumorigenesis via inhibiting p16(INK4A) and p14(ARF) expression*. *Biochim Biophys Acta*, 2008. **1782**(11): p. 642-8.

40. Dovey, J.S., S.J. Zacharek, C.F. Kim, and J.A. Lees, *Bmi1 is critical for lung tumorigenesis and bronchioalveolar stem cell expansion*. Proc Natl Acad Sci U S A, 2008. **105**(33): p. 11857-62.
41. Tsuda, H., S. Hirohashi, Y. Shimosato, Y. Ino, T. Yoshida, and M. Terada, *Low incidence of point mutation of c-Ki-ras and N-ras oncogenes in human hepatocellular carcinoma*. Jpn J Cancer Res, 1989. **80**(3): p. 196-9.
42. Challen, C., K. Guo, J.D. Collier, D. Cavanagh, and M.F. Bassendine, *Infrequent point mutations in codons 12 and 61 of ras oncogenes in human hepatocellular carcinomas*. J Hepatol, 1992. **14**(2-3): p. 342-6.
43. Bruggeman, S.W., D. Hulsman, E. Tanger, T. Buckle, M. Blom, J. Zevenhoven, O. van Tellingen, and M. van Lohuizen, *Bmi1 controls tumor development in an Ink4a/Arf-independent manner in a mouse model for glioma*. Cancer Cell, 2007. **12**(4): p. 328-41.
44. Liu, J., L. Cao, J. Chen, S. Song, I.H. Lee, C. Quijano, H. Liu, K. Keyvanfar, H. Chen, L.Y. Cao, B.H. Ahn, N.G. Kumar, Rovira, II, X.L. Xu, M. van Lohuizen, N. Motoyama, C.X. Deng, and T. Finkel, *Bmi1 regulates mitochondrial function and the DNA damage response pathway*. Nature, 2009.
45. Tward, A.D., K.D. Jones, S. Yant, S.T. Cheung, S.T. Fan, X. Chen, M.A. Kay, R. Wang, and J.M. Bishop, *Distinct pathways of genomic progression to benign and malignant tumors of the liver*. Proc Natl Acad Sci U S A, 2007.
46. Wojtowicz, J.M. and N. Kee, *BrdU assay for neurogenesis in rodents*. Nat Protoc, 2006. **1**(3): p. 1399-405.
47. Nelsen, C.J., D.G. Rickheim, M.M. Tucker, L.K. Hansen, and J.H. Albrecht, *Evidence that cyclin D1 mediates both growth and proliferation downstream of TOR in hepatocytes*. J Biol Chem, 2003. **278**(6): p. 3656-63.
48. Cheng, G., A.E. Lewis, and J.L. Meinkoth, *Ras stimulates aberrant cell cycle progression and apoptosis in rat thyroid cells*. Mol Endocrinol, 2003. **17**(3): p. 450-9.

Chapter 6

Summary and Conclusions

Signaling pathways are essential to the control of cellular processes, such as proliferation and survival. However, abnormal regulation of these signaling mechanisms is also characteristic of human cancer. Loss in the control of these pathways is thought to be the resulting effects of genetic or epigenetic alterations that arise during carcinogenesis. In particular, a range of these aberrations, including β -catenin, c-Met, and Ink4A, has been implicated in human HCC (Ch.1). Previous microarray studies from our laboratory alone have identified changes in the expression of 113 genes due to loss or gain in DNA copy number, yet their roles in liver carcinogenesis are poorly understood (Ch.2) [1]. Therefore, the capability of these genetic alterations to promote liver tumorigenesis was examined in this dissertation.

Among these implicated pathways, up-regulation of Ras/MAPK signaling occurs in almost all human HCC [2]. Furthermore, stimulation of this pathway by Ras mutations in combination with oncogenes, such as β -catenin, has been demonstrated to result in the development of liver tumors *in vivo* [3]. Mutations of Ras are frequent in many cancers, including pancreatic carcinoma, yet these aberrations are quite rare in liver cancer, suggesting that other components of the pathway may be involved in the over-activation of Ras/MAPK signaling. Indeed, our study in Chapter 2 has identified RTK feedback inhibitor Spry2 to be down-regulated and deleted in ~40% of human HCC samples. Since Spry2 has been demonstrated to repress Ras/MAPK signaling, it is possible that this

inhibitor may function as a tumor suppressor during the development of HCC. Spry2 was subsequently expressed in HCC cells and analyzed for changes in proliferation. Overexpression of this inhibitor was found to reduce proliferation in these cells, which correlates to another similar finding [4]. These findings suggest the potential of Spry2 as a tumor suppressor, yet its role needed to be further evaluated *in vivo*.

To this end, a dominant negative form of Spry2 (Spry2Y55F) was generated and expressed alone or in combination with a constitutively active form of β -catenin (Δ N90- β -catenin) into the mouse liver by the sleeping beauty transposon and hydrodynamic injection system and monitored for tumor progression. While transfection of Spry2Y55F or Δ N90- β -catenin did not alter the liver morphology, expression of both targets sufficiently induced the formation of liver tumors in ~50% of the injected mice. Further analysis revealed proliferation, angiogenesis, as well as, Ras/MAPK signaling to be elevated in these tumors. These findings support the role of Spry2 as a tumor suppressor during liver carcinogenesis *in vivo*.

Although Ras/MAPK signaling is up-regulated in Spry2Y55F/ Δ N90- β -catenin tumors, we did not detect activation of this pathway in Spry2Y55F injected livers (data not shown). This observation suggests that since Spry2 functions as a feedback inhibitor, it is likely that Ras/MAPK signaling needs to be initially activated by another component of the pathway in order for the loss of Spry2 function to prolong the signal. This may be the case in our Spry2Y55F/ Δ N90- β -catenin mouse model because an increase in the mRNA expression of RTK EGFR was observed in the tumor samples. It is possible that Spry2Y55F may enhance EGFR signaling to promote liver tumor progression in this

model. However, the role of this receptor in Spry2Y55F/ Δ N90- β -catenin induced liver tumorigenesis needs to be further examined.

Our data in Chapter 2 suggest that other factors of the Ras/MAPK pathway could potentially synergize with the absence of Spry2 to promote signaling of this pathway during hepatocarcinogenesis. Recent findings have identified a correlation between activation of RTK c-Met and reduced expression of Spry2 in human HCC (Calvisi et al, unpublished data). In addition, Spry2 has been demonstrated to regulate c-Met signaling in HCC cells upon exposure to growth factor HGF (Calvisi et al, unpublished data). Based on these findings, c-Met over-expression may act in combination with the loss of Spry2 to promote liver carcinogenesis. Therefore, the study in Chapter 3 examined the relationship between c-Met and Spry2 in liver tumor progression. In order to assess the role of both factors in the development of HCC, c-Met and/or Spry2Y55F were injected into Ink4A/Arf null mice. Although Spry2Y55F expression did not affect liver morphology, over-expression of c-Met resulted in the emergence of pre-neoplastic lesions, but not tumors, in the liver. However, the co-expression of Spry2Y55F and c-Met induced the formation of liver tumors in 50% of the injected animals. Furthermore, both Ras/MAPK and Akt signaling are increased in these tumor samples. These findings indicate that although c-Met can induce pre-neoplastic lesions in the liver, the addition of Spry2Y55F enhances c-Met signaling and allows for transformation into a malignant tumor phenotype.

Interestingly, although Akt signaling is elevated in Spry2Y55F/c-Met tumors, changes in this pathway were not detected in Spry2Y55F/ Δ N90- β -catenin tumors. Furthermore, Spry2 has been demonstrated to inhibit Akt signaling by increasing the

expression of inhibitor PTEN, yet no changes in PTEN expression were detected in the Spry2Y55F/c-Met tumors [5]. This observation suggests that the mechanisms of Spry2 repression in Akt signaling may be dependent on cell type. Since Akt signaling is known to be induced by c-Met activity, Spry2Y55F may likely be enhancing this effect in the Spry2Y55F/c-Met murine model [6]. However, the role of Akt signaling in Spry2Y55F and c-Met induced liver tumorigenesis will need to be assessed.

As these studies have suggested so far, Ras/MAPK signaling plays an important role in liver tumor progression, yet a second oncogene is needed in order to fully promote the development of HCC. In particular, activated β -catenin mutations were found in c-Met transgenic mice and subsequently demonstrated to promote hepatocarcinogenesis in combination with the over-expression of c-Met [7, 8]. Further analysis of c-Met/ β -catenin tumors revealed up-regulation of CCND1 expression, a downstream target of β -catenin, in these samples. Since CCND1 has been demonstrated to induce HCC *in vivo*, this cell cycle regulator may be an important downstream component of c-Met/ β -catenin induced liver tumorigenesis. The study in Chapter 4, therefore, assessed the relationship between CCND1, β -catenin, and c-Met during hepatocarcinogenesis. Co-expression of CCND1 and c-Met did promote the formation of liver tumors in FVB mice, although at a lower frequency and longer latency in comparison to the c-Met/ β -catenin model. Closer histological analysis of CCND1/c-Met tumors showed the tumors to be adenomas, unlike the c-Met/ β -catenin tumors, which comprised of HCC. Interestingly, the loss of CCND1 did not deter, but appears to have accelerated c-Met/ β -catenin induced liver carcinogenesis in CCND1 null mice. Our data indicates that CCND1 is sufficient, but not required for liver tumor progression induced by c-Met and β -catenin.

Other downstream targets, in addition to CCND1, may be required to promote β -catenin signaling during hepatocarcinogenesis. Such factors should be assayed to determine if they can stimulate liver tumorigenesis. In addition to the observed acceleration in tumor progression, an increase in the expression of CCND2 was also detected in c-Met/ β -catenin expressing tumors and uninjected normal liver from CCND1 null mice. Implication of this cell cycle regulator in cancers, such as gastric cancer, suggests a role for CCND2 in carcinogenesis [9]. Whether CCND2 is involved in liver tumorigenesis needs to be determined.

The study in Chapter 5 has identified Bmi1 to be up-regulated in human HCC. *In vitro* analysis indicates that induced loss of this polycomb repressor represses HCC cell proliferation, which is similar to a previous finding [10]. In addition, co-expression of Bmi1 and activated Ras (RasV12) led to liver tumor formation in 78% of the injected FVB mice. These observations support the role of Bmi1 as an oncogene in liver carcinogenesis. Ink4A and Arf are known targets of Bmi1 during normal cell processes, such as proliferation, as well as in cancer [11, 12]. However, we did not observe any changes in the expressions of Ink4A or Arf by the loss of Bmi1 in HCC cell lines. Interestingly, Ink4A and Arf protein levels were elevated in Bmi1/RasV12 tumor samples. Although Ras can induce expressions of both Ink4A and Arf (Chapter 1), transfection of RasV12 and/or Bmi1 into isolated mouse hepatocytes did not increase the expressions of either target. Taken altogether, our findings indicate that Bmi1 and RasV12 promote hepatocarcinogenesis in an Ink4A/Arf independent manner. Identification of additional Bmi1 mechanisms will certainly help in understanding how Bmi1 promotes liver tumor progression. A recent study suggests that loss of Bmi1 is capable of stimulating the DNA

damage response pathway [13]. We also observe elevated mRNA levels of DNA response genes *p53* and *ATM*. Further analysis of this pathway may implicate an additional function of Bmi1 in the development of HCC.

The studies in this dissertation have validated clinical findings and identified a set of oncogenes and tumor suppressors, when de-regulated, are capable of stimulating liver carcinogenesis. Moreover, our findings provide us with a better understanding of the signaling systems involved in the development of HCC. Specifically, the implication of Spry2 as a tumor suppressor in Chapters 2 and 3 has established a mechanism by which Ras/MAPK signaling can be activated in hepatocarcinogenesis. Given that this pathway is up-regulated in almost all HCC, further analysis of how Spry2 represses Ras/MAPK signaling in the liver may lead to the development of novel therapeutic targets. Studies in Chapters 4 and 5 have found oncogenes, CCND1 and Bmi1 to be sufficient in promoting liver tumor progression in combination with activated Ras signaling. These findings clearly demonstrate that HCC progression is a multistep process that requires the de-regulation of more than one gene. However, future studies will need to be performed in order to determine the mechanisms of these genetic interactions during the development of this disease.

The method used to generate the mouse models in these studies has allowed us to assess the role of clinical relevant genetic alterations during hepatocarcinogenesis in an efficient and timely manner. Such animal models could prove to be quite useful in therapeutic applications. Drugs designed to target a specific factor or signaling pathway can be tested in these models to assess whether inhibition of one or a combination of these factors leads to liver tumor regression.

In closing, the studies in this dissertation have demonstrated the potential of genes, implicated in human HCC, to act as tumor suppressors or oncogenes during liver cancer progression and provided us with useful models for future research in the development of HCC and/or therapeutics.

Reference:

1. Chen, X., S.T. Cheung, S. So, S.T. Fan, C. Barry, J. Higgins, K.M. Lai, J. Ji, S. Dudoit, I.O. Ng, M. Van De Rijn, D. Botstein, and P.O. Brown, *Gene expression patterns in human liver cancers*. *Mol Biol Cell*, 2002. **13**(6): p. 1929-39.
2. Calvisi, D.F., S. Ladu, A. Gorden, M. Farina, E.A. Conner, J.S. Lee, V.M. Factor, and S.S. Thorgeirsson, *Ubiquitous activation of Ras and Jak/Stat pathways in human HCC*. *Gastroenterology*, 2006. **130**(4): p. 1117-28.
3. Harada, N., H. Oshima, M. Katoh, Y. Tamai, M. Oshima, and M.M. Taketo, *Hepatocarcinogenesis in mice with beta-catenin and Ha-ras gene mutations*. *Cancer Res*, 2004. **64**(1): p. 48-54.
4. Fong, C.W., M.S. Chua, A.B. McKie, S.H. Ling, V. Mason, R. Li, P. Yusoff, T.L. Lo, H.Y. Leung, S.K. So, and G.R. Guy, *Sprouty 2, an inhibitor of mitogen-activated protein kinase signaling, is down-regulated in hepatocellular carcinoma*. *Cancer Res*, 2006. **66**(4): p. 2048-58.
5. Edwin, F., R. Singh, R. Endersby, S.J. Baker, and T.B. Patel, *The tumor suppressor PTEN is necessary for human Sprouty 2-mediated inhibition of cell proliferation*. *J Biol Chem*, 2006. **281**(8): p. 4816-22.
6. Birchmeier, C., W. Birchmeier, E. Gherardi, and G.F. Vande Woude, *Met, metastasis, motility and more*. *Nat Rev Mol Cell Biol*, 2003. **4**(12): p. 915-25.
7. Wang, R., L.D. Ferrell, S. Faouzi, J.J. Maher, and J.M. Bishop, *Activation of the Met receptor by cell attachment induces and sustains hepatocellular carcinomas in transgenic mice*. *J Cell Biol*, 2001. **153**(5): p. 1023-34.
8. Tward, A.D., K.D. Jones, S. Yant, S.T. Cheung, S.T. Fan, X. Chen, M.A. Kay, R. Wang, and J.M. Bishop, *Distinct pathways of genomic progression to benign and malignant tumors of the liver*. *Proc Natl Acad Sci U S A*, 2007.
9. Takano, Y., H. Takenaka, Y. Kato, M. Masuda, T. Mikami, M. Saegusa, and I. Okayasu, *Cyclin D1 overexpression in invasive breast cancers: correlation with cyclin-dependent kinase 4 and oestrogen receptor overexpression, and lack of correlation with mitotic activity*. *J Cancer Res Clin Oncol*, 1999. **125**(8-9): p. 505-12.
10. Chiba, T., S. Miyagi, A. Saraya, R. Aoki, A. Seki, Y. Morita, Y. Yonemitsu, O. Yokosuka, H. Taniguchi, H. Nakauchi, and A. Iwama, *The polycomb gene product BMII contributes to the maintenance of tumor-initiating side population cells in hepatocellular carcinoma*. *Cancer Res*, 2008. **68**(19): p. 7742-9.
11. Fan, C., L. He, A. Kapoor, A. Gillis, A.P. Rybak, J.C. Cutz, and D. Tang, *Bmi1 promotes prostate tumorigenesis via inhibiting p16(INK4A) and p14(ARF) expression*. *Biochim Biophys Acta*, 2008. **1782**(11): p. 642-8.
12. Dhawan, S., S.I. Tschen, and A. Bhushan, *Bmi-1 regulates the Ink4a/Arf locus to control pancreatic beta-cell proliferation*. *Genes Dev*, 2009. **23**(8): p. 906-11.
13. Liu, J., L. Cao, J. Chen, S. Song, I.H. Lee, C. Quijano, H. Liu, K. Keyvanfar, H. Chen, L.Y. Cao, B.H. Ahn, N.G. Kumar, Rovira, II, X.L. Xu, M. van Lohuizen, N. Motoyama, C.X. Deng, and T. Finkel, *Bmi1 regulates mitochondrial function and the DNA damage response pathway*. *Nature*, 2009.

Publishing Agreement

It is the policy of the University to encourage the distribution of all theses, dissertations, and manuscripts. Copies of all UCSF theses, dissertations, and manuscripts will be routed to the library via the Graduate Division. The library will make all theses, dissertations, and manuscripts accessible to the public and will preserve these to the best of their abilities, in perpetuity.

Please sign the following statement:

I hereby grant permission to the Graduate Division of the University of California, San Francisco to release copies of my thesis, dissertation, or manuscript to the Campus Library to provide access and preservation, in whole or in part, in perpetuity.

Susie Lee
Author Signature

1/7/10
Date